EMERGENCE OF RICH DYNAMICAL BEHAVIOUR IN NETWORKS OF COUPLED CANDLE-FLAME OSCILLATORS: SYNCHRONIZATION, AMPLITUDE DEATH, AND CHIMERAS

A Project Report

submitted by

KRISHNA MANOJ

in partial fulfilment of the requirements
for the award of the degree of

BACHELOR OF TECHNOLOGY & MASTER OF TECHNOLOGY

DEPARTMENT OF AEROSPACE ENGINEERING
INDIAN INSTITUTE OF TECHNOLOGY MADRAS

JUNE 2020

CERTIFICATE

This is to certify that the project report titled **EMERGENCE OF RICH DYNAMICAL BEHAVIOUR IN NETWORKS OF COUPLED CANDLE-FLAME OSCILLATORS: SYNCHRONIZATION, AMPLITUDE DEATH, AND CHIMERAS**, submitted by **Krishna Manoj**, to the Indian Institute of Technology Madras, for the award of the degree of **Bachelor of Technology** and **Master of Technology**, is a bona fide record of the research work done by her under our supervision. The contents of this report, in full or in parts, have not been submitted to any other Institute or University for the award of any degree or diploma.

Prof. R. I. Sujith
Research Guide
Professor
Dept. of Aerospace Engineering
IIT Madras, Chennai 600 036

Place: Chennai

Date: 1st June 2020

ACKNOWLEDGEMENTS

Foremost, I would like to thank my God, The Almighty, who showers His blessing on all His creations and smiles at their success.

I would like to express my sincere and heartfelt gratitude to my advisor, Prof. R. I. Sujith, who held my hand while I climbed the first steps of my research path. His constant belief in me motivated me to overcome all the hurdles and obstacles which came our way. The motivational conversations we had were beyond all the motivation I gained from stories, books, and movies he suggested. I am highly inspired by his vision, passion, sincerity, and dedication to all his research irrespective of the simplicity or the complexity of the project. His nature of looking at all his students, undergraduate, graduate, and postgraduate students, through the same lens as his own kids and having equally high expectations from all his students is truly remarkable and motivates us to reach our goal. While being the teaching assistant for his thermodynamics course, I learnt how to present our thoughts to a young audience, and experience the joy of teaching and inspiring a class of students. I am also thankful for his involvement and guidance throughout the project and for his friendship and empathy, which guided me through my hard times. I could not have imagined having a better advisor to guide me through my first steps of research.

I am extremely thankful to Dr. Samadhan A. Pawar, who guided me through the stairs of research. He taught me the methodology to carry out research and corrected me in every step of the way. His dynamism, down to earth mentality, and eagerness to discover, learn and conquer new fields of expertise is indeed an inspiration for me to continue my academic journey. I extend my earnest gratitude to him, for teaching me the very basics of how to conduct a literature survey to the difficulties which arrive while drafting the manuscript. He was always there to guide me in the right direction, whenever I strayed off, both personally and academically. I extend my earnest gratitude to him who was always there to support me and help me through every crisis. I am truly thankful for his help while designing and conducting experiments, analysing and drafting the results, and dealing with emotional and stressful situations. Without his

constant guidance and push, I cannot have imagined reaching all the milestones in my research path. More than being my mentor, he was my best friend and the big brother I always wished for. Both Prof. R. I. Sujith and Dr. Samadhan Pawar moulded me into a better researcher and on top that a better person.

I am honoured and grateful to collaborate with Prof. Jurgen Kurths, Prof. Elena Surovyatkina, Dr. Sirshendu Mondal, Dr. D. Premraj, Suraj Dange, and Subham Banerjee. Adding their varied perspectives on the topic of research helped in transforming the project continuously towards perfection. I am also thankful to Dr. Bala Pesala from the Council of Scientific and Industrial Research (CSIR) Chennai, under whom I completed my summer internship on the theoretical modelling of candle-flame oscillators. I would also like to thank my lab mates Dr. Vishnu R. Unni, Amitesh Roy, R. Manikandan, R. Mithun, K. V. Reeja , Dr. Abin Krishnana, P. Induja, K. Praveen, J. V. Alan, and Sruthi Tandon for helping me conduct complex experiments, correcting my manuscripts, and providing their valuable comments on my research. I am also thankful for all the stimulating discussion with all my lab mates, which improved my clarity on research. I am also thankful to Prof. Ram Ramaswamy for the suggestion for constructing the modified candle-flame oscillators. I am also incredibly grateful to my cherished friends, Vedashri G. and H. M. Aravind. They guided me towards choosing my research advisor and were beside me throughout my research path, holding my hands through all my fears, and helping me find my passion for research. I also wish to thank the assistance of Thilakaraj and Anand in the manufacturing process of all the experimental setups used in my projects. I also express my gratitude to Jabasteena and other office staffs in the department who helped me with all the official works and documents.

I would also like to convey my vote of thanks to my professors and friends at IIT Madras for their endless support. I would like to thank my HODs, Prof. K. Bhaskar, Prof. P. Sriram, and Prof. H. S. N. Murthy, for their support and encouragement throughout my undergraduate years. I would also like to thank Prof. Luoyi Tao and Prof. Ranjith Mohan for being highly inspirational professors and guiding me to tackle all my academic difficulties. I am also grateful to my ultimate Frisbee team at IIT Madras and my batch mates who lit my face with a smile throughout my undergraduate years. Finally, I would like to thank my parents for their support and encouragement to pursue my dreams. I am also grateful to my brothers, Adhvaid and Aryan, who always looked up to me as an inspiration, which is a constant driving force during tough situa-

tions. I am also thankful to my aunt and uncle, who always believed in me and inspired me throughout my life.

ABSTRACT

KEYWORDS: Candle-flame Oscillators; Synchronization; Amplitude Death; Phase-flip Bifurcation; Weak Chimera; Chimera; Minimal Network

Nonlinear phenomena emerging from the coupled behaviour of a network of oscillators have attracted considerable research attention over the years, of which, symmetry-breaking phenomena such as chimera, clustering, and weak chimera along with amplitude death and phase-flip bifurcation are some noteworthy examples. Understanding these global dynamical behaviour exhibited by a network of coupled oscillators has been a topic of extensive research in many fields of science and engineering. Various factors govern the resulting dynamical behaviour of such networks, including the number of oscillators and the coupling schemes between them. Although these factors are seldom significant in a large population of oscillators, a small change in these factors can drastically affect the global behaviour in small populations. Therefore, recent studies focus on the discovery of such phenomena in a system with minimum number of oscillators, as their insights can equally be applied to the dynamics of large, spatially extended systems. Moreover, the individual occurrence of the aforementioned phenomenon has been a focus of most studies in the past. Therefore, a collective existence of all these phenomena in single system is rarely observed.

The primary aim of the present project report is to provide the experimental existence of several phenomena, including symmetry-breaking phenomena such as clustering, weak chimera, and chimera along with theoretically reported states of in-phase and anti-phase chimera and other states of synchronization and oscillation quenching, in a network of two or more coupled candle-flame oscillators, exhibiting limit cycle oscillations in the uncoupled state. In the case of two candle-flame oscillators, we observe the transition from in-phase synchronization (IP) to the state of anti-phase synchronization (AP) via the intermediate state of amplitude death (AD) as the distance between the oscillators is increased. As the strength of coupling between the oscillators is increased

by increasing the number of candles in an oscillator, we report a decrease in the span of AD region between the states of in-phase and anti-phase oscillations, leading up to the point of phase-flip bifurcation (PFB). Although theoretical research has postulated the coexistence of AD and PFB upon variation of different control parameters, such an occurrence has not been reported in practical systems. We provide the first experimental evidence of the coexistence of AD and PFB in a physical system, comprising of a coupled pair of candle-flame oscillators.

The investigation is further extended to present the first experimental study highlighting the existence of several states of symmetry-breaking coupled dynamics of an array of four non-locally coupled candle-flame oscillators, as the distance between them is varied. We also provide an experimental confirmation of different dynamical states, including in-phase, anti-phase, and multi-phase weak chimera. Hence by varying the coupling structure in a network of four oscillators, we observe the emergence of phase locking, amplitude quenching, and chimera states. In many practical systems, one (or more) among these states is considered undesirable. Therefore, we bring out the possibility of evading the undesirable occurrence of phase-locking, amplitude quenching, and chimera states by smart control of the coupling parameters.

In the subsequent analysis of the project report, we provide an experimental investigation on the effect of factors, such as number, coupling strength and topology of the oscillators, on the coupled behaviour of a minimal network of candle-flame oscillators. We found that when the oscillators are strongly coupled, the global behaviour of the network exhibits in-phase synchrony and amplitude death, which remains independent of the number and the topology of oscillators. However, when they are weakly coupled, the global behaviour of the network exhibits the occurrence of multiple stable states which alternately switch in time. In addition to such states of clustering, chimera, and weak chimera, we report the first experimental evidence of partial amplitude death in a network of candle-flame oscillators. We also show that the networks with closed-loop topology tend to hold global synchronization for longer duration as compared to those with open-loop topology.

Finally, the experimental results obtained from coupled pair and quadruplet of candle-flame oscillators are compared with a generic mathematical model of time-delay coupled Stuart-Landau oscillators. We observe that the dynamics observed in coupled

Stuart-Landau oscillators show high similarity to those observed in candle-flame oscillators. Thus, we understood that coupled candle-flame oscillators exhibit a variety of dynamical behaviour depending on the number of oscillators, the coupling strength, and the topological arrangement of the oscillators. The results obtained can be used as a benchmark for several theoretical studies on coupled oscillators using generic mathematical oscillators. Further, due to the simple and generic nature of these oscillators, we can conclude that the results obtained from candle-flame oscillators can be extended to various other fields of engineering including biological, ecological, mechanical and electrochemical systems.

TABLE OF CONTENTS

LIST OF FIGURES

ABBREVIATIONS

AD	Amplitude Death
AP	Anti-phase Synchronization
CH	Chimera
CL	Clustering
DS	Desynchronization
FFT	Fast Fourier Transform
fps	frames per second
IP	In-phase Synchronization
PAD	Partial Amplitude Death
PFB	Phase-flip Bifurcation
P. V.	Cauchy Principle Value
SL	Stuart-Landau Oscillator
TS	Transition States
WC	Weak Chimera

NOTATION

Uppercase Roman

$A(t)$	Instantaneous amplitude
$I_i(t)$	Instantaneous value of heat release rate fluctuations in oscillator i, a.u.
I_H	Signal obtained after Hilbert transformation
$I_{(i,rms)}$	Root mean square value of $I_i(t)$, $a.u.$
K	Coupling strength between two oscillators
N	Number of oscillators in a network
N_C	Number of candles in an oscillator
$Z(t)$	Instantaneous amplitude of SL oscillator

Lowercase Roman

d	Distance between two oscillators, m
d_x	Distance in x direction, m
d_y	Distance in y direction, m
f	Frequency, Hz
t	Time, s

Greek Alphabets

$\phi_i(t)$	Instantaneous value of phase of oscillator i, $degrees$
$\Delta\phi_{ij}$	Phase difference between oscillator i and j, $degrees$
ρ	Pearson's correlation coefficient
τ	Time delay between two oscillators
τ_x	Time delay in x direction
τ_y	Time delay in y direction
θ_i	Instantaneous phase of spatial oscillator i, $degrees$
ω_i	Angular frequency of oscillator i, Hz
$\zeta(t)$	Analytical signal

Notation

$\|x\|$	Absolute value of x
$\bar{x}$	Mean of x
$\dot{x}$	Time derivative of x

CHAPTER 1

Introduction

Coupled behaviour emerging from the interaction of oscillators have become an extensive area of research due to the emergence of various intriguing nonlinear phenomena as a consequence of coupling between them (Kuramoto, 1984; Glass and Mackey, 1988; Winfree, 2001; Strogatz, 2004). Both theoretical and experimental studies have flurried into the literature on different aspects of the coupled phenomenon discovered in various systems found in nature. Starting from the motions of coupled pendula (Kapitaniak *et al.*, 2014) and extending towards suppressing coronavirus spread (Savi *et al.*, 2020), collective behaviour as a consequence of mutual interaction has attracted research attention since many decades (Blasius *et al.*, 1999; Selkoe, 2000; Néda *et al.*, 2000; Glass, 2001; Strogatz *et al.*, 2005*a*).

Nevertheless, recent studies focus on the classification of diverse amounts of dynamical states that emerge due to coupling between oscillators. Those dynamical states range from synchronization (Pikovsky *et al.*, 2003), clustering (Pecora *et al.*, 2014), oscillation quenching (Saxena *et al.*, 2012) to symmetry-breaking phenomena such as chimera (Abrams and Strogatz, 2004), and weak chimera (Ashwin and Burylko, 2015). Studies on such coupled behaviours reveal their importance in various physical, biological, chemical, ecological, and engineering systems (Mizuno *et al.*, 1989; Dolnik and Marek, 1988; Hansel and Sompolinsky, 1992; Roy and Thornburg Jr, 1994; Schäfer *et al.*, 1998; Strogatz, 1998; Reddy *et al.*, 1998, 2000).

The occurrence of these dynamical states has been studied in networks where the number of oscillators range from an order of one (Kapitaniak *et al.*, 2014; Hart *et al.*, 2016) to thousand (Kuramoto and Battogtokh, 2002). It is interesting to note that in a large network of coupled oscillators, the addition or removal of a few oscillators does not affect the global dynamical behaviour of the entire system (Wickramasinghe and Kiss, 2013). Furthermore, in such a network of oscillators, a change in the topological position (or coupling arrangement) of a few oscillators might not affect the overall response of the system. However, these observations exhibited by a large network of

oscillators may not be applicable to the networks where the number of oscillators is very few (i.e., the minimal oscillator network).

Coupled behaviour of oscillators in minimalist networks (number of oscillators 2 to 10) has shown several interesting dynamical behaviours. These networks are very susceptible to the addition or removal of an oscillator and also to a change in the topological arrangement of oscillators in a network. Any change in these properties would result in drastic changes in the global behaviour of the system (Wickramasinghe and Kiss, 2013). The addition of an oscillator increases the degrees of freedom of the system, increasing the complexities in the behaviour of the system.

For example, in a system of coupled candle-flame oscillators, when the number of oscillators is two, the system shows three prominent behaviours which are asymptotically stable in time such as in-phase synchronization, anti-phase synchronization, and desynchronization (Kitahata *et al.*, 2009). While, as the number of oscillators is increased to three and located in an equilateral triangle arrangement, the system shows a drastic change in its global dynamical behaviour from showing a single stable dynamical state seen in two oscillators to the presence of multiple stable states. These states include in-phase synchronization, amplitude death, partial in-phase, and rotation mode (Okamoto *et al.*, 2016). Due to the presence of only a few number of oscillators, the data acquisition and analysis process of an individual oscillator is much simpler in minimal networks when compared to large networks of oscillators. Yet another advantage of studying minimal oscillators is that the insights obtained from such minimal systems can be equally applied to the dynamics of large, spatially extended systems (Hart *et al.*, 2016).

Furthermore, studies on minimal oscillator networks primarily focus on the discovery of various dynamical states including all symmetry-breaking states, and the states of synchronization and oscillation quenching in individual systems, such as lasers (Hart *et al.*, 2016), electrochemical oscillators (Wickramasinghe and Kiss, 2013), and mechanical oscillators (Kapitaniak *et al.*, 2014). The collective existence of all these dynamical states in a single system is rarely studied. Further, many symmetry-breaking dynamical states such as in-phase and anti-phase weak chimera (Maistrenko *et al.*, 2017) have only been observed in theoretical studies and, therefore, an experimental observation of all such theoretically discovered are also to be reported.

1.1 Objectives and Overview of the Project Report

The present study is a quest for the experimental evidence of all aforementioned nonlinear phenomena observed in an autonomous system with minimum number of coupled candle-flame oscillators. The parameters varied in the case of candle-flame oscillators are the distance between the candle-flame oscillators, the number of candles in an oscillators, number of oscillators and the topology in which the oscillators are arranged. With the variation of these parameters one at a time keeping the other parameters constant, we observe the presence of weak chimera, chimera, clustering, in-phase, anti-phase and multi-phase chimera, in addition to other states such as synchronization and oscillation quenching in a network of coupled candle-flame oscillators. The coupled dynamics exhibited by candle-flame oscillators show high similarity with the behaviour exhibited by time-delay coupled Stuart-Landau oscillators.

Therefore, based on the current understanding of the literature on minimal oscillators in general and on the experimental studies on candle-flame oscillators, we come up with the following specific objectives for the present report. The list of objectives is given below.

1. Study the emergence of various dynamical states observed due to the coupled interaction of candle-flame oscillators. Then, characterize different states of synchronization observed in these oscillators using tools from synchronization theory and nonlinear dynamics.
2. Examine the coupled dynamics exhibited by a pair (two) of coupled candle-flame oscillators, under the variation of two parameters, the distance between two oscillators and the number of candles constituting each oscillator, and study the dynamical behaviour exhibited by the system.
3. Investigate the occurrence of various symmetry-breaking phenomena, including weak chimera, chimera, and clustering in a system of four coupled candle-flame oscillators placed in a rectangular topology. Analyze the amplitude, phase, and frequency characteristics of each of the dynamical state exhibited by these oscillators for various combinations of distance between the oscillators.
4. Examine the effect of topology on the coupled behaviour of a minimal network of candle-flame oscillators. Examine different open-loop (straight and star) and closed-loop topologies (triangle and square) of minimal networks consisting of two to four oscillators. Finally, study the coupled behaviour of an annular network of oscillators to understand the effect of increase in the number of oscillators in the topology on the global behaviour of the network.
5. Lastly, investigate the ability of the generic mathematical model of time-delay

coupled Stuart-Landau oscillators in supplementing the experimental results observed in coupled candle-flame oscillators.

The organization of the report is presented as follows.

In **Chapter 2**, a basic introduction of the synchronization theory, with the history, and applications, is provided. The chapter also provides a summary of tools that have been devised to study synchronization of coupled oscillators. It ends with a detailed description of various dynamical states observed in coupled oscillators in general.

Chapter 3 summarizes the various experimental setups implemented in the study of coupled candle-flame oscillators. It discusses the manufacturing of candle-flame oscillators and the experimental techniques and tools used in the analysis of the coupled dynamics of these oscillators.

In **Chapter 4**, we discuss the experimental results obtained from the mutual interaction of a pair of candle-flame oscillators. The chapter is divided into two sections: one where similar oscillators are coupled and the other with dissimilar oscillators are coupled. The first experimental coexistence of amplitude death and phase-flip bifurcation in a coupled pair of candle-flame oscillators is discussed in this chapter.

The experimental investigation of coupled dynamics of four candle-flame oscillators in a rectangular arrangement for various combination of distance between these oscillators is delineated in **Chapter 5**. The study on the presence of several nonlinear phenomena such as synchronization, amplitude death, clustering, and chimeras in a system of four coupled candle-flame oscillators is presented.

The dependence of topological arrangement on the coupled behaviour of networks with minimal number of oscillators is described in **Chapter 6**. Systems consisting of two, three, and four oscillators are subjected to various types of open-loop (straight & star) and closed-loop (triangular & square) topological arrangements. Further, the investigation is extended to annular (close-loop) topologies consisting of five to seven oscillators.

In **Chapter 7**, the generic mathematical model of time-delay coupled Stuart-Landau oscillators is used to supplement the experimental results of two and four coupled candle-flame oscillators. Finally, conclusions derived from the present report are provided in **Chapter 8**. This chapter also includes the scope for future work.

CHAPTER 2

Introduction to Synchronization Theory

Synchronization leading to self-organization within a population of oscillators due to their mutual coupling has awed the human minds since time immemorial (Pikovsky *et al.*, 2003). Following the observation of mutual adjustment of rhythms of pendulum clocks (see Fig. 2.1), Huygens in the 17^{th} century named this behaviour as sympathy, later called synchronization (Huygens, 1665), wherein all oscillators adjust their timescales to a common value upon coupling (Pikovsky *et al.*, 2003). The pendulum clocks, which were on the same wall and therefore connected with the same beam, synchronized due to the high strength of coupling provided by the presence of the beam. The pendulums exhibited a mutual adjustment in their time periods which eventually led to complete locking of their motions to a common time period. This temporal sympathy of oscillatory pendulum clocks is called synchronization. During the process of synchronization, coupled oscillators exhibit an adjustment of frequencies, from different values observed during their uncoupled state to a common value achieved at the state of synchronization.

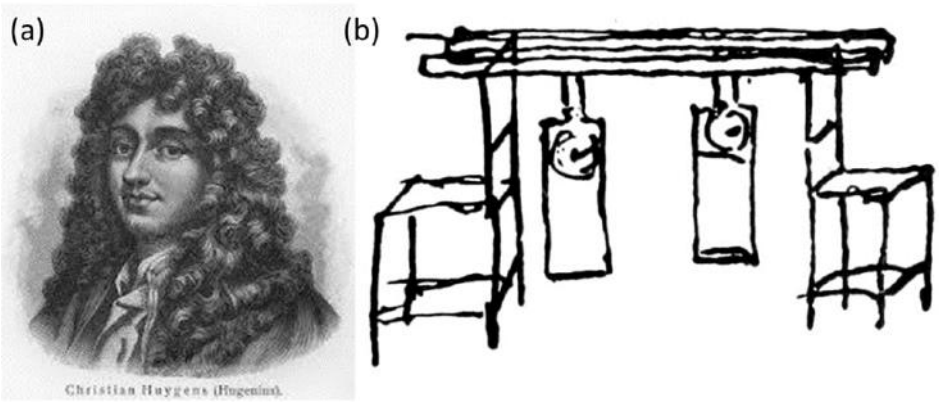

Figure 2.1: (a) Photo of Christiaan Huygen with his (b)sketch on the experiment involving a pair of pendulum clocks attached on a single beam to understand the synchronization phenomenon between them which resulted due to the kicks that their swings gave each other using the wall as a medium. The figure is adapted from Pikovsky *et al.* (2003).

In order to observe and characterize the phenomenon of synchronization, the system needs to satisfy two sufficient conditions: the first one is that all the oscillators

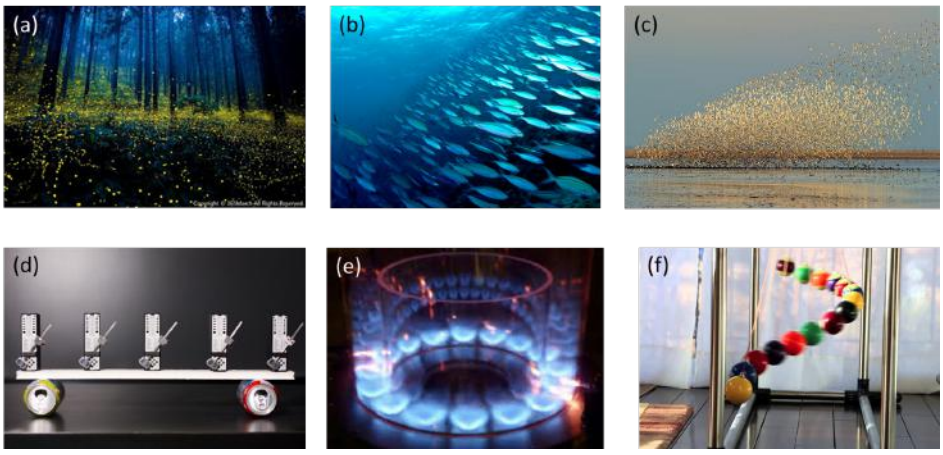

Figure 2.2: Examples of synchronization of a population of oscillators forming mind-blowing ordered patterns including (a) swarms of fireflies (exhibiting synchronized lighting), (b) school of fishes (swimming in harmony), and (c) flocks of birds, along with the synchronization of minimal oscillators of (d) coupled metronomes, (e) annular burners, and (f) coupled pendulums. Public Source: http://clarke.dickinson.edu/steven-strogatz/

present in the system must exhibit self-sustained oscillations and two covers the existence of coupling between these oscillators. Various studies that followed the discovery by Huygens discuss the variation of the strength of coupling between the oscillators on the synchronization behaviour of the system. Subsequently, both experimental and theoretical studies (Kuramoto and Battogtokh, 2002; Koseska *et al.*, 2013; Wickramasinghe and Kiss, 2013) have shown the existence of various types of coupled behaviour apart from synchronization. Such coupled behaviour include weak chimeras (Ashwin and Burylko, 2015; Wojewoda *et al.*, 2016), chimeras (Hart *et al.*, 2016; Kemeth *et al.*, 2018) and oscillation quenching (Koseska *et al.*, 2013) in populations of oscillators. A detailed description of each of the dynamical state observed is provided in the subsequent sections. The characterization of each of the dynamical state is performed by using various tools from synchronization theory.

2.1 Tools to Detect Synchronization of Oscillators

To characterize the dynamical behaviour of a system of coupled oscillators, tools from synchronization theory are used to analyze the time series obtained ($I(t)$) from each oscillator. The time series of an oscillator gives the instantaneous value of amplitude of the oscillator. Various characteristics of the oscillation such as the root mean square amplitude (I_{rms}) of the oscillation, maximum and minimum value of the oscillation,

and the frequency of oscillations (calculated using FFT) can be easily calculated.

A visual inspection of these quantitative measure gives a fairly clear picture of the dynamics of the oscillators, in terms of their correlations and other interactions. Frequency synchronized and desynchronized oscillators can be identified by calculating the values of their dominant frequencies of oscillations. Oscillators having identical dominant frequencies are identified as frequency synchronized, while those having different frequencies are referred as desynchronized.

2.1.1 Instantaneous Phase Calculation

To shed light to other characteristics of the signal in coupled oscillators, we investigate the behaviour of instantaneous phase values of each oscillator. The mutual synchronization features of two oscillators due to change in the control parameter are characterized by calculating the instantaneous phase difference between their signals. To calculate the instantaneous phase of a signal, we use the analytic signal approach based on Hilbert transform. Hilbert transform derives an analytic representation of a time series signal, that is, the real signal is extended into the complex plane. The analytical signal ($\zeta(t)$) thus obtained will have the original signal ($I(t)$) as its real part and its corresponding Hilbert transform ($I_H(t)$) as its imaginary part (that is, $\zeta(t) = I(t) + iI_H(t)$). Here, $I_H(t)$ is given by

$$I_H(t) = \frac{1}{\pi} P.V. \int_{-\infty}^{\infty} [(I(\tau))/(t-\tau)d\tau] \tag{2.1}$$

where $P.V.$ is the Cauchy principle value.

Therefore, the analytical signal can be written in the form $\zeta(t) = A(t)e^{i\phi(t)}$, where $A(t)$ corresponds to the instantaneous amplitude and $\phi(t)$ corresponds to the instantaneous phase of the signal.

The relative phase ($\Delta\phi_{1,2}$) between two signals is calculated from the difference in the instantaneous phases of these signals with time as follows (Pikovsky *et al.*, 2003),

$$\Delta\phi_{1,2}(t) = \phi_2(t) - \phi_1(t) \tag{2.2}$$

and the condition for phase locking between the two signals is given by,

$$|\Delta\phi_{1,2}(t)| \leq constant \tag{2.3}$$

The synchronization in oscillations restricts the variation in the relative phase to remain bounded, thence exhibiting fluctuations around a constant value of the phase difference. When the oscillators reach a state of desynchronization, the phase difference between them no longer remains bounded, a situation known as phase drifting (Pikovsky *et al.*, 2003).

The mean value of the absolute phase angle between the signals of coupled oscillators can be calculated as,

$$(|\Delta\phi|) = \frac{1}{N}\Sigma_{j=1}^{N}|\Delta\phi_j| \tag{2.4}$$

where N is the number of data points in the signal.

2.1.2 Pearson's Correlation Coefficient

In order to calculate the amplitude correlation between the signals of coupled oscillators, we use a measure of Pearson's correlation coefficient (ρ). This measure quantifies the linear correlation between two signals (I_1 and I_2) of coupled oscillators. Its value lies in between +1 and -1, and has a direct correlation with the slope of the amplitude correlation plot (a plot between I_1 and I_2). The value of the correlation coefficient is given by,

$$\rho = \frac{N(\Sigma I_1 I_2) - (\Sigma I_1 \Sigma I_2)}{\sqrt{(N\Sigma I_1^2 - (\Sigma I_1)^2)(N\Sigma I_2^2 - (\Sigma I_2)^2)}} \tag{2.5}$$

where all summations are from $n = 1$ to N.

2.2 Coupled Behaviour of Oscillators

The tools from synchronization theory are used to characterize the various dynamical behaviour exhibited by the mutual interaction between oscillators. Coupled oscillators tend to exhibit a plethora of dynamical behaviour depending on various parameters such as inherent characteristics of the oscillators, delay in the coupling between oscillators,

and coupling structure present in the network. The following are a list of each of these thought-provoking phenomena exhibited by coupled oscillators.

2.2.1 In-phase and Anti-phase Synchronization

Mutual coupling between two oscillators plays a vital role in the global dynamics exhibited by the system. The occurrence of such coupled dynamics further depends on the type and the intensity of coupling. Weak coupling locks only phases of the signals and gives rise to states such as in-phase synchronization and anti-phase synchronization. Due to the presence of coupling between the oscillators, both the oscillators are locked to oscillate at identical frequencies. However, during in-phase synchronization, the oscillators are locked with a constant phase shift of 0 degrees and the oscillators tend to reach their respective minima and maxima, simultaneously. On the other hand, during anti-phase synchronization, the phase difference between the two oscillators is 180 degrees. This results in an oscillator reaching its maxima while the other reaches its minima and vice versa.

2.2.2 Amplitude Death and Partial Amplitude Death

Strong mutual coupling affects both the phase and the amplitude of coupled oscillations, causing the reduction or complete cessation of oscillations in all the oscillators. Such a dynamical behaviour wherein all the oscillators approach a common steady state due to coupling is referred to as amplitude death and was discovered by Strutt and Rayleigh in a system of two organ pipes. The phenomenon of amplitude death finds a lot of research attention due to its applicability in many systems. Amplitude death is highly desirable in many systems where the presence of oscillations tends to be detrimental to the system. This includes thermoacoustic systems (Dange *et al.*, 2019*a*), ecological systems (Yoshida *et al.*, 2003), disease-spread systems (Duncan *et al.*, 1997) etc. On the contrary, oscillation quenching is considered hazardous in systems such as neuronal networks causing diseases such as Alzheimer's and Parkinson's Disease (Mizuno *et al.*, 1989).

Another phenomenon of quenching where the oscillators, does not reach a homogeneous steady state rather separate into a different stable state having a non zero am-

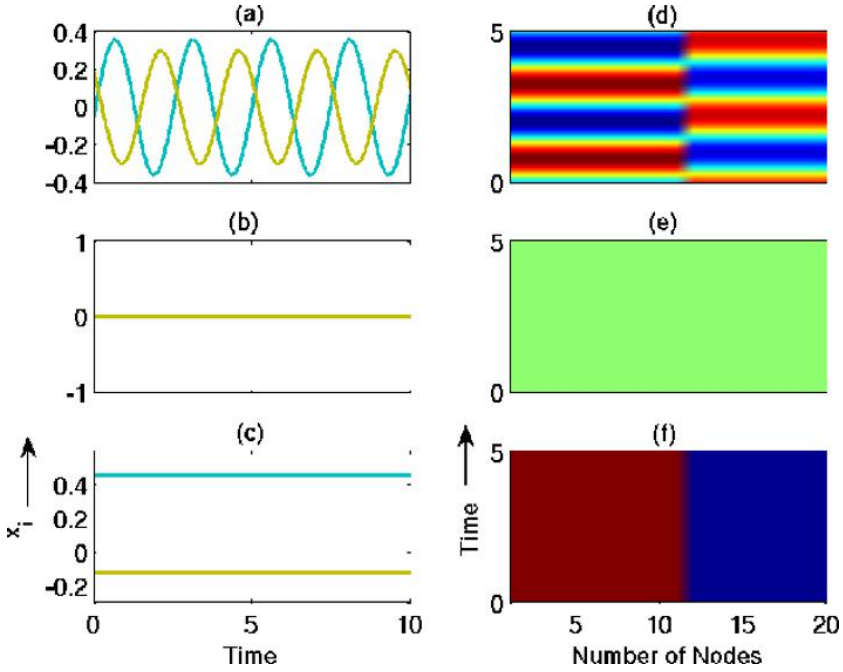

Figure 2.3: Time series of (a) - (c) two oscillators and (d) - (f) twenty oscillators exhibiting the states of synchronization, amplitude death, and oscillation death, respectively. In (a), the oscillators are locked with the phase shift of 180 degrees and are exhibiting anti-phase synchronization. However, in the case of (d), where we have twenty nodes of oscillators, we observe that nearly half the population is exhibiting in-phase synchronization and are anti-phase synchronized with the other half of the population, who among themselves are in-phase synchronized. Such behaviour is referred to as clustering. In (b),(e), we observe the nonlinear phenomenon of amplitude death, where all the oscillators reach a homogeneous steady state. In (c),(f), we observe the phenomenon of oscillation death where the oscillators reach in-homogeneous steady states having non zero amplitudes. The figure is adapted from Nandan *et al.* (2014).

plitude is referred to as oscillation death (Premalatha *et al.*, 2018). In some situations, mutual coupling does not necessarily lead to quenching of oscillations in all the coupled oscillators; it may result in a coexistence of oscillatory and steady states, which is referred to as partial amplitude death (Atay, 2003). The only experimental evidence of the state was found in a system consisting of two prototypical thermoacoustic oscillators called as the horizontal Rijke tube (Dange *et al.*, 2019*a*).

2.2.3 Desynchronization

When the mutual interaction between oscillators is very weak, the oscillators tend to oscillate independent of the presence of the second oscillator. The oscillators have different frequencies, and the phase difference monotonically decrease or increase, and such behaviour in the phase shift between the oscillators is referred to as phase drifting.

2.2.4 Phase-flip Bifurcation

The abrupt jump observed in the frequency of oscillation or the mean phase difference between the oscillators when the system flips from in-phase synchronization to anti-phase synchronization or vice versa, as the parameter is varied. In the system of coupled oscillators as the delay in coupling is increased, for higher coupling strength, we observe the direct transition from in-phase to anti-phase synchronization. The oscillators have a lower value of dominant frequency during in-phase synchronization, which jumps to a higher value during anti-phase synchronization. Along with this jump in the frequency of an oscillator, we also observe a corresponding rise in the mean phase difference value, which abruptly shifts from 0 degrees to 180 degrees as the system transitions to anti-phase synchronization from in-phase synchronization.

2.2.5 Clustering

Due to the presence of a varied coupling structure, the population of oscillators separates into different synchronized groups, depending upon the instantaneous properties (amplitude or phase) of their signals. Such a state of coupled dynamics is referred to as clustering (Wickramasinghe and Kiss, 2013; Premalatha *et al.*, 2018). Here, the

oscillators belonging to the same cluster exhibit equal instantaneous phases which are different from the other clusters, while all the oscillators in the population oscillate with identical frequencies. From Fig. 2.4, we observe that oscillators {1,3} form one cluster and oscillators {2,4} form another cluster.

Recent studies describe the phenomena of slow breathing and fast breathing clusters, where the oscillator dynamics intermittently switches between the states of desynchrony and clustering. For the state of slow breathing clusters, the oscillators exhibit clustering and desynchronized states for a longer duration when compared to the state of fast breathing clusters. A novel type of clustering dynamics observed in a network of three mutually coupled oscillators is called rotating clusters (Okamoto *et al.*, 2016), where we observe the temporal switching from one type of cluster to another type of cluster. To elaborate, the system exhibiting a particular form of clustering transitions into another form of clustering in time. Both the forms of clustering observed in a rotating clustered state need not have identical frequencies.

2.2.6 Weak Chimera

Ashwin and Burylko (2015) recently discovered the state of weak chimera, a symmetry-breaking phenomena found in minimal (3 to 6 oscillators) network of coupled phase oscillators. Weak chimera is defined as the state where two or more frequency-synchronized oscillators coexist with one or more oscillators having different frequencies with respect to the synchronized group. The pioneering experimental evidence of weak chimera state was reported by Wojewoda *et al.* (2016) in a system of three coupled pendula, followed by experimental and theoretical studies on pendulum-like nodes (Maistrenko *et al.*, 2017), electrochemical oscillators (Bick *et al.*, 2017), and Stuart-Landau oscillators (Kemeth *et al.*, 2018).

Various types of weak chimera is observed in oscillators. A recent theoretical study by Maistrenko *et al.* (2017) reported the existence of various types of weak chimera, including in-phase and anti-phase chimera. During in-phase chimera, the system divides into two pairs of in-phase synchronized oscillators, while retaining desynchrony between the pairs. The state of anti-phase weak chimera, which displays similarity to the state of in-phase weak chimera, with the only difference being the synchroniza-

tion mode exhibited by the pair of oscillators is an anti-phase mode of synchronization. Another similar case would be the clustered weak chimera where a single clustered synchronized group of oscillators coexist with a multi-clustered synchronized group of oscillators while retaining desynchrony between the groups.

2.2.7 Chimera

Chimera is one of the theoretically (Kuramoto and Battogtokh, 2002; Abrams and Strogatz, 2004; Martens *et al.*, 2013; Abrams *et al.*, 2008; Sheeba *et al.*, 2009; Omel'chenko *et al.*, 2010; Shanahan, 2010; Schmidt, 2015; Larger *et al.*, 2013) and experimentally (Tinsley *et al.*, 2012; Hagerstrom *et al.*, 2012; Martens *et al.*, 2013; Kapitaniak *et al.*, 2014; Wickramasinghe and Kiss, 2013; Nkomo *et al.*, 2013; Gambuzza *et al.*, 2014; Hart *et al.*, 2016; Mondal *et al.*, 2017) well-studied cases of weak chimera. Discovered by Kuramoto and Battogtokh (2002) in complex Ginzburg-Landau oscillators and named by Abrams and Strogatz (2004), chimera is a symmetry-breaking phenomenon where oscillators having identical individual properties and coupling structure separate into phase-locked (synchronized) and phase-drifting (desynchronized) group of oscillators. Within the last decade, different types of chimera came into the light such as clustered chimera (Sethia *et al.*, 2008; Sheeba *et al.*, 2009; Martens *et al.*, 2013; Nkomo *et al.*, 2013; Sethia *et al.*, 2013), breathing chimera (Abrams *et al.*, 2008; Sheeba *et al.*, 2009), symmetric and asymmetric chimera (Omel'chenko *et al.*, 2010), metastable chimera (Shanahan, 2010), type-I chimera and type-II chimera (Schmidt, 2015), and virtual chimeras (Larger *et al.*, 2013), characterized on the basis of instantaneous phase and amplitude relations between oscillators.

Apart from the theoretical studies discussed so far, experimental investigations of chimera have also been reported in literature. The pioneering experimental studies showing the existence of chimera in a natural system used coupled chemical oscillators (Tinsley *et al.*, 2012) and coupled map lattices (Hagerstrom *et al.*, 2012). Further experimental studies observed the existence of chimera in mechanical oscillators, such as coupled pendula (Kapitaniak *et al.*, 2014), metronomes (Martens *et al.*, 2013), electrochemical oscillators (Nkomo *et al.*, 2013; Wickramasinghe and Kiss, 2013), electronic oscillators (Gambuzza *et al.*, 2014), optical oscillators (Hart *et al.*, 2016), and in thermoacoustic systems (Mondal *et al.*, 2017). Chimera states have also been predicted

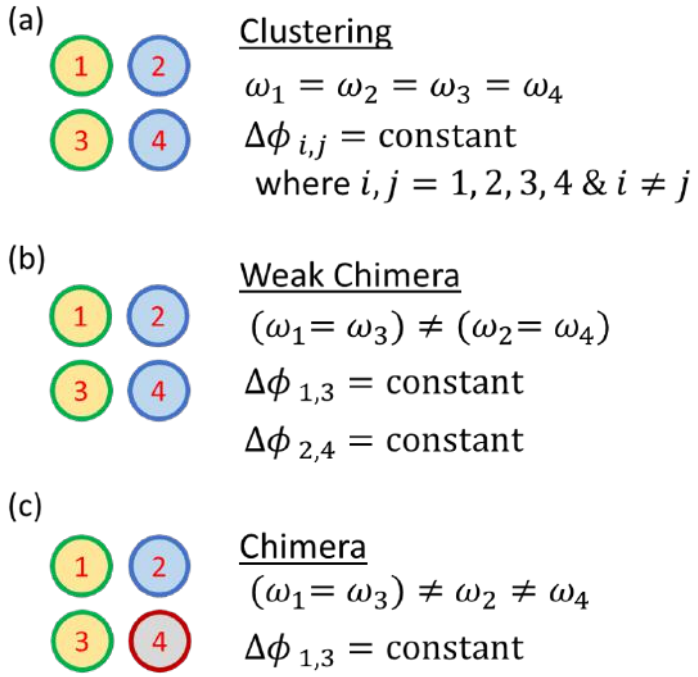

Figure 2.4: Schematic diagrams involving four oscillators exhibiting the dynamical states of (a) clustering, (b) weak chimera, and (c) bare minimum chimera. During clustering, all oscillators have identical frequencies (ω), and the phase difference between the oscillators remain constant. The formation of separate frequency synchronized groups (oscillators pair {1,3} having the equal frequencies, which are different from that of {2,4} is referred to as weak chimera. During chimera, we observe the existence of a single frequency synchronized group {1,3} coexisting with oscillators having different frequencies.

for different global (Kaneko, 1990), weak non-local (Kuramoto and Battogtokh, 2002) and local couplings (Clerc *et al.*, 2016). The pioneering study by Hart *et al.* (2016) experimentally witnessed the existence of chimera in system of four globally coupled chaotic optoelectronic oscillators which is the minimal network of oscillators required to support the state.

Having discussed the various types of intriguing coupled dynamics exhibited by coupled oscillators, we move to understand the effect of topology and other parameters on the stability of the aforementioned states in a network of coupled oscillators.

2.3 Minimal Network of Oscillators

A change in the topology of oscillators in a network changes the coupling arrangement of these oscillators. For example, in a line or a ring network, the oscillators are locally coupled to their nearest neighbours; whereas, in a star network, only the central oscillator is coupled to all peripheral oscillators. Wickramasinghe and Kiss (2013) studied the effect of network structure on the selection of self-organized patterns in coupled chemical oscillators. When six oscillators are coupled in an extended triangular network, they observed the presence of the partially synchronized state, where the strongly coupled oscillators in the core of the triangle synchronize easily when compared to the weakly coupled peripheral oscillators. Non-local coupling of 20 oscillators in a ring showed the possibility of chimera state for a transient duration on nearly 100 cycles.

Further, they also observed that globally coupled relaxation chemical oscillators tend to form a clustered state. Their investigation on the effect of coupling topology on the synchronization characteristics of chaotic oscillators showed that the oscillators coupled in a closed-loop topology (e.g., square, triangle, or ring) synchronized faster than those coupled in an open-loop topology (e.g., linear or star). Although their study talks about the effect of topology on global synchrony of chaotic oscillators, the details of individual dynamical states observed due to a change in coupling strength in each topological arrangement and effect of change in topology on the dynamical states of coupled limit cycle oscillators is yet to be discussed.

A theoretical study on Kuromoto oscillators by Ashwin and Burylko (2015) also examined the various coupling structure associated with minimal oscillators consisting of

4, 6, and 10 oscillators. They considered various coupling configurations (bi-directional coupling with different strengths) on a closed-loop topology and discovered the state of weak chimera in the network. The stability and the variations in weak chimera exhibited for the different coupling configurations are discussed. Although they investigated the state of weak chimera for varied coupling configurations, the exhibition of other dynamical states is not discussed in the study. A study conducted by Hart *et al.* (2016) reported the presence of various dynamical states, including bare minimum chimera, global synchrony, and clusters in four optoelectronic oscillators. The coupling structure between the oscillators is varied by changing the values of coupling parameters, which are global coupling strength and coupling delay. The stability of the chimera state and its relation to the phenomenon of clustering is also discussed. Although these previous studies separately provide insights on the role of coupling structure and number of oscillators on the dynamics exhibited by the oscillators in a network, the current study has comprehensively delineated the explicit dependence of the global behaviour of the system on the change in the number of oscillators, the coupling topology, and the strength of coupling between the oscillators in a network.

CHAPTER 3

Experimental Setup

Candle-flame oscillators are one among the simplest and economical oscillators which exhibit various complex dynamical behaviours including synchronization (Kitahata *et al.*, 2009), amplitude death (Okamoto *et al.*, 2016), phase-flip bifurcation and, clustering, chimeras and weak chimeras.

3.1 Construction of a Candle-flame Oscillator

To understand, the coupled dynamics of coupled candle-flame oscillators, the primary concern would be the construction of a candle-flame oscillator. From observations from our day-to-day life, we observe that a single candle does not exhibit any sort of oscillations except the transient flickering in the flame. In order to construct a candle-flame oscillator which exhibits self-sustained limit cycle oscillations, there are two different approaches: one is to bundles candles to form a single flame or manufacture a candle with four wicks. Both these techniques are elaborated in the following sections.

The candles used in the present experimental study were of cylindrical shape, made up of paraffin wax having a length of 15 cm and a diameter of 0.8 cm. A group of three or more such candles ($N_C \geq 3$) were placed together in order to produce stronger self-sustained oscillations. These candles were tied to keep them intact and burnt after keeping their wicks close enough such that they burn to form a single flame that exhibits limit cycle oscillations. This set of candles is then referred to as a single candle-flame oscillator. The average frequency of natural oscillations of a single isolated candle-flame oscillator, each consisting of four candles, obtained from ten independent trial experiments is measured to be 11.6 Hz with a standard deviation of $\pm$ 0.3 Hz. The resolution of frequency in the amplitude spectrum of the signals is approximately equal to 0.1 Hz.

In all the previous studies on candle-flame oscillators (Kitahata *et al.*, 2009; Okamoto *et al.*, 2016; Dange *et al.*, 2019*a*; Nagamine *et al.*, 2017), the candle-flame oscillators

used are made by bundling three or more candles together and lighting them to form a compound flame, exhibiting limit cycle oscillations. However, experiments with such candle-flame oscillators are susceptible to errors due to various inherent disturbances, such as uneven evaporation and burning of candles in an oscillator, leading to an uneven reduction in their heights and maintenance of vertical orientation of the wick are a few such issues. Therefore, the manufacturing of a candle consisting of four wicks deems to make the experiments easier and less cumbersome, by enhancing the repeatability with an evenly burning oscillator having stronger oscillations sustaining for a longer duration. In experiments, we make a candle-flame oscillator of length 12 cm and a diameter of 2 cm with four wicks placed in a square arrangement being 1 cm apart, as shown in Fig. 3.1(a). The candle-flame oscillator created using a single candle with four wicks exhibits limit cycle oscillations with nearly the same amplitude and frequency as the earlier used candle-flame oscillator made up of multiple candles.

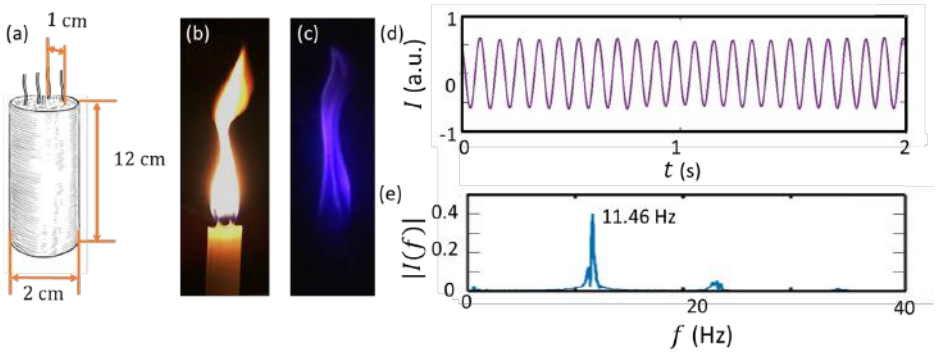

Figure 3.1: (a) Schematic of the candle-flame oscillator. (b) A normal image of the flame luminosity and (c) a filtered CH* chemiluminescence image of the flame of a candle-flame oscillator. (d) The time series of the flame intensity (I), presenting the self-sustained limit cycle oscillations shown by an isolated candle-flame oscillator. (e) The amplitude spectrum corresponding to these oscillations shows a dominant frequency of 11.46 Hz.

3.2 Data Acquisition and Post-processing

The instantaneous image of the normal flame luminosity and CH* chemiluminescence field of the candle-flame oscillator are shown in Figs. 3.1(b, c), respectively. The dynamics produced by the candle-flame oscillators are captured using a high-speed imaging technology of iPhone7S (frame rate of 240 Hz) fitted with a CH* chemiluminescence filter (wavelength of 435 nm and 10 nm full width at half maximum) for 60 s.

The data are acquired at 239 frames per second for 60 s for each configuration to have a broader view of the system dynamics. A waiting time of 60 s is enforced after each change in the configuration, to remove the transient effects and let the oscillators reach a steady state.

The presence of the CH* filter facilitates the removal of noisy fluctuations associated with the black body emission of the soot in the flame (see Fig. 3.1b) and provides information about the actual heat release rate fluctuations (indicated as blue colour in Fig. 3.1c) present in the flame (Hardalupas and Orain, 2004) of a candle-flame oscillator. The analysis of the data set acquired at every configuration is performed after cropping the portion of each frame in such a way that no two flames of the oscillators appear in a single cropped frame. The instantaneous value of the heat release rate fluctuations is obtained by summing up the local brightness values of the flame in a given frame (as shown in Fig. 3.1c) and a time series of such fluctuations is obtained by performing the same operation for the entire video. The limit cycle oscillations exhibited in the heat release rate by an isolated oscillator are presented in Fig. 3.1(d) and the amplitude spectrum of these oscillations are shown in Fig. 3.1(e). We observe the natural frequency of an isolated oscillator as 11.46 $\pm$ 0.2 Hz. The frequency resolution in the amplitude spectrum of the signal is approximately 0.017 Hz, calculated as the ratio of sampling frequency to the total number of samples (Frequency resolution $= \frac{F_s}{N_s} = \frac{240}{14400}\ 0.017$).

3.3 A Network of Two Oscillators

In order to study the coupled interaction between a pair of such candle flame oscillators, high-speed imaging of the reaction zone was captured. By moving the candle-flame oscillator placed on a movable platform against the stationary one, we vary the edge to edge distance (D) between them (Fig. 3.2a) which leads to a corresponding change in d ($D = d + 0.02$ cm). Here, d is varied from 0 cm to 2 cm in steps of 0.2 cm, and 2 cm to 8 cm in steps of 0.5 cm. The characteristic distance (d) at which various synchronization modes are observed may vary with $\pm$ 0.2 cm with experiments. An acrylic plate with hexagonal packing of drilled holes of 0.4 cm radius is fixed on each platform to ensure that the oscillators are held firmly in place. The traverse system,

used to vary d by moving the platform, has a least count of 0.05 cm. The entire system is mounted on a raised platform (height 50 cm) to avoid ground effects on the dynamics of the candle-flame oscillations. All experiments were performed in a closed quiescent room with a completely dark environment.

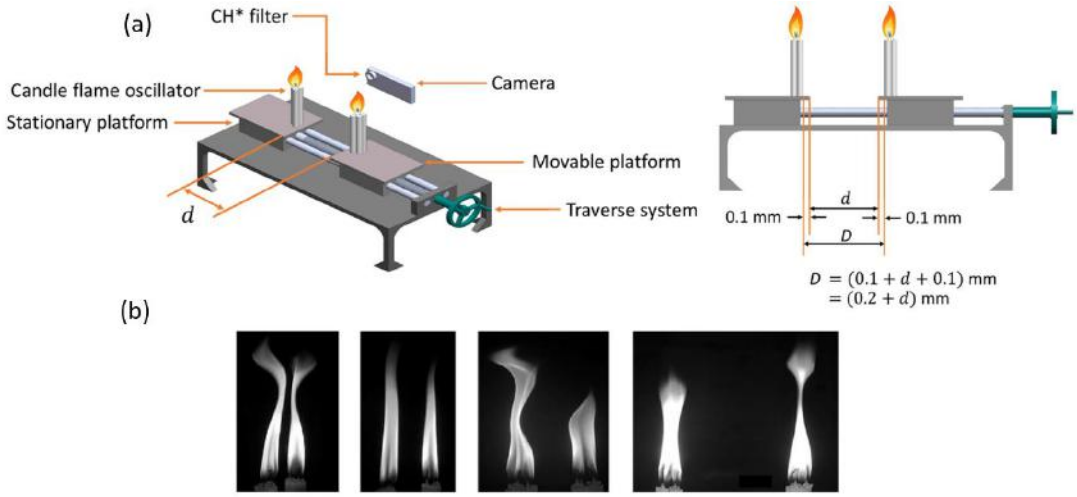

Figure 3.2: (a) Schematic of the experimental setup (isometric and side view) used for studying the coupled behaviour of a pair of candle-flame oscillators by varying the distance between them. One oscillator is mounted on a stationary platform and the other on a movable platform. The latter is moved with the help of a traverse system, thereby varying the distance (d) between them, which in turn, varies the edge to edge distance between the oscillators (D). High-speed images of heat release rate fluctuations, at each value of d, were acquired using a camera with a CH* chemiluminescence filter mounted in front of it. Similar experiments were conducted by varying the number of candles in each oscillator from 3 to 8. (b) Snapshots of the flame images as captured at characteristic distances between the oscillators highlighting the oscillatory states of IP ($d = 0$ cm), AD ($d = 1$ cm), AP ($d = 2$ cm) and desynchronization ($d = 7$ cm), respectively.

The later part of our study uses coupled similar pair of oscillators with N_C varying from 3 to 8 (refer Fig. 4.5), whose isolated oscillator characteristics are shown in Fig. 4.4. We consider the number of candles per oscillator (of the identical oscillator-pair) as another control parameter (N_C) and repeat the same experiment for six different values for the parameter (N_C = 3, 4, 5, 6, 7, 8). The second scenario of our study explores the dynamics of a coupled dissimilar pair of oscillators, and its results are discussed in Chapter 4.

3.4 A Network of Four Oscillators

The setup to study the coupled dynamics of four candle-flame oscillators consists of two platforms, one stationary and the other movable, each consisting of two candle-flame oscillators [Figs. 3.3(a,b)]. The distances between the centres of the oscillators, d_x and d_y, are varied as control parameters from 2 to 7 cm in steps of 0.5 cm. All experiments are conducted in a dark room with a quiescent environment.

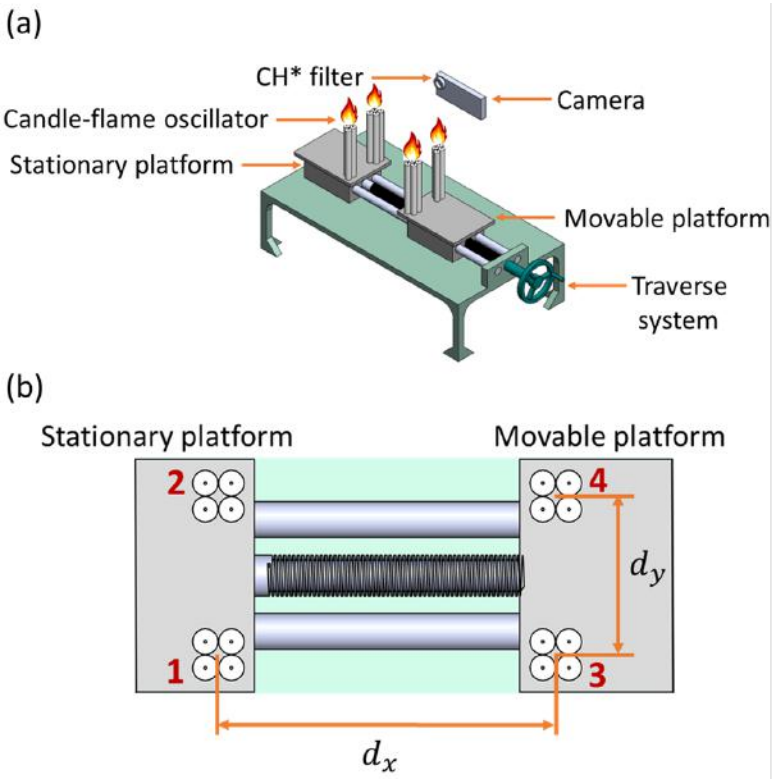

Figure 3.3: (a) Isometric view and (b) top view of the experimental setup of four candle-flame oscillators. (c) A schematic representation of the topology of the Stuart-Landau oscillators, highlighting the organization of time delays (τ_x, τ_y and τ_d) and coupling strength (K_i) between the oscillators.

As the distances between the oscillators are varied, they exhibit different dynamical states. These dynamics are captured using the high-speed imaging feature of iPhone 5S outfitted with a CH* chemiluminescence filter (wavelength centred at 435 nm with a bandwidth of 10 nm). With the employment of the filter, the luminous intensity of the flame would correspond to the local heat release rate of the flame in each frame (Hardalupas and Orain, 2004). Images for each combination of d_x and d_y are captured at a frame rate of 119 fps for 10 s. The global heat release rate value for each candle-flame oscillator at a given instant (or frame) is obtained after isolating the oscillator and summing up the luminous intensity values (local heat release rate) of the oscillator. The

global heat release rate values are then normalized with their respective instantaneous amplitudes obtained from the Hilbert transform of the signal (Pikovsky *et al.*, 2003). Thus, four different time series, corresponding to each oscillator, are obtained for each combination of distances.

3.5 Investigating the Dependence on Configuration

In order to study the effect of the number of oscillators in a network and the change in the topology of coupling between the oscillators, we couple two to four such candle-flame oscillators and measure their dynamical response for every coupling configuration. The number of ways in which oscillators can be arranged in a network topology depends on the number of oscillators interacting in the system (see Fig. 3.4). An acrylic platform with markings for each of the topological arrangement is used to mount these oscillators during experiments. The platform is placed on a table of the height of 80 cm from the ground to avoid ground effects on the dynamics of the coupled oscillators. All experiments are performed in a completely dark closed room with quiescent ambient conditions. Around 20 experiments are performed for each topological arrangement, and the percentage occurrence of each dynamical state is calculated, taking into account all these experimental trials.

We note that the interaction of oscillators is primarily influenced by their nearest neighbours. Therefore, we indicate the neighbours of an oscillator by the concept of degree of an oscillator (Barabási *et al.*, 2016). Here, the degree of the oscillator is a quantifier of the number of nearest neighbours surrounding each oscillator. In the case of two oscillators as shown in Fig. 3.4(a), the only possible combination involves the mutual interaction between both the oscillators, assigning a degree of 1 for both the oscillators. When the number of oscillators in the system is increased to three as presented in Fig. 3.4(b), two topological arrangements are possible in the system. The straight (linear) topology of the network (see Fig. 3.4b-i) where the degree of the central oscillator is 2, as it is in a direct influence with the other oscillators placed at equidistance from it, and the edge ones have a degree of 1. In a triangular topology of the network, each oscillator interacts with every other oscillator with equal strength and, therefore, the degree of each oscillator remains 2 (see Fig. 3.4b-ii). For the case

where the number of oscillators is increased to 4, the number of network topologies possible also increases. Three such topologies are investigated in this study, namely straight (Fig. 3.4c-i), star (Fig. 3.4c-ii), and square (Fig. 3.4c-iii), where the degree of each oscillator is also indicated.

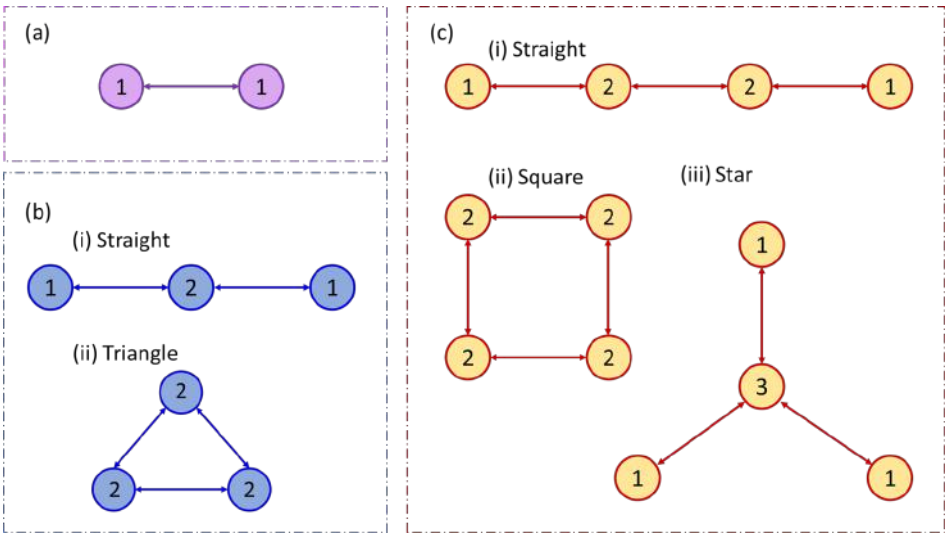

Figure 3.4: Various topological arrangements possible with the number of candle-flame oscillators (indicated as nodes in a network) increased as (a) two, (b) three, and (c) four in a network. The degree of each node corresponds to the number of its nearest neighbours, which is marked on each oscillator. The arrows indicate the presence of bidirectional coupling between the nearest oscillators and the distance between the oscillators connected by the arrows, referred to as link distances (d), are kept constant in a network.

The second parameter which would dictate the global dynamical behaviour of a network of oscillators is the distance between adjacent oscillator. The distances between oscillators in a given topology, marked with the links between the oscillators, are kept equal to facilitate symmetric coupling. This distance between the oscillators which is marked by an arrow in Fig. 3.4 is referred to as link distance (d). After fixing the link distance and topological arrangement, high-speed imaging of each experiment is performed. The position of the camera is varied for each topology to obtain distinct flames for each oscillator in a single frame. Further analysis of the data obtained was carried out using various tools from time series analysis and synchronization theory (Pikovsky *et al.*, 2003).

CHAPTER 4

Coupled Dynamics of a Pair of Candle-flame Oscillators

System of coupled oscillators has become an extensive area of research due to the emergence of various intriguing nonlinear phenomena such as synchronization, AD and PFB (Winfree, 2001; Kuramoto, 2012; Strogatz, 2004; Pikovsky *et al.*, 2003). Although most of the theoretical studies indicate the individual or combined occurrence of AD and PFB (Saxena *et al.*, 2012; Karnatak *et al.*, 2010; Arumugam *et al.*, 2016; Sharma *et al.*, 2016; Karnatak *et al.*, 2007), an experimental evidence of their coexistence in a physical system has not been reported to the best of our knowledge. Here, we investigate the coexistence of AD and PFB for the first time in a physical system. To demonstrate such transitions, control parameters such as the distance between the oscillators (d) and the number of candles in each oscillator (N_C) are varied. The transition is described here, in candle-flame oscillators having two configurations: similar pair (both oscillators having the same value of N_C) and dissimilar pair (both oscillators having different values of N_C).

4.1 Coupled Behaviour of Identical Pair of Coupled Candle-flame Oscillators

To study the coupled behaviour of similar candle-flame oscillators, we couple two such oscillators, each having an N_C of 4, and vary the distance d between these oscillators. Figure 4.1 shows the dynamical states manifesting IP, AD, AP and desynchronized oscillations observed due to mutual interaction between the candle-flame oscillators over various values of d. At small values of d (0 cm to 1 cm), they exhibit IP synchronization, during which the time series of each oscillator (I_1 and I_2) fluctuates with nearly 0

The results presented in this chapter are published in K. Manoj, S. A. Pawar and R. I. Sujith, Experimental Evidence of Amplitude Death and Phase-Flip Bifurcation between In-Phase and Anti-Phase Synchronization *Scientific reports*, 8, 11626, (2018).

degrees phase difference (Fig. 4.1a). The collapse in the amplitude correlation plot (I_1 against I_2) into a line having a slope of positive unity (Fig. 4.1a) reasserts the presence of IP state. When d is increased beyond 1 cm, we notice a cessation of oscillations in both oscillators (Fig. 4.1b). We refer to this state as AD. The cluster of trajectory around the origin in the amplitude correlation plot implies the presence of AD in the signal (Fig. 4.1b).

When d is sufficiently high (2 cm to 5 cm), both oscillators regain their oscillatory behaviour. However, at these distances, both oscillators exhibit AP synchronization, wherein the time series of each oscillator shows a phase difference of nearly 180 degrees (Fig. 4.1c). Collapsing of the amplitude correlation plot into a line with a slope close to negative unity (Fig. 4.1c) reaffirms the AP synchronization of these oscillators. As d is increased further (beyond 5 cm), we observe desynchronization (DS) of coupled candle-flame oscillators. During this state, we see an increased presence of IP oscillations in between AP oscillations in an arbitrary manner (Fig. 4.1d). This increased switching between IP and AP is further reflected in the amplitude correlation plot, wherein the plot fills the entire plane (Fig. 4.1d).

Apart from these steady states observed at particular ranges of d (shown in Figs. 4.1a-d), we also see transition states (TS) at the boundaries of AD. Figures 4.1(e),(f) show the existence of such states in the transition from IP to AD, and AD to AP, respectively. The silent region represents AD, whereas the bursts show IP oscillations in Fig. 4.1(e) and AP oscillations in Fig. 4.1(f). The evidence of such transition states further reasserts that the transition from IP to AD and that from AD to AP is not sudden, but happens gradually.

Furthermore, we quantify the synchronization behaviour of candle-flame oscillators with the change in d using various quantitative measures such as dominant frequency (f) of oscillations (Fig. 4.2a) and PearsonâĂŹs correlation coefficient (ρ) between the signals (Fig. 4.2b). When two oscillators are in IP state (Fig. 4.2a), we observe that the dominant frequencies of both the oscillators are below their uncoupled frequency value. As these oscillators transition from IP to AP via AD state, we notice a sudden jump in the values of their dominant frequencies (Fig. 4.2a) to a value greater than their uncoupled frequency. A possible explanation for this variation in frequencies is the change in the interaction of vortices formed due to the instabilities of buoyancy-driven

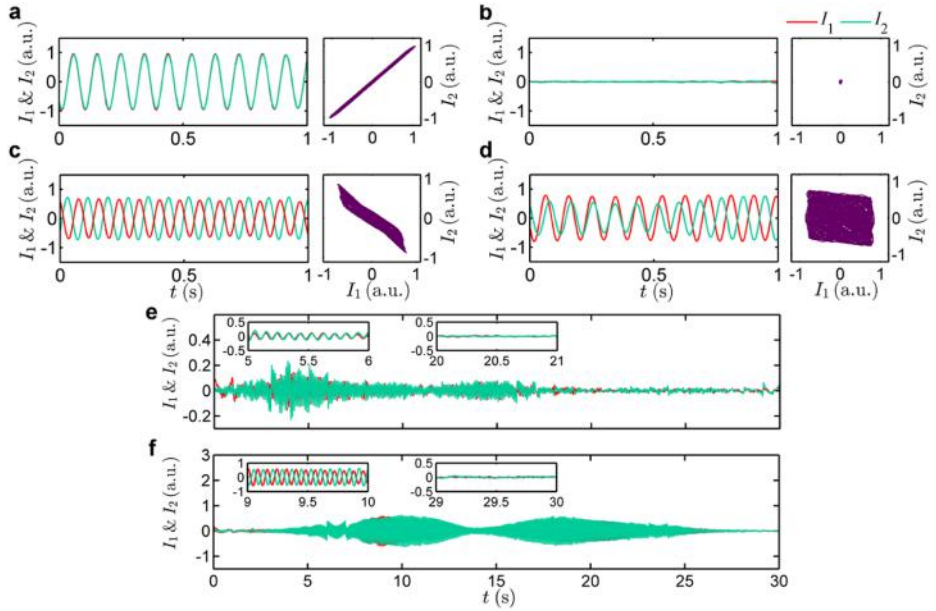

Figure 4.1: (a)-(d) Time series of heat release rate fluctuations (I_1 and I_2) obtained from individual oscillators and their corresponding amplitude correlation plot (a plot between I_1 and I_2) are shown for IP, AD, AP, and desynchronized state of oscillations, respectively. These states are observed when the value of d is 0 cm, 1 cm, 2 cm, and 7 cm, respectively. I_1 and I_2 correspond to the instantaneous values of the heat release rate fluctuations of the oscillator on the stationary platform and the movable platform, respectively. (e),(f) The transition states observed in a pair of candle-flame oscillators when the oscillators are 0.5 cm and 1.5 cm apart, respectively. In (e), the time-series oscillate alternately between IP and AD states, while in (f), the oscillations alter between AD and AP states.

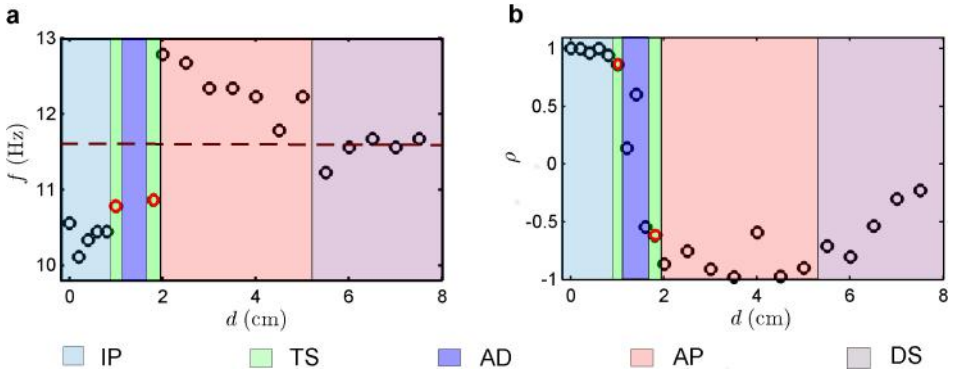

Figure 4.2: The variation of (a) dominant frequency (f) and (b) PearsonâĂŹs correlation coefficient (ρ) as a function of d for a pair of candle-flame oscillators. The horizontal dotted line in a corresponds to the dominant frequency of 11.6 Hz obtained from the individual oscillator in an uncoupled state. The red circles correspond to the transition states (TS) where the frequency peak in the amplitude spectra represents the oscillatory regions observed in the signals of these states.

flows around the oscillating flame of each candle-flame oscillator (Okamoto *et al.*, 2016; Dange *et al.*, 2019*b*). When the oscillators are nearby, the inner portions of the vortices merge with each other resulting in the inhibition of oscillations and thereby a reduction in their frequencies.

On the contrary, when the oscillators are sufficiently far apart, alternate formation of such vortices enhances the oscillation in each oscillator leading to an increase in their natural oscillation frequency. During the state of AD (Fig. 4.2a), we do not observe any dominant peak in the amplitude spectra of both the oscillators, due to the complete disappearance of vortex formation in both the oscillators. However, we see the presence of oscillations during the transition states, which correspond to the two points in the TS zone of Fig. 4.2(a), observed at the boundaries of AD. As d is further increased, we observe a decrease in the frequencies of both the oscillators due to a reduction in the interaction between them, finally reaching the value of frequency of an isolated oscillator in the DS region (Fig. 4.2a).

This synchronization behaviour is also reflected in the plot of the PearsonâĂŹs correlation coefficient (ρ) (Fig. 4.2b). If the two oscillators are in the IP state, the slope in the amplitude correlation plot tends to positive unity (Fig. 4.1a), so does the value of ρ (Fig. 4.2b). Conversely, for the AP state, we see a slope which tends to negative unity (Fig. 4.1c) and the value of ρ falls near minus one (Fig. 4.2b). When the oscillators are in the desynchronized state (Fig. 4.1d), the value of ρ approaches zero (Fig. 4.2b).

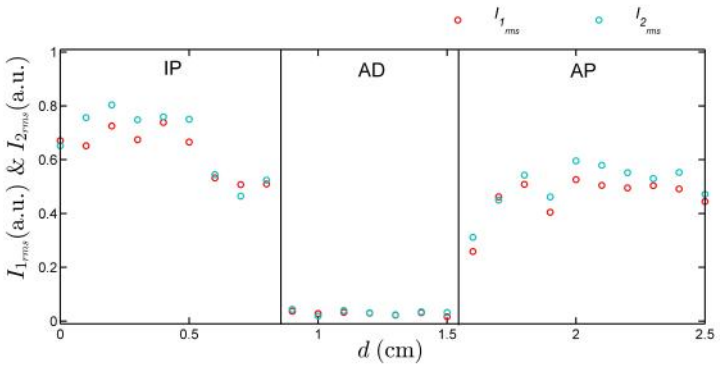

Figure 4.3: Variation in the root mean square value of the signals obtained from a system of coupled candle-flame oscillators with distance (d) between them. The lines provided show the approximate boundaries of each dynamical state of in-phase synchronization (IP), amplitude death (AD) and anti-phase synchronization (AP)

Figure 4.3 highlights the variation of the root mean square value of the signals

($I_(1, rms)$ and $I_(2, rms)$) as the distance between a pair of coupled candle-flame oscillators (d) is changed, wherein each oscillator consists of four candles ($N_c = 4$). The plot is divided into three different regions of coupled dynamics depending on the characteristics of the signals observed during these states. Starting from the in-phase (IP) mode of oscillation, the root mean square value of each oscillator decreases gradually and eventually reaches a value near zero during the amplitude death (AD) state. When the oscillators regain oscillations in the state of anti-phase (AP) oscillation, after AD, the root mean square value of oscillations begins to increase and reach a nearly constant value. This behaviour of the variation in amplitudes of signals acquired from coupled-candle flame oscillators with distance (d) between them is similar when N_c equals 3 and 5.

To conclude, IP oscillations can be characterized by the drop in the frequency value as well as ρ tending to positive unity. In contrast, AP oscillations are characterized by an increase in the frequency value when compared to the uncoupled oscillator as well as ρ tending to negative unity. The transition from IP to AP in the frequency plot in Fig 4.2(a) is interposed by the region of AD state. As the oscillators move to desynchrony, the frequency fluctuates around the frequency of uncoupled oscillators along with ρ moving towards 0, highlighting the reduction in interaction between the oscillators. We also observe a gradual decrease in the amplitude of oscillation as we approach the state of AD from either side, i.e., as the distance is increased (IP to AD) or decreased (AP to AD).

Finally, we investigate the effect of variation in the number of candles (N_C) in candle-flame oscillators. Increase in N_C, from 3 to 8, in an isolated oscillator leads to an increase in the amplitude and a small change in the frequency of oscillations, see Fig. 4.4. The dominant frequency of oscillations exhibited by such oscillators, obtained from their amplitude spectra, always lies in between 10 Hz to 12 Hz for different values of N_C (see Fig. 4.4a). This observation of frequency is in accordance with an important characteristic found in most of the buoyant diffusion flames, that the universal value of the flickering frequency lies in a range of 10-20 Hz, irrespective of the type of system considered (Buckmaster and Peters, 1988). The error bar indicates the ensemble average of frequencies and the root mean square value of the oscillations performed over ten experiments. We also observe a slight decrease in the value of the mean of the dominant frequency of an oscillator as N_C is increased (in Fig. 4.4a). The variation of root mean

square value for each candle-flame oscillator exhibits an increasing trend as the number of candles (N_C) in an oscillator is increased (in Fig. 4.4b). As N_C is increased, the rate of fuel supplied to the flame of an oscillator increases. Hence, the oxygen required for complete combustion of the fuel increases. This leads to an increased surface area and volume of the flame, which are essential to satisfy this increased oxygen requirement.

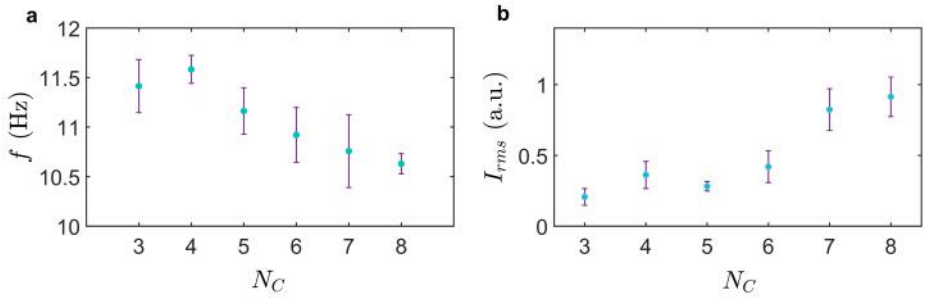

Figure 4.4: Characteristic properties of limit cycle oscillations produced by an isolated candle-flame oscillator with varying number of candles (N_C) in an oscillator. Variation of (a) dominant frequency (f) and (b) root mean square value (I_rms) of self-sustained limit cycle oscillations produced by an isolated candle-flame oscillator when the number of candles (N_C) in the oscillator is changed.

Figure 4.5 demonstrates the effect of variation in the number of candles (N_C) in the coupled dynamics of a pair of candle-flame oscillators. From Fig. 4.5a, we observe that the regions of AD (including both AD and transition states) are observed to decrease with increasing N_C. At lower N_C (e.g. 3, 4 and 5), AD is observed over a considerable interval of d, whereas at higher N_C (e.g. 6 and 7), the likeliness of observing perfect AD becomes zero and only regions of transition states are observed. As N_C is further increased to 8, we observe the phenomenon of phase-flip bifurcation (PFB), where the oscillators exhibit a sudden transition from a state of IP to AP oscillations, bypassing the intermediary AD state. During this transition, we observe a sudden jump in the relative phase between the oscillators from near 0 degrees to 180 degrees, at the bifurcation point (Fig. 4.5b). In addition to this, while in IP state, we also observe a reduction in the frequency of both the oscillators from the value at their uncoupled state, followed by an abrupt jump in the frequency during the onset of AP state (Prasad *et al.*, 2008) (Fig. 4.5c).

With increasing N_C, we observe a reduction in the AD region along with an ad-

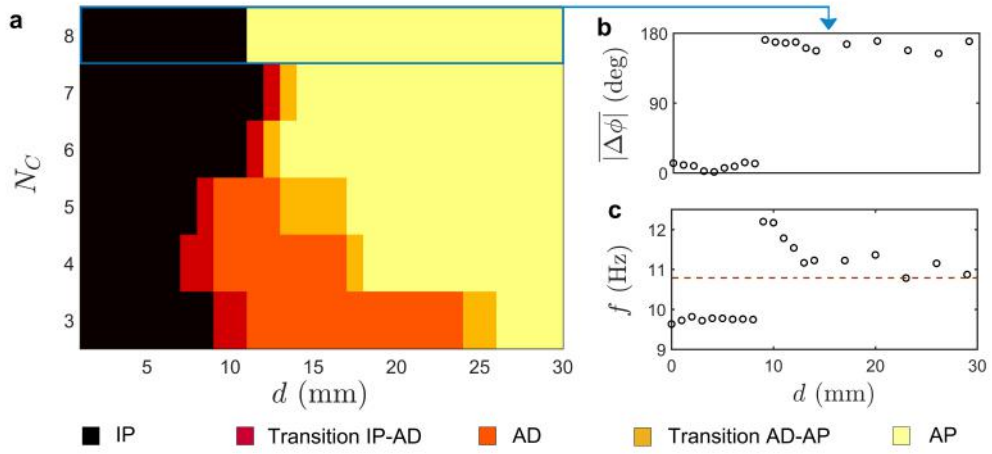

Figure 4.5: (a) The mapping of the occurrence of various states of coupled dynamics in a pair of candle-flame oscillators with variation in two control parameters, d and N_C. N_C is varied from 3 to 8, while d is increased from 0 to 30 mm in steps of 1 mm. (b), (c) The variation in the dominant frequency and the time-averaged value of absolute relative phase, respectively, with d for a pair of candle-flame oscillators consisting of $N_c = 8$, highlights the phenomena of PFB.

vancement in the onset of AP oscillations (Fig. 4.5a). We conjecture that with increasing N_C, the amplitude of oscillations of individual oscillators increases due to insufficient air supply (see Fig. 4.4), which in turn, increases the coupling strength between them. The enhancement in the amplitude of the candle-flame oscillations reduces the possibility of displaying AD and develops a tendency in the coupled oscillators to move to a state of higher frequency (AP state, see Fig. 4.2a) so as to satisfy their oxygen needs. To conclude, the dominance of the AD or PFB exhibited by the system is decided by the control parameter N_C. At lower N_C, AD dominates whereas, at higher N_C, PFB prevails.

4.2 Coupled Behaviour of Dissimilar Pair of Candle-flame Oscillators

Hitherto, we investigate the coupled dynamics of a dissimilar pair of oscillators, where the number of candles (N_c) in each of the coupled oscillators is different. In Fig. 4.6, we show the instantaneous value of the heat release rate fluctuations, I_4 corresponds to the oscillator consisting of 4 candles mounted on the movable platform, and I_6 corresponds

to an oscillator with 6 candles mounted on the stationary platform. These states are observed at different distances (d) between the oscillators of 0 cm, 1.2 cm, 2 cm and 7.5 cm, respectively. We observe that the flame dynamics observed at various values of d in a dissimilar pair of oscillators is very much akin to that observed in a similar pair (that is, the same number of candles in both oscillators) shown in Fig. 4.1. The amplitude of oscillation is observed to be different for each oscillator, which is due to the difference in the amplitudes of their individual oscillations (see Fig. 4.4b).

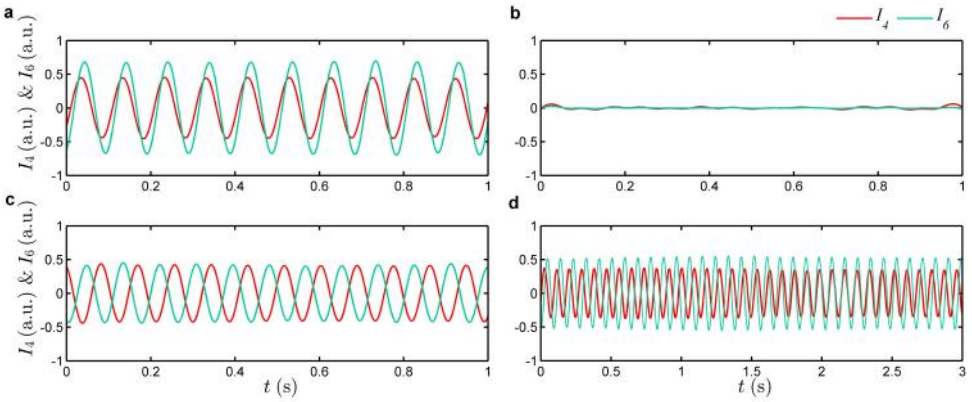

Figure 4.6: (a)-(d) The temporal variation of heat release rate fluctuations corresponding to in-phase (IP), amplitude death (AD), anti-phase (AP) and desynchronized states of oscillations, respectively, for a coupled dissimilar pair of candle-flame oscillators.

Figure 4.7 presents the dependence of dominant frequency (f) and PearsonâĂŹs correlation coefficient (ρ) on the distance between the oscillators (d) for a dissimilar pair of candle-flame oscillators. During in-phase (IP), we observe a drop in the frequency of both the oscillators compared to their uncoupled frequency value along with a near positive one value of ρ. Whereas, during the onset of anti-phase (AP), the frequency exhibits a significant rise accompanied by the value of ρ near negative one. During the desynchronized state (DS), the frequency of the coupled oscillators fluctuates around their individual isolated frequencies, and the value of ρ tends to zero. Hence, we conclude that the dynamic transition of coupled dissimilar candle-flame oscillators is near identical to that of similar candle-flame oscillators (see Fig. 4.2), except for the presence of transition states.

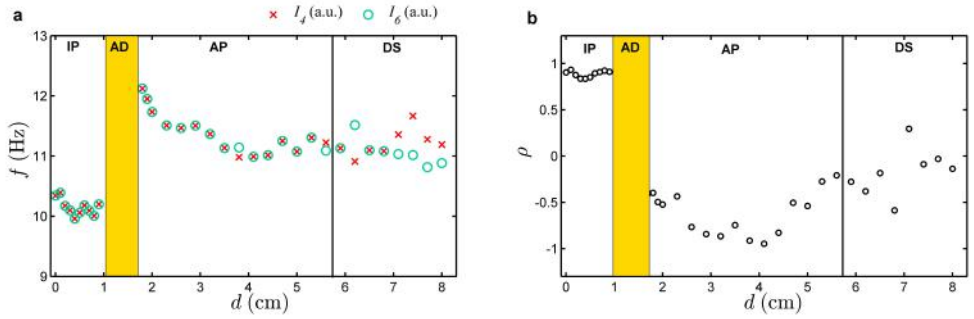

Figure 4.7: Variation in (a) the dominant frequency (f) and (b) the PearsonâĂŹs correlation coefficient (ρ) with d for a coupled dissimilar pair of candle-flame oscillators. The presence of amplitude death (AD) region observed in between the IP and AP states is highlighted in both (a) and (b).

4.3 Conclusions and Discussion

Here, we examine the coupled interaction of candle-flame oscillators by varying two system parameters (d and N_C). We demonstrate the experimental observation of the presence of AD in between IP and AP states along with PFB in the same physical system. AD can be achieved by various types of coupling such as diffusive, time-delay, conjugate and dynamic (Saxena *et al.*, 2012). Among these, AD due to time-delay (Reddy *et al.*, 1998; Strogatz, 1998) and indirect coupling (conjugate, relay, environmental diffusive) (Sharma *et al.*, 2016; Karnatak *et al.*, 2007; Sharma *et al.*, 2012) are often observed in physical systems, for instance, biological or chemical oscillators. Time-delay is intrinsic in such systems, as a finite amount of propagation time is required for transmission of the signal from one oscillator to another. In contrast, during indirect coupling, the oscillators are coupled through an intermediate medium (environment).

Recent studies (Prasad *et al.*, 2008; Sharma *et al.*, 2016, 2012; Cruz *et al.*, 2010) have shown that these types of couplings are also responsible for the manifestation of PFB. Since time-delay and indirect (through an intermediate medium) couplings are the most important factors responsible for the demonstration of PFB along with AD (Prasad *et al.*, 2008; Sharma *et al.*, 2016; Karnatak *et al.*, 2007), we hypothesize that these coupling mechanisms could play a major role in the synchronization of coupled candle-flame oscillators as well. Such couplings are inherent in the oscillatory com-

bustion of candle flames due to the difference in parameters such as the vaporization rate of wax, the chemical kinetics, and the time required for propagation of the thermal wave from one oscillator to another through a medium of oscillatory convecting current (McCaffrey, 1979). The increase in d further induces a delay in the coupling of these oscillators, which in turn, is responsible for the demonstration of different modes of synchronization.

The coexistence of AD and PFB allows us to vary the appropriate control parameters in order to choose the most desired phenomena amongst the two. The situation of AD is undesirable in many biological systems, hence a change in a single parameter which helps us to bypass this situation by directly moving to a state of PFB might act as a solution to many non-curable diseases such as Alzheimer's and Parkinson's disease (Mizuno *et al.*, 1989; Lim *et al.*, 2017). On the contrary, AD is preferred (due to its remarkable stability) in ecological systems (Yoshida *et al.*, 2003), where an oscillatory phase would lead to the extinction of species in a long-term scenario. Thence, change in a control parameter leading to a switch from PFB to AD would help sustain various endangered species. The oscillatory transmission of measles epidemic in the United Kingdom in the 18th century which persisted up to 20th century was discovered to be IP at Birmingham and Newcastle, and AP at Cambridge and Norwich. The occurrence of AD state in such systems would have resulted in a drastic decrease in the spread of these diseases (Duncan *et al.*, 1997). Furthermore, candle being a simple diffusion flame can also replicate phenomena observed in other large diffusion flames. The application of coupled behaviour of oscillatory flames in a diffusion combustion system ranges from the propagation of natural fires resulting from accidents to human-made combustion systems such as industrial, aircraft engine and rocket burners (Forrester, 2015; Yeoh and Yuen, 2009).

CHAPTER 5

Coupled Dynamics of Four Candle-flame Oscillators in a Rectangular Topology

Several experimental and theoretical studies (Pikovsky *et al.*, 2003; Kuramoto and Battogtokh, 2002; Koseska *et al.*, 2013; Wickramasinghe and Kiss, 2013) have shown the existence of different motions of coupled behaviour such as synchronization, clustering, quenching, and chimera, in minimal populations of oscillators. Although these states have been identified in various systems, the exhibition of all such states in a single system remains deficient. Furthermore, a few dynamical states such as in-phase and anti-phase weak chimera have only been seen in a theoretical study (Maistrenko *et al.*, 2017) and the experimental evidence is yet to be reported to the best of our knowledge. Therefore, the present study is a quest for observing such phenomena in an experimental system with minimum number of coupled candle-flame oscillators, positioned in a rectangular arrangement (see Fig. 3.3a). The coupled dynamics of these oscillators are characterized through the plots of temporal variation of the normalized amplitude (I) of their oscillations and the instantaneous phase difference ($\Delta\phi$, wrapped within -180 degrees to 180 degrees) between each pair of oscillators. Various dynamical states observed for each combination of inter oscillator distances given by d_x and d_y are discussed separately below.

5.1 Symmetry-breaking Dynamical States

To gain an understanding of the various coupled dynamics exhibited by four candle-flame oscillators (explained hereafter), we examine the temporal variation of the normalized amplitude (I), wrapped instantaneous phase difference ($\Delta\phi$), and the dominant

The results presented in this chapter are published in K. Manoj, S. A. Pawar, S, Dange, S, Mondal, R. I. Sujith, E. Surovyatkina, and J. Kurths, Synchronization route to weak chimera in four candle-flame oscillators *Physical Review E*, 100, 062204, (2019).

frequencies (f) of each oscillator. The relative phase ($\Delta\phi$) is calculated for each combination of oscillators as the difference between the instantaneous phases, obtained from the Hilbert transform (Pikovsky *et al.*, 2003). Oscillator pairs exhibiting synchronized behaviour display a constant phase difference between them and oscillate at identical frequencies. On the other hand, desynchronized oscillators exhibit phase-drifting behaviour in time and oscillate at different frequencies. Various dynamical states observed for each combination of inter oscillator distances, shown by d_x and d_y in Fig. 3.3(b), are individually discussed below.

5.1.1 Types of Weak Chimera

We witness the experimental evidence of weak chimera states in coupled candle-flame oscillator system. The first case of weak chimera is presented in Fig. 5.1(a), where a group of three synchronized oscillators {1, 3, and 4} coexists with a desynchronized oscillator 2, when d_x = d_y = 7 cm. Oscillators 1 and 3 are in-phase synchronized and oscillator 4 exhibits an anti-phase synchronization with them. In contrast, oscillator 2 separates itself as the desynchronized oscillator, exhibiting a phase-drifting behaviour with the synchronized group of oscillators.

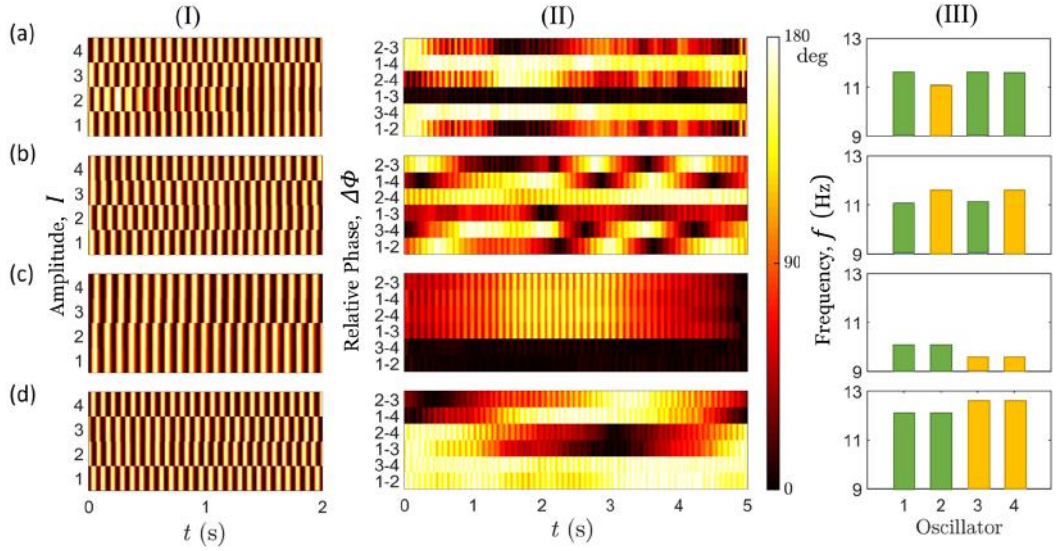

Figure 5.1: The temporal variation of (I) amplitude of each candle-flame oscillator, (II) relative phase between all combinations of such oscillator pairs, and (III) the values of dominant frequencies of each oscillator for different states of coupled dynamics characterized as (a) weak chimera, (b) multi-phase weak chimera, (c) in-phase chimera, and (d) anti-phase chimera. Oscillators having the same colour in (III) possess equal frequencies.

We report the discovery of the novel state of multi-phase weak chimera, where the oscillators in a frequency synchronized group exhibit different phase-locking behaviour from the other group while retaining desynchrony between them. In our system, an anti-phase synchronized oscillator pair coexists with an in-phase synchronized oscillator pair [Fig. 5.1(b)], while both pairs are desynchronized with each other. The oscillators {1, 3} are in-phase synchronized while the oscillators {2, 4} are anti-phase synchronized, when d_x = 5 cm and d_y = 7 cm.

A recent theoretical study by Maistrenko *et al.* (2017) showed the possibility of other states of weak chimera such as imperfect chimera, chaotic chimera, anti-phase chimera, and in-phase chimera in a theoretical model of three pendulum-like nodes. Here, we report the maiden experimental observation of such in-phase and anti-phase chimera states in candle-flame oscillators. During in-phase chimera [Fig. 5.1(c)], the system divides into two pairs of in-phase synchronized oscillators, {1, 2} and {3, 4}, while retaining desynchrony between those pairs when d_x = 7 cm and d_y = 4 cm. The state of anti-phase chimera [Fig. 5.1(d)] displays similarity to the state of in-phase chimera shown in Fig. 5.1(c) with the only difference being the synchronized pair of oscillators exhibiting an anti-phase mode of synchronization. Such a state of anti-phase chimera is observed for d_x = 5 cm and d_y = 6 cm.

5.1.2 Bare Minimum Chimera

A yet another specific case of weak chimera which is thoroughly investigated is the state of bare minimum chimera (Hart *et al.*, 2016), where a system of four oscillators separates into pairs of synchronized and desynchronized oscillators. We observe the existence of such a chimera state at a distance of d_x = d_y = 6 cm. In Fig. 5.2(a,b), we see the oscillators {1, 3} that exhibit anti-phase synchronization coexisting with the desynchronized pair of oscillators {2, 4}.

The stability of chimera states in small populations of oscillators has been studied widely by many researchers. The chimera states which are found in large populations of oscillators are considered to be a stable phenomenon due to its long lifetime (Wolfrum and Omel'chenko, 2011). As the number of oscillators in the population decreases, the transient nature of chimera state has been observed to increase due to the finiteness

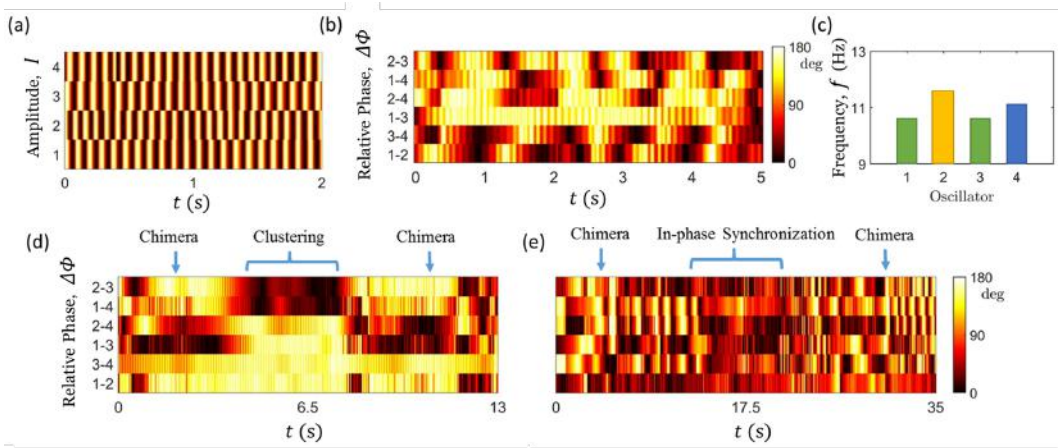

Figure 5.2: The temporal variation in the (a) amplitude of each oscillator, (b) the relative phase between each pair of oscillators and (c) frequencies of each oscillator. (d), (e) The plots of relative phase representing the states of alternating chimera states seen in the experiments where the existence of chimera is observed to mediate between the states of clustering and in-phase synchronization, respectively.

(Wolfrum and Omel'chenko, 2011).

The study by Wolfrum and Omel'chenko (2011) recognizes chimera as chaotic transients. According to their study, chimeras observed in small populations are transient in nature, wherein we would observe a sudden collapse of the coupled dynamics from a chimera state to a fully coherent state after a long time span. A study on six coupled electrochemical oscillators (Wickramasinghe and Kiss, 2013) has shown the existence of chimera as a long transient phenomenon that occurs over 90 to 100 cycles and later collapses to the coherent states. In another study by Omelchenko *et al.* (2016), they reported the usage of tweezers to stabilize the chimera states observed in small populations of oscillators, where the chimera state is observed to have a finite lifetime and exhibits a random-walk behaviour. Various other control strategies have also been used to stabilize the chimera states in minimal oscillator networks (Sieber *et al.*, 2014; Bick and Martens, 2015). Subsequent studies showed the existence of chimera in small systems to mediate between coherent states (Ma *et al.*, 2010; Panaggio and Abrams, 2015). The phenomenon of alternating chimera is one such example.

The chimera state found in candle-flame oscillators is observed to mediate between coherent states (clustering states or in-phase synchronized states), due to their low stability in small populations, commonly referred to as alternating chimera (Ma *et al.*, 2010). In Fig. 5.2(d), we observe that the system dynamics transition from the chimera

state, with oscillators $\{3, 4\}$ as the synchronized pair and oscillators $\{1, 2\}$ as the desynchronized pair, to a clustering state where the oscillators separate into two clusters of synchronized oscillators (detailed explanation is provided subsequently) and later returns to the chimera state. During the chimera state, the oscillator pair $\{3, 4\}$ exhibits nearly anti-phase synchronization and the other oscillators 1 and 2 remain desynchronized. As the dynamics transition to the clustering state, we observe that the oscillators 1 and 2 are synchronized with the oscillators 4 and 3, respectively, with a zero degree phase shift. The oscillator pair $\{1, 4\}$ and $\{2, 3\}$ form two clusters oscillating at a frequency of 11.5 Hz with anti-phase synchronization between the clusters.

On the other hand, in Fig. 5.2(e), we observe that the chimera state is followed by the state of in-phase synchronization, which yet again transitions to the chimera states. The oscillator pair $\{1, 2\}$ remains in-phase synchronized, having nearly zero degrees phase shift throughout the time series. In contrast, the oscillators 3 and 4 are desynchronized within themselves and with the synchronized pair during the chimera state. The oscillators are in-phase synchronized within themselves and the others, and have an oscillation frequency of 10.8 Hz during the epoch of in-phase synchronization. We observe the existence of the chimera state for an average of 80 cycles in both the cases of alternating chimera.

5.2 Homogeneous Coupled Behaviour

Hitherto, we have discussed the existence of symmetry-breaking states where we observe a combined existence of synchronized and desynchronized oscillators upon coupling. Hereon, we will discuss the presence of only synchronization states observed at various distances between coupled candle-flame oscillators. These states are observed when the oscillators are placed close to each other.

5.2.1 In-phase Synchronization and Amplitude Death

When the oscillators are very close to each other at $d_x = d_y = 2$ cm [Fig. 5.3(a)], we observe that every oscillator (oscillators 1 to 4) attains maximum and minimum amplitudes simultaneously, exhibiting in-phase synchronization (Pikovsky *et al.*, 2003) at

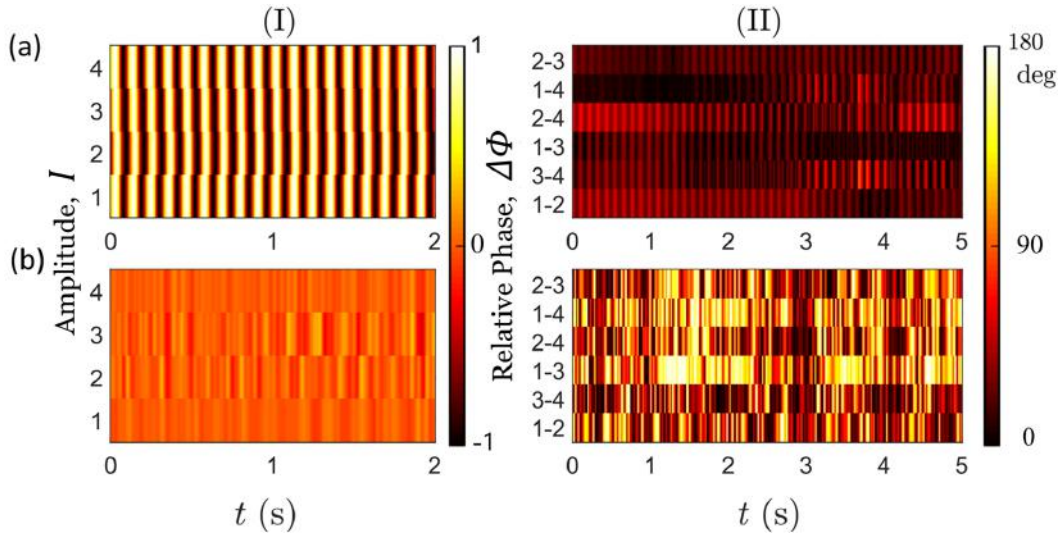

Figure 5.3: Plots of temporal variation in (I) amplitude of each candle-flame oscillator and (II) instantaneous phase difference between all combinations of oscillator pairs for the states of (a) in-phase synchronization, and (b) amplitude death

a frequency of approximately 10.7 Hz. As the oscillators are positioned a small distance apart (d_x = d_y = 4 cm), the coupling between them leads to the simultaneous quenching of oscillations in all the oscillators. This state where all the oscillators occupy a homogeneous steady state due to mutual coupling is referred to as amplitude death (Koseska *et al.*, 2013). The amplitude plot of this state [Fig. 5.3(b)] shows minor fluctuations around zero, highlighting the lack of oscillations in the system. The instantaneous Hilbert phases of these oscillators, although physically undefined due to the lack of narrow-band oscillations (Pikovsky *et al.*, 2003), do not show any particular trend for this state.

5.2.2 Clustering States

When the candle-flame oscillators are moved to a distance of d_x = 1 cm and d_y = 4 cm, the population of these oscillators separates into different clusters, depending on the values of instantaneous properties (amplitude and phase) of their signals (Wickramasinghe and Kiss, 2013; Premalatha *et al.*, 2018). Here, the oscillators belonging to the same cluster exhibit equal instantaneous phases that are different from the other clusters; while all the oscillators in the population carry an identical frequency of approximately 11 Hz. In Fig. 5.4(a), the oscillator pairs {1, 2} and {3, 4} separate into two clusters which exhibit anti-phase synchronization between them. An interchange

in the distances d_x and d_y (i.e., d_x = 4 cm and d_y = 1 cm) results in the formation of a clustering state shown in Fig. 5.4(b). During this state of clustering, the oscillators belonging to the same clusters are now on different platforms.

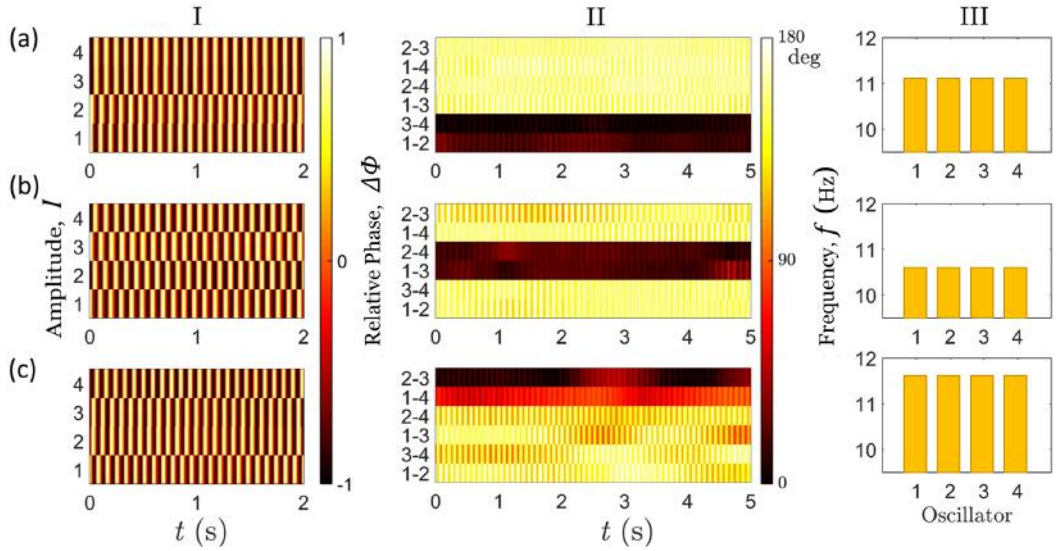

Figure 5.4: Variation in (I) amplitude, (II) relative phase, and (III) dominant frequency of each candle-flame oscillator during different states of clustering. In all three types of clustering exhibited by four candle-flame oscillators, we observe the presence of two clusters, each consisting of two oscillators and anti-phase synchronization between the clusters.

Apart from the aforementioned types of clustering where adjacent oscillators group together into a cluster, we also observe clustering between diagonal pair of oscillators (d_x = 3 cm and d_y = 3 cm). During diagonal clustering of oscillators, the oscillators which exhibit in-phase synchronization would be on diagonally opposite ends of the rectangle, and the adjacent oscillators display anti-phase synchronization [as shown in Fig. 5.4(c)]. For each state of clustering shown in Fig. 5.4(a) âĂŞ (c), we observe a difference in the frequency of oscillations, due to the existence of low frequency during in-phase synchronization and high frequency during anti-phase synchronization (Kitahata *et al.*, 2009). In Fig. 5.4 (a) and (b), we observe only slight variation in frequency due to their symmetric coupling structure, i.e. the coupling structure at d_x = 1 cm and d_y = 4 cm is symmetric to the coupling structure during d_x = 4 cm and d_y = 1 cm. During diagonal clustering, we observe a very high frequency value as all the neighbouring oscillators exhibit anti-phase synchronization, which itself has a higher frequency (Kitahata *et al.*, 2009). In all three states of clustering exhibited by the system of four candle-flame oscillators, we observe the presence of two clusters, each consisting of two oscillators. Other types of clustering, where three oscillators

group into one cluster and the fourth oscillator oscillate at a constant phase difference from the former, are also observed as transient phenomena and hence not discussed.

5.3 Route to Weak Chimera

Having discussed all the observed prominent synchronization and symmetry-breaking states in an experimental four oscillator system, let us now compare their behaviour on a two-parameter bifurcation plot. Figure 5.5 shows the overall mapping of the coupled dynamics of candle-flame oscillators at various values of coupling parameters (d_x and d_y). This plot projects all the possible modes of coupled oscillations exhibited by four limit cycle oscillators considered in our study at a given combination of coupling parameters. It also helps us examine the various available routes to traverse from a given mode of oscillations to another and to smartly control the system dynamics by the selection of the preferred route.

In non-locally coupled candle-flame oscillators, the mutual interaction or coupling between them decreases with an increase in the distance, refer Chapter 4. In Fig. 5.5, we observe the exhibition of in-phase synchronization when the oscillators are placed very close to each other, due to the presence of strong interaction between them. When either d_x or d_y is increased, keeping the other at a very low value, we observe various states of clustering due to the difference in the synchronization properties between pairs of oscillators. On the other hand, a slight increase in the values of both d_x and d_y leads to the exhibition of amplitude death in their dynamics. With further increase in the values of d_x and d_y, we observe the presence of desynchrony in the system, through the states of chimera and weak chimeras.

An interesting feature of the two-parameter bifurcation plot is its symmetry [Fig. 5.5]. We observe a spatial symmetry in the coupled dynamics of four candle-flame oscillators about the diagonal line of the bifurcation plot. An interchange in d_x and d_y would not make much significant changes in the dynamics of the group of oscillators. This fact further confirms the repeatability of these experiments.

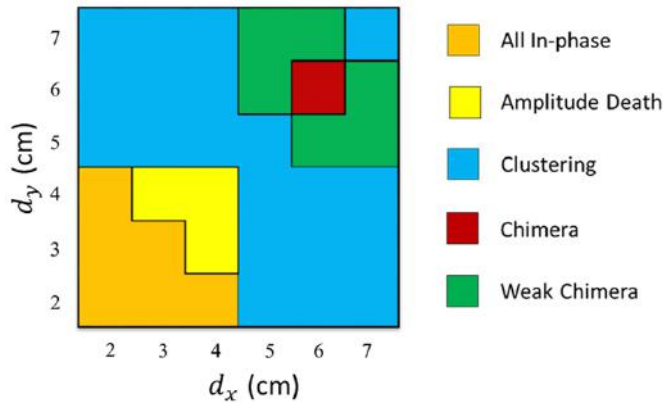

Figure 5.5: Two-parameter bifurcation plots between distances d_x & d_y depicting the presence of various dynamical states observed in a system consisting of four candle-flame oscillators exhibiting limit cycle oscillations.

5.4 Conclusions and Discussion

To summarize, in the present study, we provide an experimental evidence to the emergence of rich dynamical behaviours exhibited by a system with a minimal number (N = 4) of coupled candle-flame oscillators due to a change in their topological arrangement. Various coupled dynamics, including in-phase synchronization, amplitude death, clustering, and chimeras are observed. We report the discovery of the novel state of multi-phase weak chimera. Further, we provide the first experimental evidence of weak chimera states such as in-phase chimera, anti-phase chimera, which were observed previously in theoretical studies. Hence, by varying the coupling between the oscillators, we bring forth various routes of transition from one dynamical state to another.

In many practical systems, one among these states is undesirable. For example, phase-locked (or synchronization) states leading to amplitude growth are unwanted in many oscillatory systems such as, thermoacoustic systems (Pawar *et al.*, 2017; Raaj *et al.*, 2019), pedestrians on the Millennium Bridge (Strogatz *et al.*, 2005*b*), ecological systems (Yoshida *et al.*, 2003), the spread of epidemics (Duncan *et al.*, 1997) and epileptic seizures (Timmermann *et al.*, 2002). On the other hand, amplitude death proves dangerous in neural systems, causing the occurrence of AlzheimerâĂŹs (Lim *et al.*, 2017) and ParkinsonâĂŹs disease (Mizuno *et al.*, 1989). The difficulty in controlling the oscillatory states enhances during the partial synchronization states, such as chimera and weak chimera. Therefore, a transition from these undesirable states in such oscillatory systems to the desired state is possible with smart control of the coupling parameters.

CHAPTER 6

Effect of Topology on the Dynamical Behaviour of Coupled Candle-flame Oscillators

The coupled dynamics of candle-flame oscillators in a network depends on the number of oscillators, the distance between each oscillator, and the topological arrangement of these oscillators. The coupled interaction between these oscillators engenders a plethora of dynamical states in the system. The discussion in Chapter 4 presented the coupled dynamics exhibited by two candle-flame oscillators as the distance between them is varied. The topology of two oscillators in a network is shown in Fig. 3.1(a), where we observe the existence of four dynamical states. These include in-phase synchronization (for $d \leq 0.5$ cm), amplitude death (for 0.75 cm < d < 1.25 cm), anti-phase synchronization (for 1.5 cm <$d \leq 3.5$ cm), and desynchronization (for d> 3.5 cm). The existence of these states is asymptotically stable in time.

In our subsequent analysis, the distances corresponding to each of these dynamical states are subjected to various topological arrangements when the number of oscillators in the network is increased to 3 and 4. To elaborate, anti-phase synchronization is observed at a distance of $d = 3$ cm in a system of two coupled oscillators. All the other network topologies discussed in Fig. 3.1(b) and Fig. 3.1(c) are investigated by keeping the distance of $d = 3$ cm between the oscillators and the effects of the change in the number of oscillators and the network topology on the coupled behaviour of the system is investigated. A similar analysis is performed for distances corresponding to other afore-mentioned dynamical states, which includes $d = 0$ cm for in-phase synchronization, $d = 1$ cm for amplitude death, and $d = 4$ cm for desynchronization.

6.1 Behaviour of Strongly Coupled Oscillators

For link distances of 0 cm and 1 cm between two candle-flame oscillators, we observe dynamical states of in-phase synchronization and amplitude death, respectively

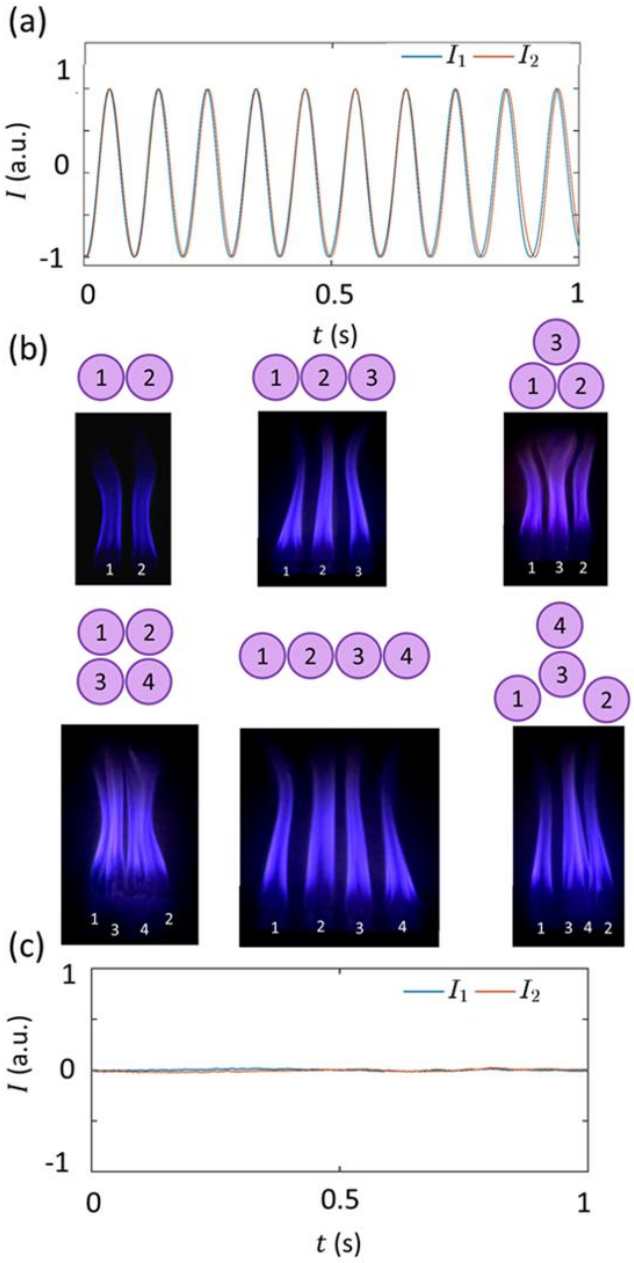

Figure 6.1: Time series of the heat release rate fluctuations corresponding to (a) in-phase synchronization ($d = 0$ cm) and (c) amplitude death ($d = 1$ cm) obtained from coupled pair of oscillators. Snapshots of the candle-flame oscillators corresponding different topologies as discussed in Fig. 3.1 for link distances that correspond to in-phase synchronization ($d = 0$ cm).

(Fig. 6.1a and Fig. 6.1c). The representative time series of the heat release rate fluctuations corresponding to each dynamical state (i.e., in-phase synchronization and amplitude death) are shown for two oscillators are shown in Fig. 6.1(a),(c). In the case of in-phase synchronization, all oscillators reach their corresponding maximum and minimum amplitudes simultaneously; thus, exhibiting a phase-shift of nearly 0 degrees between their oscillations. On the other hand, the state of amplitude death is charac-

terized by simultaneous quenching of oscillations in both the oscillators, where all the oscillators theoretically reach a homogenous steady state, but in experiments, they show minimal noisy fluctuations around the mean value of zero.

As the number of oscillators in a network is increased, the possible ways of constructing networks also change, as discussed in Fig. 3.4. In Fig. 6.1, we observe that the variation in the number of oscillators or a change in a network topology for a fixed number of oscillators, for $d = 0$ cm does not disturb the existence of the coupled dynamical states observed in candle-flame oscillators (Fig. 6.1b). Similar behaviour is exhibited for $d = 1$ cm with all oscillators existing in the state of amplitude death and is not presented here. Hence, we observe that the existence of the states of in-phase synchronization and amplitude death at $d = 0$ cm and 1 cm, respectively, is independent of the number of oscillators and their topological arrangement. The presence of stronger coupling between the oscillators at small link distances and the existence of high stability of the dynamical states might be a plausible reason for the occurrence of these invariant states in a network of candle-flame oscillators. However, this observation is not true for the case where link distances between oscillators are larger than 2 cm ($d > 2$ cm).

6.2 Behaviour of weakly coupled oscillator networks

When the distance between two oscillators is between 2 cm $< d <$ 3.5 cm, we observe the presence of anti-phase synchronization, and when $d \geq$ 3.5 cm, these oscillators exhibit desynchronization behaviour. As the number of oscillators becomes greater than 2, at these distances, we observe an increase in the complexity of coupled dynamics observed in the network of candle-flame oscillators. At higher distances, we witness the emergence of several symmetry-breaking states of coupled dynamics, which are elaborated in the subsequent parts of the paper (see Figs. 6.2 - 6.5). We observe that these oscillators tend to exhibit multiple stable dynamical states for a specified distance and topology of oscillators. Note that each dynamical state is observed for a minimum of 100 oscillatory cycles and, therefore, we do not consider them as transient dynamics.

The coupled dynamics of oscillators gradually shifts from one dynamical state into another with time. This transition happens either via a transient change in the frequency of a few oscillators or a momentary quenching of a few oscillators, observed for a

duration of approximately 3 to 5 s (a maximum of 50 cycles), to adjust their dynamics to satisfy the subsequent dynamical state. In the following paragraphs (Figs. 6.2 - 6.4), we discuss various dynamical states which are exhibited by candle-flame oscillators at link distances greater than 2. We note that the distances corresponding to each dynamical state discussed in Figs. 6.2 - 6.4 are not specified, as multiple dynamical states are observed for a given distance and vice versa (multiple distances for which we observe a given dynamical state). An overall description of the occurrence of these states is summarized in Fig. 7.2.

6.2.1 Dynamical Behaviour of Three-oscillator Networks

To characterize the coupled dynamics exhibited by a network of three and four candle-flame oscillators, we plot the temporal variation of the instantaneous phase difference between the pair of oscillators. The absolute value of the relative phase (wrapped between -180 degrees to 180 degrees) obtained after applying the Hilbert transformation (Pikovsky *et al.*, 2003) on the signal, as shown in Fig. 6.2(I). If the phase difference between two oscillators is near zero deg, they exhibit in-phase synchronization; whereas, if the oscillators have a near 180 degrees phase shift, they are in a state of anti-phase synchronization. In this manner, the synchronization characteristics of oscillator pairs in a network decide the global behaviour of the network. A bar chart depicting the dominant frequency of each oscillator at a given state is shown in Fig. 6.2(II).

When the number of oscillators in the system is three, we observe various states of coupled dynamics as the topology and distance between the oscillators in a network are varied. Four possible dynamical states observed in a three-oscillator network of candle-flame oscillators are shown in Fig. 6.2(a-d). In Fig. 6.2(a), we plot the dynamical features of a state of clustering of oscillators, where three oscillators exhibit an equal frequency and maintain a constant phase difference between each other. We observe that the phase difference between the oscillator pairs {1, 2}, {2, 3}, and {3, 1} are nearly 84 deg, 152 deg, and 68 deg, respectively, and all oscillators exhibit a dominant frequency of 11.03 Hz. We note that unlike the states of clustering observed previously in these candle-flame oscillators, refer Chapter 4, where the phase shift between the oscillator pairs is either 0 or 180 deg, in our system, these oscillators are synchronized at a phase shift other than 0 or 180 deg.

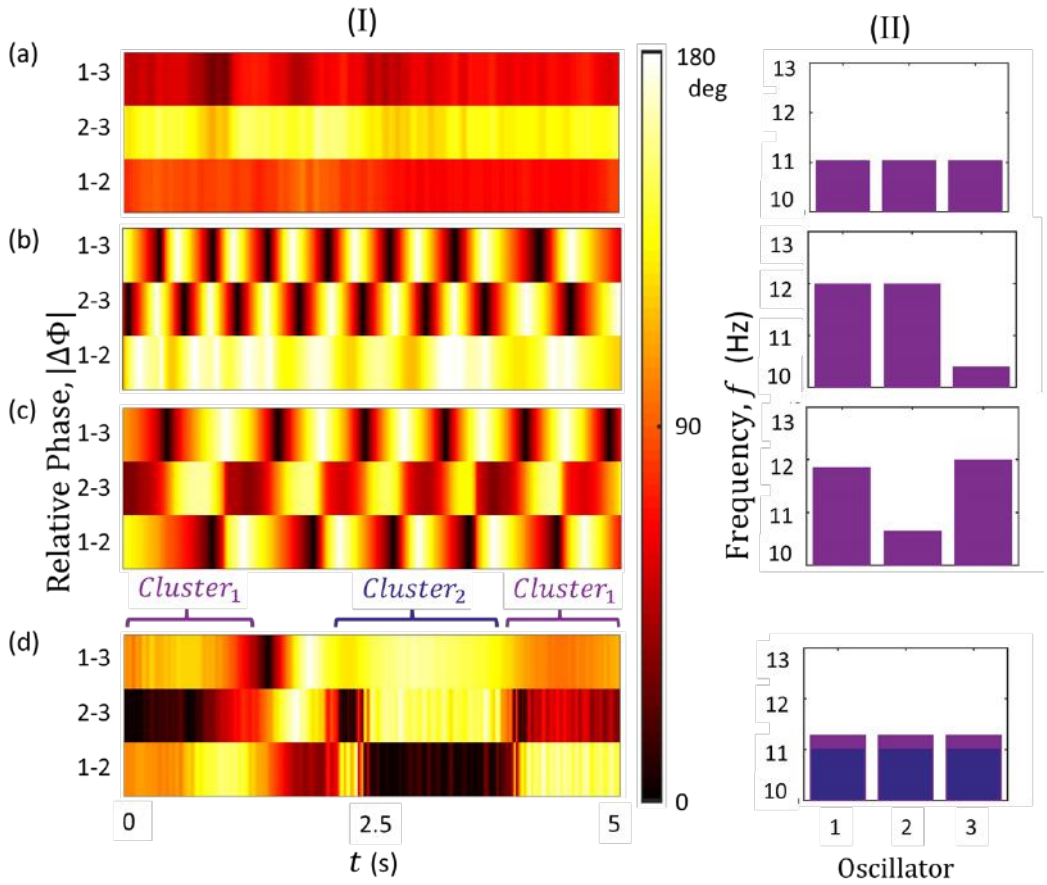

Figure 6.2: (I) Temporal variation of the relative phase between a pair of oscillators and (II) the frequency distribution of all oscillators for the dynamical states of (a) clustering, (b) weak chimera, (c) desynchronization, and (d) rotating clusters observed in a network of three coupled candle-flame oscillators.

In Fig. 6.2(b), we show the dynamical behaviour of the state of weak chimera (Ashwin and Burylko, 2015) observed in a three-oscillator network. The state is characterized by the presence of a pair of frequency synchronized oscillators, which are desynchronized with the third oscillator due to a difference in the frequency. Here, we notice that the oscillator pair {1, 2} are anti-phase synchronized and their synchronization frequency is 11.99 Hz; whereas, the oscillator 3 is desynchronized with the pair {1, 2} as it exhibits a frequency of 10.39 Hz. We also observe the presence of complete desynchrony in the system of three oscillators (Fig. 6.2c), where oscillators 1, 2, and 3 exhibit three different frequencies which are 11.84 Hz, 10.64 Hz, and 11.99 Hz, respectively (see Fig. 3 6.2-II). The desynchronized behaviour of oscillators can be observed from the phase-drifting behaviour of the relative phase between each pair of oscillators (Fig. 6.2c-I).

A novel type of clustering dynamics observed in a network of three mutually cou-

pled oscillators is called rotating clusters, where we observe the temporal switching from one type of cluster to another type of cluster. To elaborate, the system exhibiting a particular form of clustering transitions into another form of clustering in time. Both the forms of clustering observed in a rotating clustered state need not have identical frequencies. Here, we observe two types of clustering: In the first type, oscillators 2 and 3 are in-phase synchronized, and they are anti-phase synchronized with the oscillator 1. This state of clustering is marked in Fig. 6.2(d-I) as $Cluster_1$, where all the oscillators have a frequency of 11.28 Hz, as shown in violet in Fig. 6.2(d-II). On the other hand, in the second type of cluster, the oscillators 1 and 2 are in-phase synchronized, and they are anti-phase synchronized with the oscillator 3. This type of clustering is marked as $Cluster_2$ in Fig. 6.2(d) and all oscillators show a dominant frequency of 11.08 Hz during this state (shown in blue in Fig. 6.2d-II).

6.2.2 Dynamical Behaviour of Four-oscillator Networks

In the case of a network of four oscillators, we primarily observe two types of clustered states. In the first type of the clustered state shown in Fig. 6.3(a), a pair of clusters consists of two oscillators in each. On the other hand, in the other type of the clustered state shown in Fig. 6.3(b), one cluster consisting of three oscillators and another cluster formed with a single oscillator. We observe that the oscillator pairs {1, 3} and {2, 4} are in-phase synchronized and, therefore, form two clusters in Fig. 6.3(a). Between these clusters, we observe anti-phase synchronization. During this type of clustering, all four oscillators show a dominant frequency of 12.31 Hz (Fig. 6.3a-II). On the other hand, in Fig. 6.3(b), we observe that oscillators {1, 2, 4} form one cluster of in-phase synchronized oscillations, which is anti-phase synchronized with the oscillator 3 that alone forms another cluster. Here, every oscillator in the network exhibits a frequency of 12.09 Hz (Fig. 6.3b-II).

The presence of desynchrony in the system of oscillators gives rise to the occurrence of symmetry-breaking phenomena such as chimera, weak chimera, etc. In a network of four oscillators, the coexistence of a synchronized and desynchronized pair of oscillators is referred to as chimera (Abrams and Strogatz, 2004). In Fig. 6.3(c), we observe the state of chimera in four coupled oscillators where the oscillator pair {2, 3} are synchronized and oscillate at a frequency of 11.51 Hz. The other oscillators 1 and 4 having

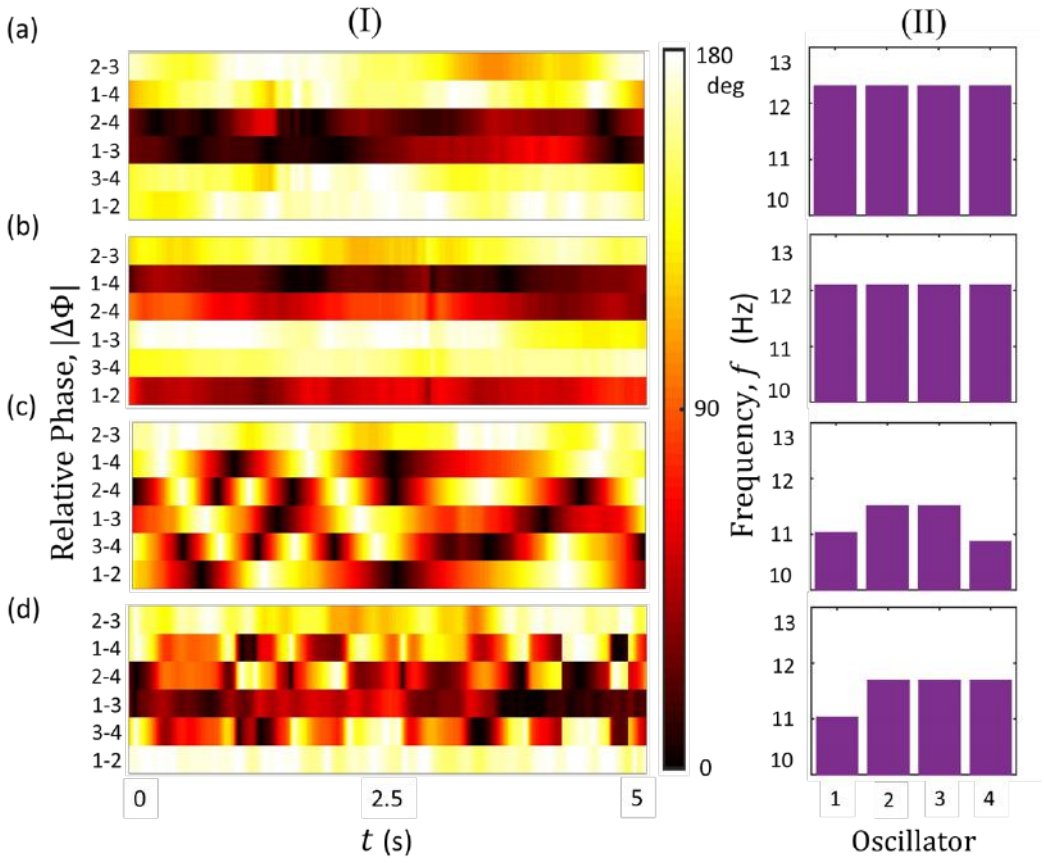

Figure 6.3: (I) The temporal variation in the relative phase between a pair of candle-flame oscillators and (II) the dominant frequency of each oscillator for the states of (a), (b) clustering, (c) chimera, and (d) weak chimera observed in a network of four coupled oscillators.

frequencies of 11.03 Hz and 10.87 Hz, respectively, are desynchronized with each other and also with the synchronized pair of oscillators. The weak chimera observed in this network of candle-flame oscillators is shown in Fig. 6.3(d), where oscillators 2, 3, and 4 are frequency synchronized having equal frequencies of 11.69 Hz, while oscillator 1 is desynchronized with all three oscillators and has a frequency of 11.09 Hz.

Apart from the aforementioned either oscillatory or completely quenched (amplitude death) states of coupled dynamics, we also witness a novel dynamical state called partial amplitude death (PAD) in a mutually coupled network of four candle-flame oscillators. Partial amplitude death is characterized by the coexistence of nearly quenched states and oscillatory states in a coupled system of oscillators (Atay, 2003). In the case of candle-flame oscillators, we report the first observation of two variants of PAD states. In the first type of PAD (Fig. 6.4a), we observe that two oscillators (1 and 4) exhibit desynchronized oscillations, while the oscillators 2 and 3 are nearly quenched

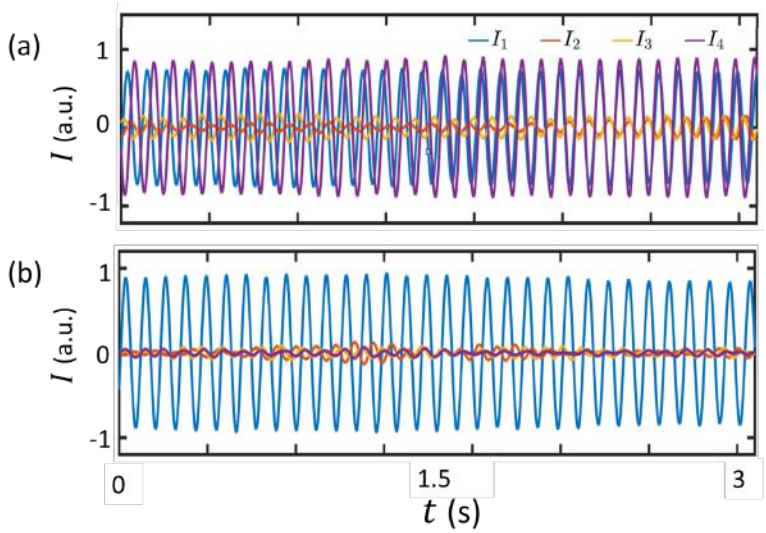

Figure 6.4: (a), (b) The time series of the heat release rate fluctuations observed during two different variants of partial amplitude death states observed in the network of four coupled candle-flame oscillators.

displaying minimal fluctuations of zero amplitude. Such a state of PAD is observed in the straight configuration of oscillators, where the outer oscillators are in the oscillatory state, and the inner two oscillators are in the quenched state. In another form of PAD, three oscillators are observed to be in the quenched state while one remains in an oscillatory state. In Fig. 6.4(b), we observe that the oscillators 2, 3, and 4 are in a quenched state, while the oscillator 1 exhibits limit cycle oscillations. Such a state is observed for the star configuration, where oscillator 1 is the central oscillator, and the other oscillators are the outer ones that surround the central oscillator.

6.2.3 Global Dynamics of Weakly Coupled Network of Oscillators

Having discussed all the dynamical states observed in a network of coupled candle-flame oscillators individually in Figs. 6.1- 6.4, we now move our attention to categorizing the occurrence of these states in networks of 3 and 4 oscillators when the link distances between the oscillators are $d = 3$ cm and 4 cm (Fig. 6.5). As mentioned previously, when the number of oscillators is greater than 3, and the distance between oscillators is larger ($d > 2$ cm), we observe the alternate occurrence of multiple stable states of coupled dynamics in a network of oscillators. As a result, to account for all these states, we plot the percentage occurrence of each dynamical state observed at each topological arrangement (Fig. 6.5). Here, the percentage indicates the average

time for which a given coupled behaviour of oscillators is observed in a system for an experimental duration of 60 s over 20 trials. For example, in the case of a straight configuration with four oscillators placed at $d = 3$ cm, we observe the occurrence of three dynamical states: clustering, chimera, and weak chimera. The percentage of occurrence of these states for the configuration is 42%, 27%, and 31%, respectively (see Fig. 6.5a).

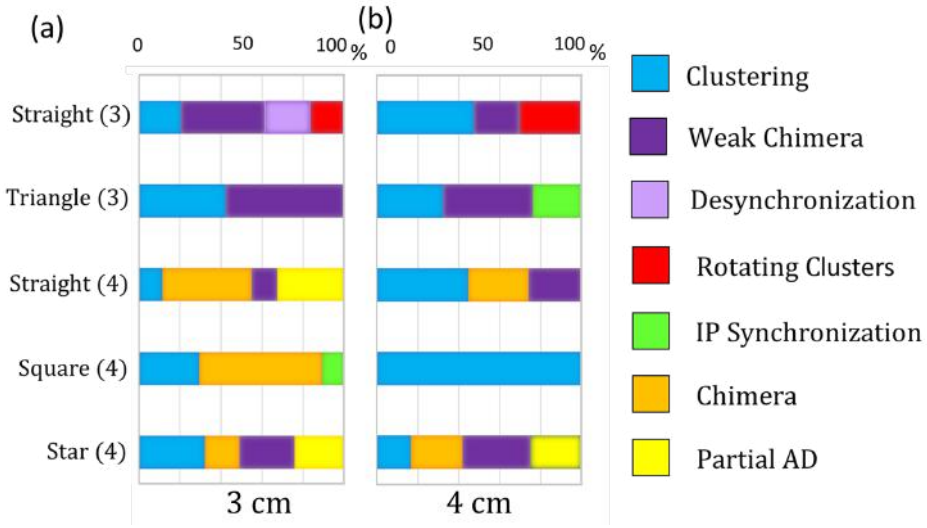

Figure 6.5: Percentage occurrence of different dynamical states in a network of couple candle-flame oscillators for a given number of oscillators (specified in braces) arranged in different topological configurations when the distance between the oscillators is (a) $d = 3$ cm and (b) $d = 4$ cm. The maximum standard deviation of the percentage occurrence of each dynamical state is approximately 13 %.

From Fig. 6.5, we observe that for a closed-loop network of oscillators (e.g., square and triangle network where all oscillators have an equal degree), one stable dynamical state of coupled oscillators dominates over the other states. For example, in the square configuration of 4 oscillators with $d = 3$ cm (Fig. 6.5a), we see the singular dominance of clustering. Similarly, for $d = 4$ cm between oscillators for the same configuration (Fig. 6.5b), chimera state dominates with 57 % than the states of clustering (28 %) and in-phase synchronization (15 %). However, such behaviour of oscillators is not as prominent in the case of a triangular network. Furthermore, we observe that the number of stable states observed for a given number of oscillators is lesser for a closed-loop network. For example, in the case of three oscillators having a link distance of $d = 4$ cm, we observe that the straight configuration displays four dynamical states, whereas the triangular configuration exhibits only two. We can also note that the global synchronization between all oscillators (state of in-phase synchronization) is observed only for closed-loop networks. On the other hand, for open-loop network topologies with a

varying degree for each oscillator, we observe an increased number of multiple stable dynamical states. For instance, in the case of star configuration for both Fig. 6.5(a) and Fig. 6.5(b), we observe the presence of four different dynamical states and all having a nearly equal probability of occurrence. We further note that the PAD states discussed in Fig. 6.4 are observed only for open-loop topologies (straight and star configuration) with four oscillators. Similarly, we observe the existence of rotating clusters only in the open-loop topology (straight configurations) with three oscillators.

As we increase the link distance without changing the topology of the oscillators, we observe the increased existence of desynchrony in the system (as oscillators have different frequencies). To elaborate, for a given topological arrangement (say, the triangular configuration with 3 oscillators), as we increase the link distance from $d = 3$ cm (Fig. 6.5a) to 4 cm (Fig. 6.5b), we observe an increase in the existence of states of weak chimera (oscillators having different frequencies) and a decrease in the occurrence of states such as in-phase synchronization and clustering (all oscillators exhibit equal frequencies). Moreover, as the number of oscillators (N) is increased from 3 to 4, we observe the emergence of states such as PAD and chimera along with the disappearance of states such as rotating clusters. We can extend such behaviour and conjecture that as the number is increased further ($N > 4$), one can expect the vanishing of highly synchronous states such as in-phase synchronization and clustering. Further, it is also notable that the stability (the oscillatory cycles for which a state is exhibited) of these symmetry-breaking states increases with an increase in the number of oscillators (Wolfrum and Omel'chenko, 2011). Therefore, we can also conjecture that an increased occurrence of symmetry-breaking states such as weak chimera and chimera can be observed in a network with a higher number of oscillators ($N > 4$) under weak coupling (higher distances).

6.3 Annular Network of Oscillators

Having discussed the various dynamical behaviour exhibited by networks of candle-flame oscillators consisting of two to four oscillators placed in various topological arrangements, we next move on to investigating the global dynamics of a ring (regular) network in detail (see Fig. 6.6). In this case, the effect of an increase in the number

of oscillators from 5 to 7 at a fixed link distance of $d = 3$ cm is investigated. In the network, as the oscillators are locally coupled to their nearest neighbours, all oscillators possess a degree of 2. From Fig. 6.5, we observe that closed-loop topologies tend to exhibit increased synchrony and stability as compared to open-loop topologies. In annular networks of oscillators, we primarily observe the states of clustering (CL), chimera (CH), and weak chimera (WC). The dynamical state having the coexistence of multiple frequency synchronized groups, each having one or more oscillators, can be categorized to a state of weak chimera. A specific case of weak chimera, where a single frequency synchronized group of oscillators coexist with a group of desynchronized oscillators is referred to as chimera.

For link distances of 0 cm and 1 cm, we observe the state of in-phase synchronization and amplitude death, respectively, irrespective of the number of oscillators present in the annular topology. This is similar to the observation of these system dynamics of other network topologies discussed in Fig. 3.4. When the link distance between the oscillators is $d = 3$ cm, the neighbouring oscillators have a tendency to exhibit anti-phase synchrony due to the alternate shedding of vortices from oscillators in each cycle (Dange *et al.*, 2019*b*). As a result, we observe a difference in the dynamics of an annular network having even number of oscillators from those having odd numbers. The existence of global synchrony, in the form of clustering, is observed in the case of networks with even number of oscillators alone. Further, we observe that during the state of clustering, the network separates into two clusters consisting of equal number of oscillators. For example, in a square network of four oscillators, the state of clustering is observed with the formation of two clusters, each having two oscillators (Fig. 6.5a). Similarly, for a ring-network of six oscillators (see Fig. 6.6b), we observe the formation of two clusters, each consisting of three oscillators. In both the cases discussed above, the formation of two clusters occurs such that adjacent oscillators belong to different clusters.

On the contrary, in ring networks having odd number of candle-flame oscillators with $N > 3$, we do not observe the existence of clustering states; however, we observe the existence of only chimera and weak chimera states. These states occur in various forms which are referred to as variants of the given dynamical state. In Fig. 6.6a âĂŞ (i),(ii) we observe the state of weak chimera where the coexistence of frequency synchronized and desynchronized oscillators occur. However, the number is the frequency

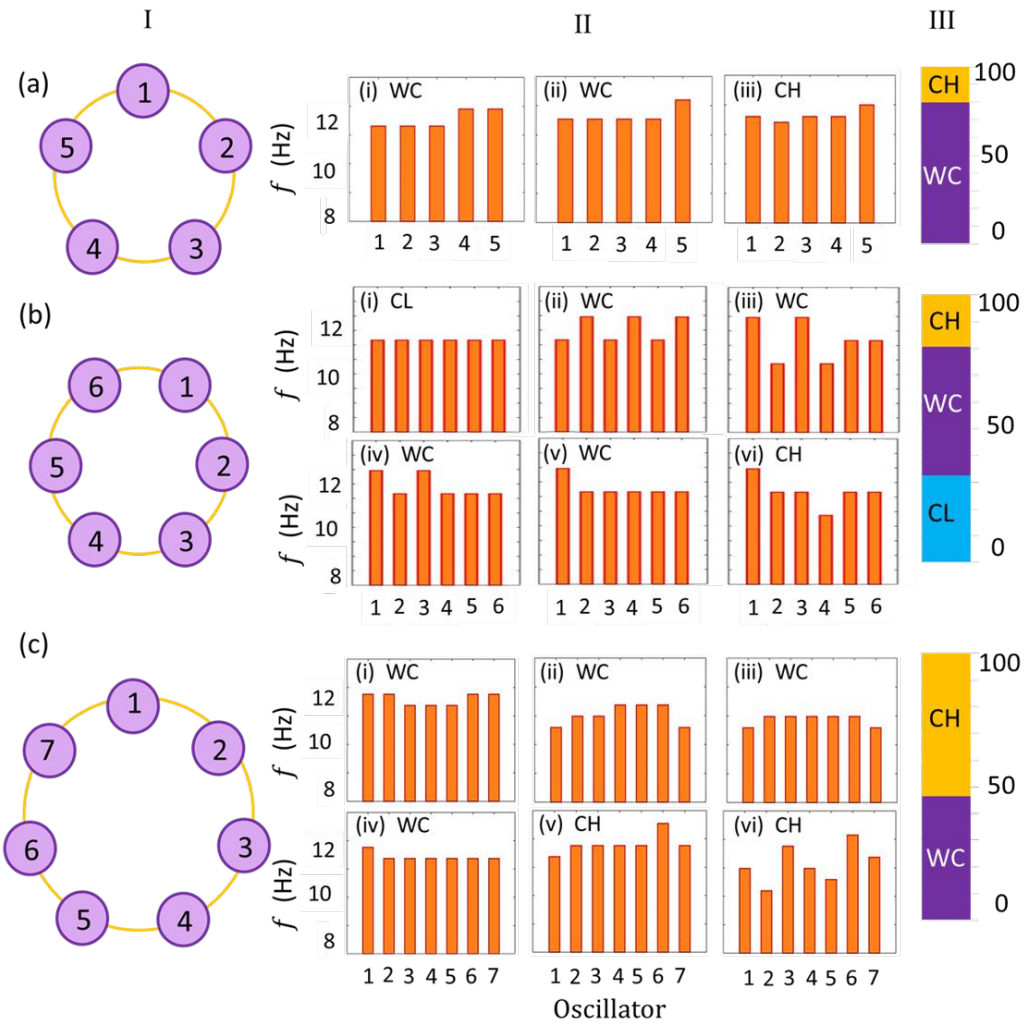

Figure 6.6: (a)-(c) The effect of an increase in the number of oscillators on the dynamical behaviour of annular network consisting of five, six, and seven oscillators, respectively. (I) Schematic of annular network topology for different oscillators, (II) bar charts of dominant frequencies of oscillations corresponding to different dynamical states, namely clustering (CL), weak chimera (WC), and chimera (CH), and (III) percentage occurrence of these dynamical states in a given experiment for these annular networks. The numbers indicated in (a) is a reference number for each oscillator.

synchronized and desynchronized groups are not the same for the weak chimera states presented. As the number of oscillators in an annular topology is increased, we observe an increase in the number of variants of weak chimera and chimera states exhibited by these oscillators. We observe the existence of two variants of weak chimera in a network with five oscillators (Fig. 6.6a-i,ii) and four variants in the network with seven oscillators (Fig. 6.6c-i-iv). Further, in a seven-oscillator ring network, we observe that the chimera states have a greater number of desynchronized oscillators (Fig. 6.6c-vi) as opposed to five oscillator ring network which predominantly has synchronized oscillators (Fig. 6.6a-iii). Furthermore, we observe an increase in the percentage occurrence

of chimera states as the number is increased from five to seven (Fig. 6.6a,c-III), which in turn, points towards the increase in the stability of these symmetry-breaking states in larger networks.

6.4 Conclusions and Discussion

To summarize, in this paper, we investigate the dependency of parameters such as the number of oscillators, coupling topology, and the strength of interaction on the global behaviour of a minimal network of limit-cycle oscillators. Towards this purpose, we perform an experimental investigation on candle-flame oscillators, where the number of oscillators in a network is increased from 2 to 4, the oscillators are coupled in closed-loop (triangle and square) or open-loop (straight and star) topologies, and the strength of coupling between the oscillators is decreased by increasing the distance between them. The closed-loop topology induces nearly equal/symmetric coupling between the oscillators (i.e., global coupling with equal degrees), while the open-loop topology represents an unequal/asymmetric coupling (i.e. non-local coupling with unequal degrees) between the oscillators. In annular networks with a fixed link distance between the oscillators, as the number of oscillators in the network is increased, we observe that the dynamics exhibited by networks consisting of even number of oscillators is different from those with an odd number. In an annular network consisting of an even number of oscillators placed 3 cm apart, the state of clustering is exhibited with the formation of two clusters, with adjacent oscillators being allotted in different clusters. On the other hand, we observe only weak chimera and chimera states in networks with odd number of oscillators and the stability of chimera states increases as the number of oscillators is increased.

When the oscillators are very close to each other, the coupling strength between them is very high. As a result, global dynamical behaviours exhibited by these oscillators, i.e., the state of in-phase synchronization ($d = 0$ cm) and amplitude death ($d = 1$ cm), are highly stable (sustained for longer duration). We also observe that the occurrence of these dynamical states is independent of other parameters, such as the number of oscillators and the network topology considered in the study. However, as the distance between the oscillators is increased ($d > 3$ cm), we observe a dependency

of the global behaviour of the network on these parameters, due to a decrease in the coupling strength between the oscillators. Such topological dependency of oscillators can be clearly depicted through the degree of each oscillator in a network. We observe the presence of multiple stable dynamical states that are alternately exhibited in time at a given distance between the oscillators. Therefore, we plot the percentage occurrence of these dynamical states for each network topology. These states include in-phase synchronization, clustering, rotating clusters, chimera, weak chimera, partial amplitude death, and desynchronization.

We notice that the occurrence of the clustering state in a network topology depends on the degree of each oscillator. For a network of three oscillators, we observe two types of clustering behaviours. One of these types of clustering, usually observed in the literature (Pecora *et al.*, 2014), consists of the phase difference between the oscillator pairs as 0 or 180 deg. Such clustering behaviour is observed for the straight (open-loop) network. The oscillators on the edge, having a degree of one, are in-phase synchronized, while this pair is anti-phase synchronized to the central oscillator, having a degree of 2 (Fig. 3.4b-i). In another type of clustering that is witnessed in a triangular (closed-loop) network, we do not observe the phase shift between the oscillators at 0 or 180 deg. We observe that the oscillators are locked in a phase difference of 84 degrees, 152 degrees, and 68 degrees (Fig. 6.1a). The unstable nature of maintaining 0 or 180 degrees due to the closed-loop arrangement with three oscillators is a possible reason behind such a state of clustering.

Furthermore, we observe the phenomena of rotating clusters in an open-loop network topology containing three oscillators. In the straight configuration, the oscillator in the centre (say, B) has a degree of two and that on edges (say, A and C) have a degree of one. Here, oscillators tend to form two clusters, where two adjacent oscillators (A and B) exhibit in-phase synchronization while maintaining anti-phase synchronization with the third oscillator (C). Due to the low stability of such a clustering state, the clusters flip and the central oscillator (B) forms a cluster (in-phase synchrony) with the oscillator C and this pair displays anti-phase synchrony with the oscillator A. Thereby, exhibiting the occurrence of rotating- like clustering behaviour in the system.

Another novel phenomenon which is observed only in open-loop network topologies (star and straight) with four oscillators, is the state of partial amplitude death

(PAD). In the straight network, we observe that the oscillators on either edge having a degree of 1 are quenched, while the other two oscillators in the middle having a degree of 2 are in a state of desynchronized oscillation (Fig. 6.4a). On the contrary, in a star configuration during the state of PAD, three oscillators on the periphery having a degree of 1 are quenched and that at the centre having a degree of 3 remains in an oscillatory state (Fig. 6.4b). We believe that a system with the coexistence of oscillators having a degree of 1 and a higher degree is pertinent for the exhibition of PAD. The oscillator having degree 1 in such systems would be quenched while the oscillators having a higher degree would remain oscillatory.

In a network of four oscillators, we observe the occurrence of chimera state in every topology except for the square topology at a distance of $d = 3$ cm (Fig. 6.5). For $d = 3$ cm, the highly stable nature of the clustering state restricts the oscillators from oscillating at different frequencies. The state of chimera in open-loop networks is observed to alternate between states of clustering and in-phase synchronization, called alternating chimera, refer Chapter 5.

Thus, the present study highlights that coupled behaviour of limit-cycle oscillators in minimal networks depends on the number of oscillators, the coupling strength between the oscillators, and the coupling structure/topology of these oscillators. Strongly coupling leads to the occurrence of a global behaviour in the network, that remain independent of the number or the topology of oscillators. However, for weakly/asymmetrically coupled oscillators, the global behaviour exhibits the occurrence of multiple states where these states alternately switch in time. We strongly believe that these results on topological dependence can be extended to other systems such as power grids, neuronal networks, vortex interactions in turbulence, and seizure dynamics.

CHAPTER 7

Generic Model for Candle-flame Oscillators: Time-delay Coupled Stuart-Landau Oscillators

The behaviour of coupled candle-flame oscillators resembles the behaviour exhibited by coupled Stuart-Landau oscillators. Stuart-Landau (SL) oscillator is a general paradigmatic model used to approximate a variety of weakly nonlinear systems near Hopf bifurcation. SL oscillators are extensively used to complement the experimental results from various system (Atay, 2010) including coupled candle-flame oscillators.

Here, the oscillators are identical (that is, the frequency of each oscillator is the same) and are coupled with time-delay coupling alone. The general equation for the well-known Stuart-Landau oscillator is given by (Reddy *et al.*, 1998; Atay, 2010)

$$Z(t) = (a + \omega - |Z(t)|^2)Z(t) \tag{7.1}$$

where $Z(t)$ is a complex variable given as $Z(t) = \sqrt{a}e^{i\omega t}$, $\sqrt{a}$ being the amplitude of the oscillator ($a > 0$) and ω being the natural frequency of oscillation. We choose the value of a (= 1) such that each oscillator exhibits a stable limit cycle oscillation in an uncoupled state.

The results presented in this chapter are published in K. Manoj, S. A. Pawar and R. I. Sujith, Experimental Evidence of Amplitude Death and Phase-Flip Bifurcation between In-Phase and Anti-Phase Synchronization *Scientific reports*, 8, 11626, (2018).

K. Manoj, S. A. Pawar, S, Dange, S, Mondal, R. I. Sujith, E. Surovyatkina, and J. Kurths, Synchronization route to weak chimera in four candle-flame oscillators *Physical Review E*, 100, 062204, (2019).

7.1 Coupled Behaviour of a Pair of Stuart-Landau Oscillators

The experimental results from coupled candle-flame oscillators having identical N_C, including the coexistence of AD and PFB and the existence of AD amidst IP and AP oscillations, is supplemented using the equations for the linearly coupled Stuart-Landau oscillators with time-delay coupling are given by

$$\dot{Z}_1(t) = [1 + i\omega_1 - |Z_1(t)|^2]Z_1(t) + K[Z_2(t-\tau) - Z_1(t)] \tag{7.2}$$

$$\dot{Z}_2(t) = [1 + i\omega_2 - |Z_2(t)|^2]Z_2(t) + K[Z_1(t-\tau) - Z_2(t)] \tag{7.3}$$

where the subscripts 1 and 2 correspond to each Stuart-Landau oscillator. The second term on the right-hand side in both the equations (2) and (3), for instance, $K[Z_2(t-\tau) - Z_1(t)]$, contributes to the time-delay coupling. In the equations, τ corresponds to the time delay and K to the coupling strength between the oscillators.

The interactions among the respective oscillators are controlled through the coupling strength K and time-delay τ. Numerical simulations are performed using a fourth-order Runge-Kutta scheme with a step size of 0.01. Here, the first 5 $\times 10^4$ time units are disregarded as transient time and the analysis is performed only on the asymptotically stable dynamical behaviour of the system.

We notice that the behaviour observed at low and high values of N_C (number of candles in an oscillator) with increasing d (distance between the oscillators) in a system of coupled candle-flame oscillators is qualitatively similar to that observed at respective low and high values of K (coupling strength) with increasing τ (time-delay) in the model of coupled Stuart-Landau oscillators. Further, we notice in experiments that with an increase in N_C, the amplitude of oscillations of an individual candle-flame oscillator increases (see Fig. 4.4b) and, we conjecture that this increase in amplitude contributes to an increase in the coupling strength between the oscillators. Further, we consider the oscillators as identical ($\omega_1 = \omega_2 = \omega$), as the natural frequency of a pair of candle-flame oscillators in their uncoupled state is nearly equal, when N_c is the same in both the oscillators. The results of coupled Stuart-Landau oscillators for the

transition from in-phase (IP) to anti-phase (AP) through the amplitude death (AD) state, and the direct transition through phase-flip bifurcation (PFB) are shown in Fig. 7.1 and Fig. 7.2, respectively. A two-parameter plot showing the variation of K with τ for these oscillators is shown in Fig. 7.3.

The initial conditions of Z_1 and Z_2 are fixed at 0.3 and 0.5, respectively, and the non-dimensional frequencies (ω) of both oscillators are kept the same at 10 throughout the study.

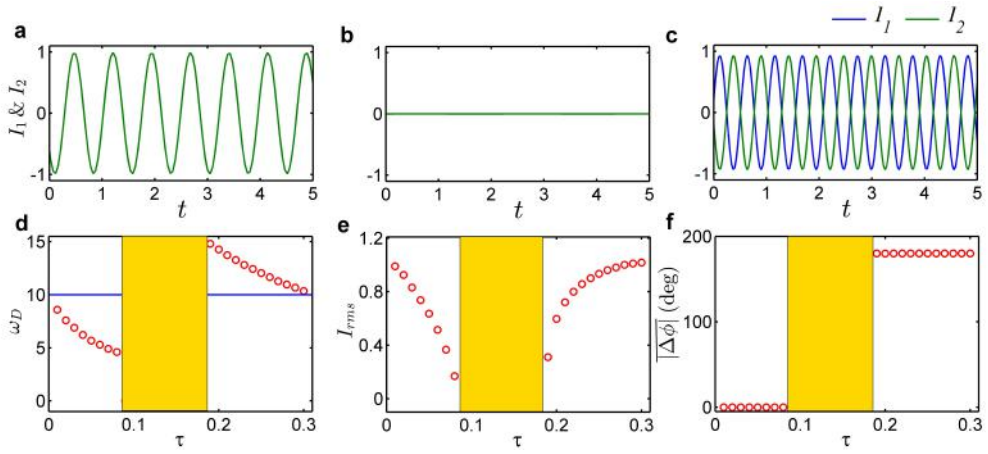

Figure 7.1: Synchronization transition from in-phase (IP) to anti-phase (AP) state via intermediate amplitude death (AD) state for coupled identical Stuart-Landau oscillators. (a)-(c) The times series of IP, AD and AP states observed for coupled Stuart-Landau oscillators for different values of time delay (τ) such as 0, 0.15 and 0.25, respectively, at a constant value of coupling strength (K) equal to 15. (d)-(f), The variation of the dominant frequency, the root mean square value of the amplitude of oscillations and the mean phase difference between the oscillators for different values of τ.

From Fig. 7.1, we see that for a constant low value of K(=15), we observe that as τ is increased, both oscillators transition from IP to AP states of oscillation via an intermediate state of AD. During IP state, the frequency of coupled oscillators is observed to decrease from the frequency of an uncoupled oscillator (ω=10, shown by the horizontal line in Fig. 7.1d), whereas it shows a significant jump during the onset of AP, which eventually decreases and approaches a value close to the frequency of an uncoupled oscillator. The response amplitude of coupled oscillators (in Fig. 7.1e) shows a continuous decrease and increase during IP and AP states, respectively. However, the amplitude of oscillations is nearly zero, showing the cessation of oscillations, during AD state. The mean phase difference between the signals of both oscillators shows a value of zero degrees during IP state and a value of 180 degrees during AP state (in Fig. 7.1f). Such

variation in the properties of coupled Stuart-Landau oscillators due to the change in delay between the oscillators for a constant value of the coupling strength is qualitatively similar to that observed in the experiments of coupled candle-flame oscillators (refer Fig. 4.1, Fig. 4.2a and Fig. 4.3), when the number of candles in an oscillator was low (3 to 5). This supports our conjecture of the importance of time delay in displaying AD state in between the states of IP and AP synchronization in a pair of coupled candle-flame oscillators.

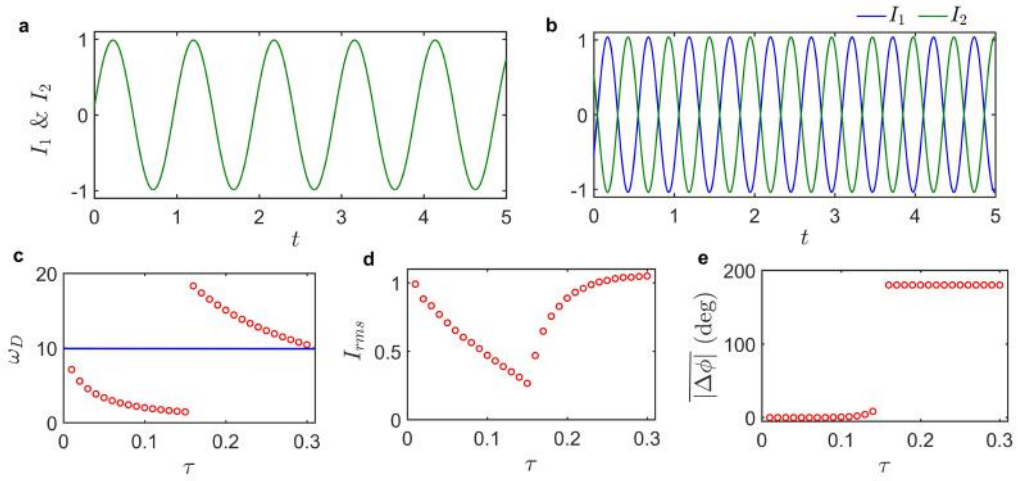

Figure 7.2: Synchronization transition from in-phase (IP) to anti-phase (AP) mode through phase-flip bifurcation (PFB) for coupled identical Stuart-Landau oscillators. The time series corresponding to (a) IP and (b) AP states of oscillations for a constant higher value of coupling strength (K = 55) obtained at different values of time delay (τ) as 0.01 and 0.25, respectively. (c)-(e), The variation of the dominant frequency, the root mean square amplitude and the mean phase difference between the oscillators with τ.

When the value of K(= 55) is considerably high as shown in Fig. 7.2, we observe a sudden transition from IP to AP state. This abrupt transition is accompanied by an equivalent jump in the value of the dominant frequency and the mean relative phase between the oscillators. In contrast, the amplitude of oscillations is observed to decrease and then increase gradually during the transition from IP to AP states. At this value of K, we observe the exhibition of PFB by coupled Stuart-Landau oscillators as a result of varying time delay between them. These results are qualitatively similar to that observed for coupled candle-flame oscillators consisting of eight candles in each oscillator (refer Figs. 4.5b,c).

Figure 7.3 shows the mapping of different dynamical states such as in-phase (IP), amplitude death (AD) and anti-phase (AP) in a parameter space of K and τ. At low

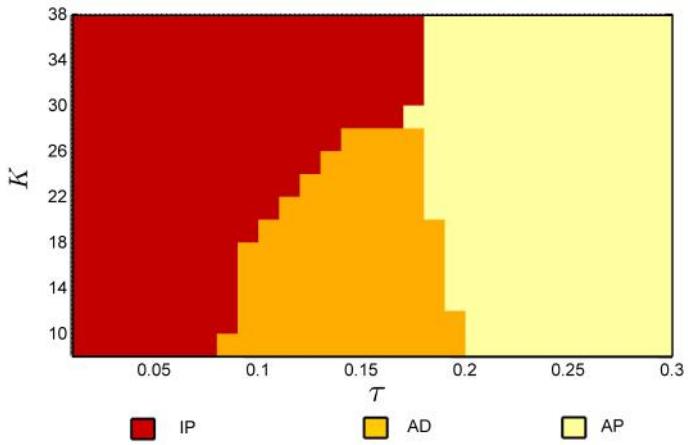

Figure 7.3: Two-parameter bifurcation plot between time delay (τ) and coupling strength (K) for a system of time-delay coupled identical Stuart-Landau oscillators.

values of K, the transition from IP to AP state happens via the AD state (refer Fig. 7.1), whose region gradually decreases as K is increased. Further, a sufficient increase in K value causes the complete disappearance of the AD zone and the emergence of a new phenomenon of phase-flip bifurcation (PFB) (refer Fig. 7.2). During PFB, the oscillators shift their coupled dynamics directly from IP to AP oscillations accompanied by a jump in the value of frequency and phase difference. Thus, the presence of time delay alone in a system of identical oscillators (oscillators with the same natural frequency) can result in the coexistence of two different phenomena such as AD and PFB. These results are very much similar to Fig. 4.5, where the distance between the coupled candle-flame oscillators contributes to the delay in their coupling and the number of candles contributes to the change in coupling strength between the oscillators.

7.2 Coupled Behaviour of Four Stuart-Landau Oscillators

The dynamics of four time-delay coupled SL oscillators with an addition of Gaussian noise in the uncoupled state is examined and compared with the results obtained from the experiments with four candle-flame oscillators. In the recent study presented in Chapter 4, time-delay coupled SL oscillators have been used to model the dynamics of two coupled candle-flame oscillators at various distances between them. They qualita-

tively captured the synchronization modes such as in-phase synchronization, amplitude death and anti-phase synchronization exhibited by these oscillators. Further, coupling of multiple SL oscillators displays various nonlinear symmetry-breaking phenomena such as clustering, chimera, and weak chimera (Premalatha *et al.*, 2018; Kemeth *et al.*, 2018). Hence, we believe that SL oscillators prove to be efficient in modelling the coupled dynamics of four candle-flame oscillators. Further, the general equation for coupled SL oscillators with time-delay coupling is given below. An additive Gaussian white noise term $\epsilon(t)$ is added in the general equation of SL oscillators to mimic the noisy fluctuations encountered in practical experiments with candle flame oscillators.

$$\dot{Z}_j(t) = [1 + i\omega_j - |Z_j(t)|^2]Z_j(t) + \Sigma_l K_{jl}[Z_l(t - \tau_{jl}) - Z_j(t)] + \sigma\epsilon(t) \tag{7.4}$$

where $j, l\epsilon$ {1,2,3, and 4}, and K_{jl} & τ_{jl} are the coupling strength and time-delay constants between the oscillators j and l, respectively. σ represents the strength of the additive noise which is kept constant at 0.2 and $\epsilon(t)$ represents the additive Gaussian white noise whose mean is zero, and the variance is proportional to the square root of the time step used for computation.

We conjecture that the time-delay constants, τ_{jl}, in the system of coupled SL oscillators (equation 7.4) are analogous to the distance between the oscillators in the experiments on coupled candle-flame oscillators. As the distance between two oscillators is increased, the time for the propagation of information from one oscillator to another also increases. Hence, the time-delay between the oscillators is directly proportional to the distance between them. On the other hand, we also assume that the strength of interaction between the oscillators is inversely related to their distance. Hence, the increase in distance decreases the coupling strength between the oscillators. This, in turn, suggests that the coupling strength decreases with the increase in time-delay. Hence, in order to capture this dependency of coupling parameters in the model, we propose a nonlinear relation between the coupling strength, K, and time-delay, τ ($K = 2.5 \times 10^(- 4.6\tau)$). The choice of such a suitable relation between coupling strength and time-delay has been made after the analysis of several possible relations and comparison of the coupled features of candle-flame oscillators discovered in experiments, as shown in the main manuscript.

Due to the rectangular topology of oscillators used in our experiments (Fig. 3.3), implying equal distance on opposite side, we define τ_x and τ_y such that $\tau_{12} = \tau_{34} = \tau_x$ and $\tau_{13} = \tau_{24} = \tau_y$. Using the analogy from the Euclidean distance, we define the time-delay between the coupling of diagonally placed oscillators as $_d = \sqrt{\tau_x^2 + \tau_y^2}$. Initial conditions and frequencies for the oscillators {1,2,3,4} are fixed at {0.3,0.3,0.5,0.5} and 10, respectively. The results of different modes of coupled dynamics obtained at various combinations of time delay and coupling strength values are explained in Figs. 7.4- 7.8.

7.2.1 In-phase Synchronization and Amplitude Death

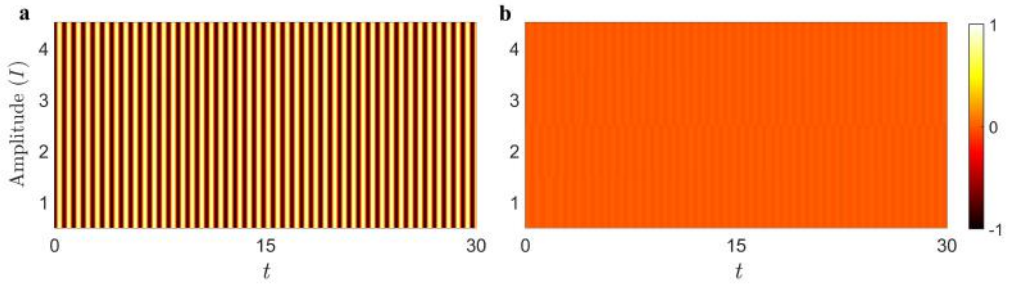

Figure 7.4: Time series (I, with oscillator index 1 to 4, shown as the normalized amplitude fluctuating between 1 and -1) for the states of (a), in-phase synchronization, and (b), amplitude death, in a system of four time-delay coupled Stuart-Landau oscillators.

During the in-phase synchronization state of oscillation (see Fig. 7.4a), all the oscillators attain maxima and minima simultaneously exhibiting a phase shift of zero degrees. This state of synchronization is observed for the {τ_x, τ_y} combination of {0.05, 0.05}, and has a frequency of oscillation of 9.3 Hz. During the state of amplitude death (see Fig. 7.4b), observed for {τ_x, τ_y} combination of {0.1, 0.1}, we observe that the amplitude of oscillations in all the oscillators simultaneously quench to a zero value, which is highlighted by the orange colour of the plot. These states of coupled dynamics are similar to the in-phase synchronization and amplitude death states observed in a system of four coupled candle-flame oscillators, presented in Fig. 5.3.

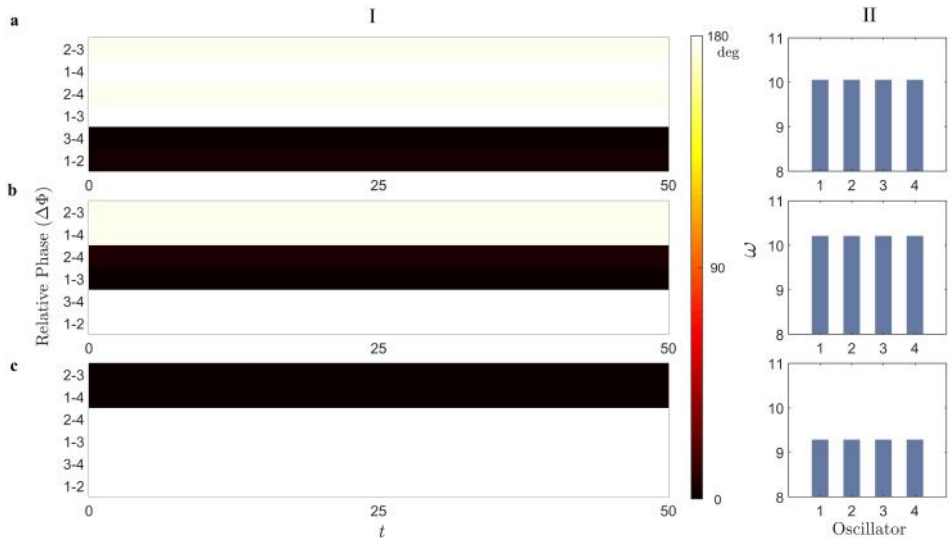

Figure 7.5: Variation in (I), the relative phase ($\Delta\phi$) between each pair of oscillators, and (II), the angular frequency (ω) of each oscillator for a system of coupled Stuart-Landau (SL) oscillators during different states of clustering. The states of clustering presented here correspond to τ_x and τ_y of (a) 0.1 $\times$ 0.4, (b) 0.3 $\times$ 0.3, and (c) 0.4 $\times$ 0.1.

7.2.2 Clustering States

During the state of clustering (see Fig. 7.5), oscillators having equal instantaneous properties (amplitude and phase) group themselves to form clusters while maintaining a constant phase difference (180 degrees in the case shown here) between each cluster. The frequency of all oscillators in a population irrespective of the cluster they belong to would remain the same during the state of clustering. In all three types of clustering exhibited by four SL oscillators, we observe the presence of two clusters, each consisting of two in-phase synchronized oscillators ($\Delta\phi$ 0 deg), and anti-phase synchronization ($\Delta\phi$ 180 deg) between the clusters. The frequencies of oscillators during each type of clustering presented in Fig. 7.5(a) to Fig. 7.5(c) are 10.0, 10.2 and 9.3 Hz, respectively. Similar states of clustering, shown in Fig. 7.5(a) to Fig. 7.5(c) are observed in the experiments with coupled candle-flame oscillators and are discussed in Fig. 5.4.

7.2.3 Symmetry-breaking States

In Fig. 7.6(a) during the state of chimera, we observe the coexistence of the in-phase synchronized oscillator pair $\{1, 3\}$ coexisting with the desynchronized pair $\{2, 4\}$. The oscillators $\{2, 4\}$ have different frequencies among themselves (i.e. 10.03 Hz and 10.02

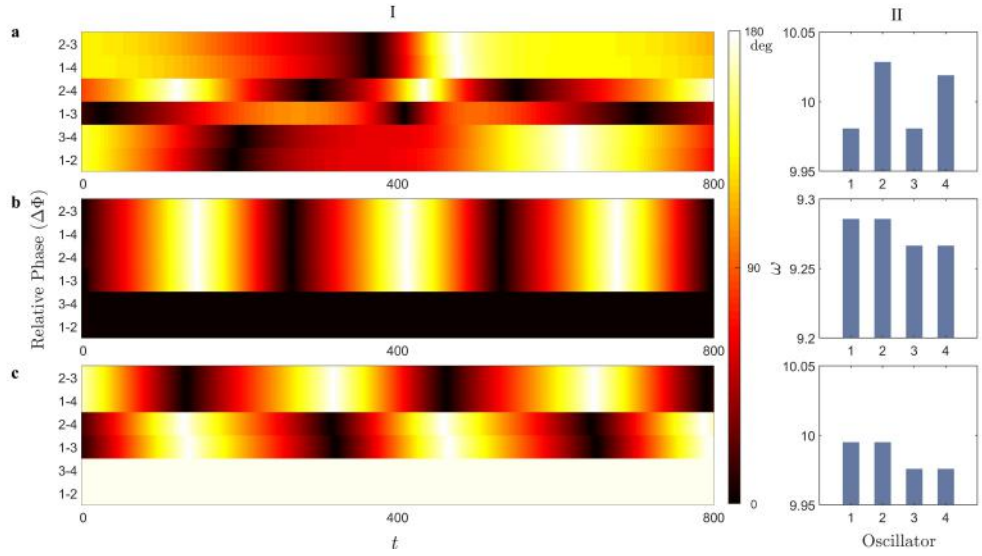

Figure 7.6: Variation in (I) the relative phase ($\Delta\phi$) between each pair of oscillators, and (II) the angular frequency (ω) of each oscillator for a system of coupled Stuart-Landau (SL) oscillators during the states of (a) chimera, (b) in-phase chimera, and (c) anti-phase chimera.

Hz, respectively), whereas the synchronized pair of oscillators exhibits a frequency of 9.97 Hz. This state corresponds to τ_x and τ_y of 0.475 $\times$ 0.425. During the state of in-phase chimera presented in Fig. 7.6(b), the oscillator pairs {1, 2} and {3, 4} exhibit in-phase synchronization while being desynchronized with each other. Hence, we observe a phase shift of zero degrees for the oscillator combinations of {1, 2} and {3, 4}, and phase drifting behaviour for all other combination of oscillators. The oscillator pair {1, 2} have equal frequencies of 9.28 Hz, while the oscillators {3, 4} oscillate at a different frequency of 9.26 Hz. A similar observation is observed in the case of anti-phase chimera presented in Fig. 7.6(c), where the oscillator pairs {1, 2} and {3, 4} are anti-phase synchronized having a phase shift of 180 degrees, and all other combinations are desynchronized. The frequency of the synchronized pair {1, 2} is 9.99 Hz, while that of the pair {3, 4} is 9.97 Hz. The presence of in-phase and anti-phase chimera states is observed for the τ_x and τ_y combinations of 0.1 $\times$ 0.5 and 0.3 $\times$ 0.5, respectively. The states of chimera, in-phase chimera and anti-phase chimera observed in coupled SL oscillators are similar to the states presented in Fig. 5.2, Fig. 5.1(c) and Fig. 5.1(d) in experiments with coupled candle-flame oscillators. Other states of weak chimera and multi-phase weak chimera (Figs. 5.1(a) and (b), respectively) observed in the experiments could not be reproduced in the system of coupled SL oscillators with the nonlinear coupling strength relation employed in the present study.

7.2.4 Global Dynamical Behaviour of the System

The two-parameter bifurcation plots depict the various states of coupled dynamics observed for each combination of $_x$ and $_y$ values in SL oscillators for each relation between coupling strength, K_i and time delay, τ_i, where subscript i corresponds to the notations x, y and d is shown in Fig. 7.7. These states include in-phase synchronization, amplitude death, clustering, weak chimeras, and chimera. The heuristic models govern the specific variation of coupling strength with time delay between the oscillators. From various trials of each relation, we found that the two-parameter bifurcation plot shown in Fig. 7.7(e), the plot with the coupling strength and time-delay relation of $K_i = 2.5 \times 10^{-4.6\tau_i}$, exhibit a close resemblance with the experimental results. However, for this specific case of coupling shown in Fig. 7.7(e), we see a few states which are not observed in the experimental results and are marked as others. These states are discussed in detail in the subsequent figure.

In Fig. 7.8(a), we observe the state of complete desynchrony where all combinations of the relative phase between the oscillators exhibit a phase drifting behaviour. The frequencies of all the oscillators during the state of complete desynchrony, observed at the τ_x and τ_y combination of 0.45 $\times$ 0.45, are different from one another. The plots Fig. 7.8(b), (c) represent the phenomena of slow breathing and fast breathing clusters, where the oscillator dynamics intermittently switches between the states of desynchrony and clustering. For the state of slow breathing clusters [shown in Fig. 7.8(b)], the oscillators exhibit clustering and desynchronized states for a longer duration when compared to the state of fast breathing clusters [shown in Fig. 7.8(c)]. The regions of clustering and complete desynchrony are marked with blue and green braces, respectively. During the states of breathing clusters (both slow and fast), the frequency of oscillators during the clustering region of oscillations is 10.07 Hz, whereas all oscillators oscillate at different frequencies from one another during the state of desynchrony. The states of slow and fast breathing clusters are observed for τ_x and τ_y combinations of 0.45 $\times$ 0.475 and 0.475 $\times$ 0.55, respectively. The states described in this figure are not observed in the experiments on four coupled candle-flame oscillators.

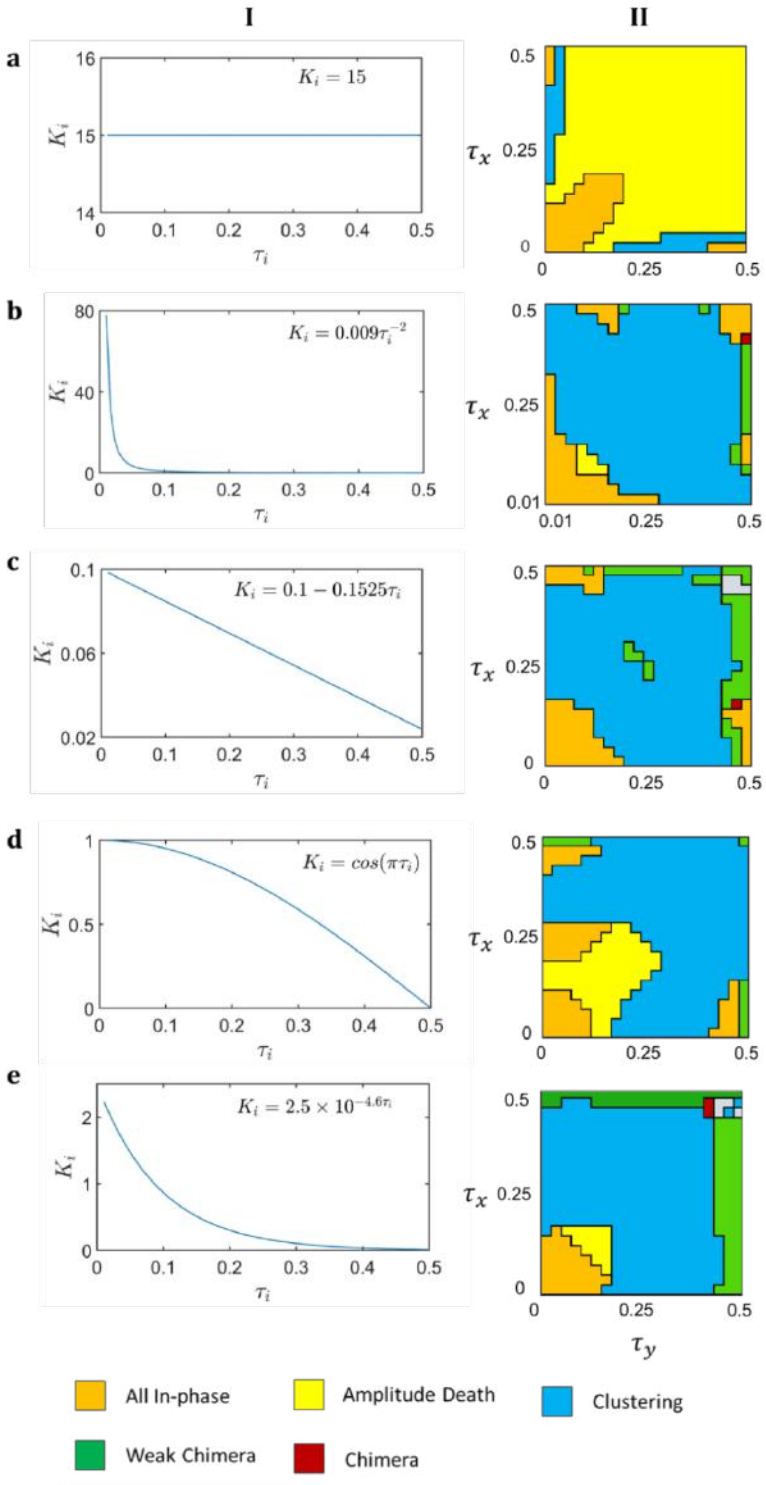

Figure 7.7: (I) The variation of coupling strength (K_i) with time delay (τ_i) for four coupled SL oscillators and (II) the corresponding two-parameter bifurcation plot obtained for various heuristic relations assumed between K_i and $_i$, where subscript i corresponds to the notations x, y and d. These relations include (a) constant, (b) inverse-square, (c) linear, (d) sinusoidal, and (e) negative exponent of 10, which are chosen to qualitatively match the dynamics of coupled candle-flame oscillators observed in experiments (see Fig. 5.5).

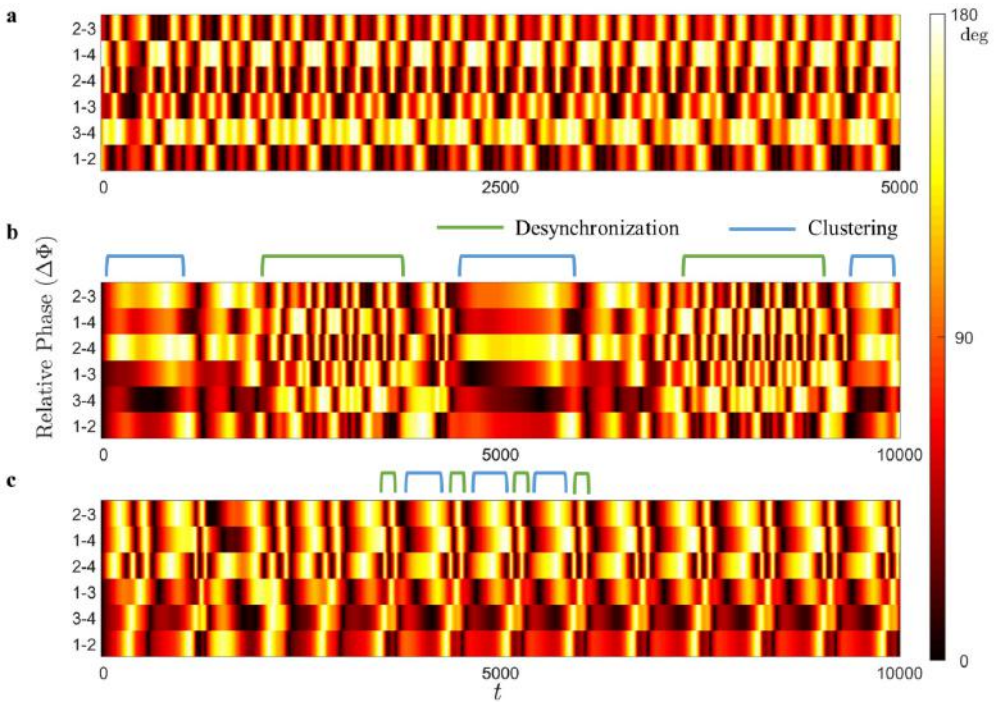

Figure 7.8: The temporal variation of the relative phase between each combination of oscillators for the states depicted as âĂŸothersâĂŹ in the two-parameter bifurcation plot shown in Fig.7.7.

7.3 Conclusions and Discussion

To summarize, we observe that the coupled dynamics exhibited by a coupled pair and quadruplet of Stuart-Landau oscillators complement the experimental results obtained from coupled candle-flame oscillators. Although a physical connection between the two oscillators is not made in the study, a thorough progressive analysis of SL oscillator is carried out to come to such a conclusion. We observe that in the case of coupled pair of SL oscillators, at low values of K, the system transitions from IP to AP via AD, whereas for high values, we observe PFB. The amplitude and frequency of the oscillators along with the mean phase difference between the oscillators for each of these dynamical state observed in SL oscillators showed the same trend as the experimental results.

In the case of four coupled SL oscillators, the determinism of the relationship between the value of K and τ for a given direction was very crucial. Many theoretical studies use various types of coupling, such as local, non-local, and global coupling strategies. In the case of candle-flame oscillators, one can easily argue the existence of non-local coupling, where the strength of coupling between the oscillators decrease with distance (or time delay). However, such a monotonic decrease can be modelled

by various means such linear, exponential and inverse square. Therefore, in order to find an approximate trend, most of the possible monotonic decrease curves, were subjected to the test, to obtain the aptest relationship, which complements the results from candle-flame oscillators.

CHAPTER 8

Conclusion and Scope for Future Work

The main focus of this project report is to investigate the dynamics exhibited by coupled candle-flame oscillators as various coupling parameters and system parameters are changed. The control parameters used in the study include distance between oscillators, the number of candles in an oscillator, the number of oscillators in a system, and the topological arrangement of oscillators. Plethora of dynamical states such as synchronization, oscillation quenching, chimera, clustering, and weak chimeras are observed in coupled candle-flame oscillators depending on the combination of control parameters.

The initial focus of the study is to understand the coupled dynamics exhibited by a pair of candle-flame oscillators as the distance between them is varied. For lower number of candles, we observed the system shift its dynamical behaviour from in-phase synchronization to anti-phase synchronization via the presence of the amplitude death state (AD). As the number of candles in an oscillator is increased, we observed an abrupt shift from in-phase to anti-phase synchronization, referred commonly as phase-flip bifurcation (PFB). Hence, the study presents the first experimental evidence of the coexistence of AD and PFB in a single system. In phase-flip bifurcation, the phases of coupled oscillators exhibit a sudden flip from in-phase (IP) to anti-phase (AP) synchronization or vice versa, due to change in the coupling parameter. During this transition, the frequencies of both oscillators also show a significant leap. We extended the study on mutual interaction between candle-flame oscillators to a system with four oscillators. We discovered the presence of the novel state of multi-phase weak chimera along with the experimental existence of many theoretically discovered states such as in-phase and anti-phase weak chimera. We also observed other dynamical states such as weak chimera, bare minimum chimera, clustering, synchronization and amplitude death.

Further, we performed an experimental investigation on the coupled behaviour of a minimal network of candle-flame oscillators by changing the number of oscillators in a network and locating them in various topological arrangements. For a given number of oscillators, we examined two types of topological arrangements such as closed-loop

(triangle and square: where the oscillators are globally coupled) and open-loop (linear and star: where they are locally coupled). We observed that when the distance between the oscillators is small, the network of oscillators exhibits the states of in-phase synchronization ($d = 0$ cm) and amplitude death ($d = 1$ cm) irrespective of the number or the topological arrangement of oscillators in the network. When the distance between the oscillators is large ($d > 2$ cm) and the number of oscillators is greater than three, we observe that the system behaviour alternately switches between one stable dynamical state to another stable dynamical state in time, for a fixed topological arrangement of oscillators in a network. With the observation of multiple stable states, we could sketch the percentage occurrence of each state at a given distance and topology. Due to the symmetric nature of coupling in closed-loop network topology, the oscillators arranged in such a topology exhibits increased synchrony and stability when compared to those in an open-loop network topology. Therefore, we investigated the dynamical behaviour of oscillators placed in a closed-loop topology (annular) for higher number of oscillators (5-7). We observed that the behaviour exhibited in networks with even number of oscillators is much different from that observed with an odd number of oscillators. These results would find application in various real-life problems such as power grids, neuronal networks, and seizure dynamics (Wickramasinghe and Kiss, 2013).

Finally, the experimental results obtained from coupled candle-flame oscillators are complemented using the numerical results obtained from a generic model of time-delay coupled Stuart-Landau oscillators. We concluded that the generic model of coupled Stuart-Landau oscillators, which is extensively used in modelling varied types of systems of oscillators, mimics the behaviour exhibited by coupled candle-flame oscillators at different distances between the oscillators. This conclusion opens a window to various fields of science and technology where the results from candle-flame oscillators can be extended to other systems including biological, electrochemical, and electronic systems. The experiments involving candle-flame oscillators, while being unconventional, are simple to conduct, and can be used to simulate synchronization phenomena of coupled flames in more complicated systems such as can-annular combustors and afterburner of a gas turbine engine (Flack, 2005).

Scope for Future Work

The study on coupled candle-flame oscillators are extensively investigated in the present project report, however, there are many scopes for future work in this field. A list of possible future extension of the present study is provided below:

- The results from candle-experiments, although are supplemented well using the model of coupled Stuart-Landau oscillators, are not yet modelled using a mathematical model based on the principles of combustion. The model developed by Kitahata *et al.* (2009) based on radiation does not capture the key dynamics of amplitude death or desynchronization observed in two candle-flame oscillators. Furthermore, this model has not yet been used to explore results from systems with more than two oscillators. Therefore, a mathematical model having a physical and chemical basis to the experimental candle-flame oscillator is to be ideated in future studies.

- Furthermore, many studies have postulated varied reasons behind the occurrence of the dynamical states in the oscillators (Kitahata *et al.*, 2009; Dange *et al.*, 2019*b*; Yang *et al.*, 2019). Therefore, a study on the computational fluid dynamical simulation of coupled candle-flame oscillator might provide more clarity on the physical reason behind the occurrence of all the dynamical states observed.

- The experimental investigation on annular topology of candle-flame oscillators performed in the present report is restricted to the link distance of 3 cm. A detailed experimental analysis by separating the possible coupling parameters such as the radius of the circle, the number of oscillators, etc. and individual investigation of these parameters would provide a clearer view on the interaction between oscillators in a annular (ring or regular) network.

- The experiments on candle-flame oscillators are primarily an experiment involving free convention. Comparing these results with experimental studies involving the coupled dynamics of burners such as bunsen burners (Ferguson *et al.*, 2005) and turbulent flames (Takagi *et al.*, 2018) that employ forced convention might provide more insights about many such practical systems.

- There is a possible scope for extending the experimental studies on candle-flame oscillators involving the investigation of external coupling mechanisms, such as the involvement of a co-flow, periodic forcing, or an addition of a boundary, disturbing the flow field around the oscillator.

- The generic mathematical model of SL oscillators is used in the present report to supplement the experimental results of mutual interaction between two and four oscillators. A study parallel to the investigation of the topological dependence of candle-flame oscillators by changing the coupling structure in a network of generic time-delay coupled SL oscillators would also find application in many fields of science.

- The experimental results obtained from coupled pair of candle-flame oscillators shows high similarity to that observed in a system of coupled pair of horizontal Rijke tubes (Dange *et al.*, 2019*a*), which is a prototypical thermoaocustic

oscillator. The oscillatory nature of coupled flames post interaction with the acoustic modes of the combustor results in the generation of large-amplitude self-sustained oscillations, known as thermoacoustic instability (Lieuwen and Yang, 2005; Culick and Kuentzmann, 2006). It is indeed very interesting to note the similarity in experimental results obtained in such varied systems. Therefore, a thorough study on this similarity and the applicability of extending the experimental results from candle-flames to the field of thermoacoustics is also very promising. These results can be used to control/mitigate thermoacoustic oscillations observed in multiple combustion systems.

REFERENCES

1. **Abrams, D. M.**, **R. Mirollo**, **S. H. Strogatz**, and **D. A. Wiley** (2008). Solvable model for chimera states of coupled oscillators. *Physical Review Letters*, **101**(8), 084103.

2. **Abrams, D. M.** and **S. H. Strogatz** (2004). Chimera states for coupled oscillators. *Physical Review Letters*, **93**(17), 174102.

3. **Arumugam, R.**, **P. S. Dutta**, and **T. Banerjee** (2016). Environmental coupling in ecosystems: From oscillation quenching to rhythmogenesis. *Physical Review E*, **94**(2), 022206.

4. **Ashwin, P.** and **O. Burylko** (2015). Weak chimeras in minimal networks of coupled phase oscillators. *Chaos: An Interdisciplinary Journal of Nonlinear Science*, **25**(1), 013106.

5. **Atay, F. M.** (2003). Total and partial amplitude death in networks of diffusively coupled oscillators. *Physica D: Nonlinear Phenomena*, **183**(1-2), 1–18.

6. **Atay, F. M.**, *Complex time-delay systems: theory and applications*. Springer, 2010.

7. **Barabási, A.-L.** *et al.*, *Network science*. Cambridge university press, 2016.

8. **Bick, C.** and **E. A. Martens** (2015). Controlling chimeras. *New Journal of Physics*, **17**(3), 033030.

9. **Bick, C.**, **M. Sebek**, and **I. Z. Kiss** (2017). Robust weak chimeras in oscillator networks with delayed linear and quadratic interactions. *Physical Review Letters*, **119**(16), 168301.

10. **Blasius, B.**, **A. Huppert**, and **L. Stone** (1999). Complex dynamics and phase synchronization in spatially extended ecological systems. *Nature*, **399**(6734), 354–359.

11. **Buckmaster, J.** and **N. Peters**, The infinite candle and its stabilityâĂŤa paradigm for flickering diffusion flames. *In Symposium (International) on Combustion*, volume 21. Elsevier, 1988.

12. **Clerc, M.**, **S. Coulibaly**, **M. Ferré**, **M. García-Ñustes**, and **R. Rojas** (2016). Chimera-type states induced by local coupling. *Physical Review E*, **93**(5), 052204.

13. **Cruz, J.**, **J. Escalona**, **P. Parmananda**, **R. Karnatak**, **A. Prasad**, and **R. Ramaswamy** (2010). Phase-flip transition in coupled electrochemical cells. *Physical Review E*, **81**(4), 046213.

14. **Culick, F.** and **P. Kuentzmann** (2006). Unsteady motions in combustion chambers for propulsion systems. Technical report, NATO RESEARCH AND TECHNOLOGY ORGANIZATION NEUILLY-SUR-SEINE (FRANCE).

15. **Dange, S.**, **K. Manoj**, **S. Banerjee**, **S. A. Pawar**, **S. Mondal**, and **R. Sujith** (2019*a*). Oscillation quenching and phase-flip bifurcation in coupled thermoacoustic systems. *Chaos: An Interdisciplinary Journal of Nonlinear Science*, **29**(9), 093135.

16. **Dange, S.**, **S. A. Pawar**, **K. Manoj**, and **R. Sujith** (2019*b*). Role of buoyancy-driven vortices in inducing different modes of coupled behaviour in candle-flame oscillators. *AIP Advances*, **9**(1), 015119.

17. **Dolnik, M.** and **M. Marek** (1988). Extinction of oscillations in forced and coupled reaction cells. *The Journal of Physical Chemistry*, **92**(9), 2452–2455.

18. **Duncan, C.**, **S. Duncan**, and **S. Scott** (1997). The dynamics of measles epidemics. *Theoretical Population Biology*, **52**(2), 155–163.

19. **Ferguson, D. H.**, **D.-H. Lee**, **T. Lieuwen**, and **G. A. Richards**, Velocity field measurements in an oscillating bunsen flame. *In Proceedings of the 2005 Joint States Meeting of the Combustion Institute*, volume 57. 2005.

20. **Flack, R. D.**, *Fundamentals of jet propulsion with applications*, volume 17. Cambridge University Press, 2005.

21. **Forrester, D. M.** (2015). Arrays of coupled chemical oscillators. *Scientific reports*, **5**, 16994.

22. **Gambuzza, L. V.**, **A. Buscarino**, **S. Chessari**, **L. Fortuna**, **R. Meucci**, and **M. Frasca** (2014). Experimental investigation of chimera states with quiescent and synchronous domains in coupled electronic oscillators. *Physical Review E*, **90**(3), 032905.

23. **Glass, L.** (2001). Synchronization and rhythmic processes in physiology. *Nature*, **410**(6825), 277–284.

24. **Glass, L.** and **M. C. Mackey**, *From clocks to chaos: The rhythms of life*. Princeton University Press, 1988.

25. **Hagerstrom, A. M.**, **T. E. Murphy**, **R. Roy**, **P. Hövel**, **I. Omelchenko**, and **E. Schöll** (2012). Experimental observation of chimeras in coupled-map lattices. *Nature Physics*, **8**(9), 658.

26. **Hansel, D.** and **H. Sompolinsky** (1992). Synchronization and computation in a chaotic neural network. *Physical Review Letters*, **68**(5), 718.

27. **Hardalupas, Y.** and **M. Orain** (2004). Local measurements of the time-dependent heat release rate and equivalence ratio using chemiluminescent emission from a flame. *Combustion and Flame*, **139**(3), 188–207.

28. **Hart, J. D.**, **K. Bansal**, **T. E. Murphy**, and **R. Roy** (2016). Experimental observation of chimera and cluster states in a minimal globally coupled network. *Chaos: An Interdisciplinary Journal of Nonlinear Science*, **26**(9), 094801.

29. **Huygens, C.** (1665). Letter to de sluse, oeuveres completes de christian huygens. *Letters*, **133**.

30. **Kaneko, K.** (1990). Clustering, coding, switching, hierarchical ordering, and control in a network of chaotic elements. *Physica D: Nonlinear Phenomena*, **41**(2), 137–172.

31. **Kapitaniak, T.**, **P. Kuzma**, **J. Wojewoda**, **K. Czolczynski**, and **Y. Maistrenko** (2014). Imperfect chimera states for coupled pendula. *Scientific Reports*, **4**, 6379.

32. **Karnatak, R.**, **N. Punetha**, **A. Prasad**, and **R. Ramaswamy** (2010). Nature of the phase-flip transition in the synchronized approach to amplitude death. *Physical Review E*, **82**(4), 046219.

33. **Karnatak, R.**, **R. Ramaswamy**, and **A. Prasad** (2007). Amplitude death in the absence of time delays in identical coupled oscillators. *Physical Review E*, **76**(3), 035201.

34. **Kemeth, F. P.**, **S. W. Haugland**, and **K. Krischer** (2018). Symmetries of chimera states. *Physical Review Letters*, **120**(21), 214101.

35. **Kitahata, H.**, **J. Taguchi**, **M. Nagayama**, **T. Sakurai**, **Y. Ikura**, **A. Osa**, **Y. Sumino**, **M. Tanaka**, **E. Yokoyama**, and **H. Miike** (2009). Oscillation and synchronization in the combustion of candles. *The Journal of Physical Chemistry A*, **113**(29), 8164–8168.

36. **Koseska, A.**, **E. Volkov**, and **J. Kurths** (2013). Oscillation quenching mechanisms: Amplitude vs. oscillation death. *Physics Reports*, **531**(4), 173–199.

37. **Kuramoto, Y.** (1984). Phase dynamics of weakly unstable periodic structures. *Progress of theoretical physics*, **71**(6), 1182–1196.

38. **Kuramoto, Y.**, *Chaos and Statistical Methods: Proceedings of the Sixth Kyoto Summer Institute, Kyoto, Japan September 12–15, 1983*, volume 24. Springer Science & Business Media, 2012.

39. **Kuramoto, Y.** and **D. Battogtokh** (2002). Coexistence of coherence and incoherence in nonlocally coupled phase oscillators. *arXiv preprint cond-mat/0210694*.

40. **Larger, L.**, **B. Penkovsky**, and **Y. Maistrenko** (2013). Virtual chimera states for delayed-feedback systems. *Physical Review Letters*, **111**(5), 054103.

41. **Lieuwen, T. C.** and **V. Yang**, *Combustion instabilities in gas turbine engines: operational experience, fundamental mechanisms, and modeling*. American Institute of Aeronautics and Astronautics, 2005.

42. **Lim, A. S.**, **H.-U. Klein**, **L. Yu**, **L. B. Chibnik**, **S. Ali**, **J. Xu**, **D. A. Bennett**, and **P. L. De Jager** (2017). Diurnal and seasonal molecular rhythms in human neocortex and their relation to alzheimerâĂŹs disease. *Nature Communications*, **8**, 14931.

43. **Ma, R.**, **J. Wang**, and **Z. Liu** (2010). Robust features of chimera states and the implementation of alternating chimera states. *EPL (Europhysics Letters)*, **91**(4), 40006.

44. **Maistrenko, Y.**, **S. Brezetsky**, **P. Jaros**, **R. Levchenko**, and **T. Kapitaniak** (2017). Smallest chimera states. *Physical Review E*, **95**(1), 010203.

45. **Martens, E. A.**, **S. Thutupalli**, **A. Fourrière**, and **O. Hallatschek** (2013). Chimera states in mechanical oscillator networks. *Proceedings of the National Academy of Sciences*, **110**(26), 10563–10567.

46. **McCaffrey, B.** (1979). Purely buoyant diffusion flames: Some experimental results[final report].

47. **Mizuno, Y.**, **S. Ohta**, **M. Tanaka**, **S. Takamiya**, **K. Suzuki**, **T. Sato**, **H. Oya**, **T. Ozawa**, and **Y. Kagawa** (1989). Deficiencies in complex i subunits of the respiratory chain in parkinson's disease. *Biochemical and Biophysical Research Communications*, **163**(3), 1450–1455.

48. **Mondal, S.**, **V. R. Unni**, and **R. Sujith** (2017). Onset of thermoacoustic instability in turbulent combustors: an emergence of synchronized periodicity through formation of chimera-like states. *Journal of Fluid Mechanics*, **811**, 659–681.

49. **Nagamine, Y.**, **K. Otaka**, **H. Zuiki**, **H. Miike**, and **A. Osa** (2017). Mechanism of candle flame oscillation: Detection of descending flow above the candle flame. *Journal of the Physical Society of Japan*, **86**(7), 074003.

50. **Nandan, M.**, **C. Hens**, **P. Pal**, and **S. K. Dana** (2014). Transition from amplitude to oscillation death in a network of oscillators. *Chaos: An Interdisciplinary Journal of Nonlinear Science*, **24**(4), 043103.

51. **Néda, Z.**, **E. Ravasz**, **Y. Brechet**, **T. Vicsek**, and **A.-L. Barabási** (2000). The sound of many hands clapping. *Nature*, **403**(6772), 849–850.

52. **Nkomo, S.**, **M. R. Tinsley**, and **K. Showalter** (2013). Chimera states in populations of nonlocally coupled chemical oscillators. *Physical Review Letters*, **110**(24), 244102.

53. **Okamoto, K.**, **A. Kijima**, **Y. Umeno**, and **H. Shima** (2016). Synchronization in flickering of three-coupled candle flames. *Scientific Reports*, **6**, 36145.

54. **Omel'chenko, E.**, **M. Wolfrum**, and **Y. L. Maistrenko** (2010). Chimera states as chaotic spatiotemporal patterns. *Physical Review E*, **81**(6), 065201.

55. **Omelchenko, I.**, **E. Omel'chenko**, **A. Zakharova**, **M. Wolfrum**, and **E. Schöll** (2016). Tweezers for chimeras in small networks. *Physical review letters*, **116**(11), 114101.

56. **Panaggio, M. J.** and **D. M. Abrams** (2015). Chimera states: coexistence of coherence and incoherence in networks of coupled oscillators. *Nonlinearity*, **28**(3), R67.

57. **Pawar, S. A.**, **A. Seshadri**, **V. R. Unni**, and **R. Sujith** (2017). Thermoacoustic instability as mutual synchronization between the acoustic field of the confinement and turbulent reactive flow. *Journal of Fluid Mechanics*, **827**, 664–693.

58. **Pecora, L. M.**, **F. Sorrentino**, **A. M. Hagerstrom**, **T. E. Murphy**, and **R. Roy** (2014). Cluster synchronization and isolated desynchronization in complex networks with symmetries. *Nature communications*, **5**(1), 1–8.

59. **Pikovsky, A.**, **M. Rosenblum**, and **J. Kurths**, *Synchronization: A Universal Concept in Nonlinear Sciences*, volume 12. Cambridge University Press, 2003.

60. **Prasad, A.**, **S. K. Dana**, **R. Karnatak**, **J. Kurths**, **B. Blasius**, and **R. Ramaswamy** (2008). Universal occurrence of the phase-flip bifurcation in time-delay coupled systems. *Chaos: An Interdisciplinary Journal of Nonlinear Science*, **18**(2), 023111.

61. **Premalatha, K.**, **V. Chandrasekar**, **M. Senthilvelan**, and **M. Lakshmanan** (2018). Stable amplitude chimera states in a network of locally coupled stuart-landau oscillators. *Chaos: An Interdisciplinary Journal of Nonlinear Science*, **28**(3), 033110.

62. **Raaj, A.**, **J. Venkatramani**, and **S. Mondal** (2019). Synchronization of pitch and plunge motions during intermittency route to aeroelastic flutter. *Chaos: An Interdisciplinary Journal of Nonlinear Science*, **29**(4), 043129.

63. **Reddy, D. R.**, **A. Sen**, and **G. L. Johnston** (1998). Time delay induced death in coupled limit cycle oscillators. *Physical Review Letters*, **80**(23), 5109.

64. **Reddy, D. R.**, **A. Sen**, and **G. L. Johnston** (2000). Experimental evidence of time-delay-induced death in coupled limit-cycle oscillators. *Physical Review Letters*, **85**(16), 3381.

65. **Roy, R.** and **K. S. Thornburg Jr** (1994). Experimental synchronization of chaotic lasers. *Physical Review Letters*, **72**(13), 2009.

66. **Savi, P. V.**, **M. A. Savi**, and **B. Borges** (2020). A mathematical description of the dynamics of coronavirus disease (covid-10): A case study of brazil. *arXiv preprint arXiv:2004.03495*.

67. **Saxena, G.**, **A. Prasad**, and **R. Ramaswamy** (2012). Amplitude death: The emergence of stationarity in coupled nonlinear systems. *Physics Reports*, **521**(5), 205–228.

68. **Schäfer, C.**, **M. G. Rosenblum**, **J. Kurths**, and **H.-H. Abel** (1998). Heartbeat synchronized with ventilation. *nature*, **392**(6673), 239–240.

69. **Schmidt, L.** (2015). *Oscillatory systems with nonlinear global coupling: from clusters to chimeras*. Ph.D. thesis, Technische Universität München.

70. **Selkoe, D. J.** (2000). Toward a comprehensive theory for alzheimer's disease. hypothesis: Alzheimer's disease is caused by the cerebral accumulation and cytotoxicity of amyloid β-protein. *Annals of the New York Academy of Sciences*, **924**(1), 17–25.

71. **Sethia, G. C.**, **A. Sen**, and **F. M. Atay** (2008). Clustered chimera states in delay-coupled oscillator systems. *Physical review letters*, **100**(14), 144102.

72. **Sethia, G. C.**, **A. Sen**, and **G. L. Johnston** (2013). Amplitude-mediated chimera states. *Physical Review E*, **88**(4), 042917.

73. **Shanahan, M.** (2010). Metastable chimera states in community-structured oscillator networks. *Chaos: An Interdisciplinary Journal of Nonlinear Science*, **20**(1), 013108.

74. **Sharma, A.**, **P. R. Sharma**, and **M. D. Shrimali** (2012). Amplitude death in nonlinear oscillators with indirect coupling. *Physics Letters A*, **376**(18), 1562–1566.

75. **Sharma, A.**, **U. K. Verma**, and **M. D. Shrimali** (2016). Phase-flip and oscillation-quenching-state transitions through environmental diffusive coupling. *Physical Review E*, **94**(6), 062218.

76. **Sheeba, J. H.**, **V. Chandrasekar**, and **M. Lakshmanan** (2009). Globally clustered chimera states in delay-coupled populations. *Physical Review E*, **79**(5), 055203.

77. **Sieber, J.**, **E. Omel'chenko**, and **M. Wolfrum** (2014). Controlling unstable chaos: stabilizing chimera states by feedback. *Physical review letters*, **112**(5), 054102.

78. **Strogatz, S.**, *Sync: The emerging science of spontaneous order*. Penguin UK, 2004.

79. **Strogatz, S. H.** (1998). Death by delay. *Nature*, **394**(6691), 316–317.

80. **Strogatz, S. H.**, **D. M. Abrams**, **A. McRobie**, **B. Eckhardt**, and **E. Ott** (2005*a*). Crowd synchrony on the millennium bridge. *Nature*, **438**(7064), 43–44.

81. **Strogatz, S. H.**, **D. M. Abrams**, **A. McRobie**, **B. Eckhardt**, and **E. Ott** (2005*b*). Theoretical mechanics: Crowd synchrony on the millennium bridge. *Nature*, **438**(7064), 43.

82. **Takagi, K.**, **H. Gotoda**, **T. Miyano**, **S. Murayama**, and **I. T. Tokuda** (2018). Synchronization of two coupled turbulent fires. *Chaos: An Interdisciplinary Journal of Nonlinear Science*, **28**(4), 045116.

83. **Timmermann, L.**, **J. Gross**, **M. Dirks**, **J. Volkmann**, **H.-J. Freund**, and **A. Schnitzler** (2002). The cerebral oscillatory network of parkinsonian resting tremor. *Brain*, **126**(1), 199–212.

84. **Tinsley, M. R.**, **S. Nkomo**, and **K. Showalter** (2012). Chimera and phase-cluster states in populations of coupled chemical oscillators. *Nature Physics*, **8**(9), 662.

85. **Wickramasinghe, M.** and **I. Z. Kiss** (2013). Spatially organized dynamical states in chemical oscillator networks: Synchronization, dynamical differentiation, and chimera patterns. *PloS One*, **8**(11), e80586.

86. **Winfree, A. T.**, *The geometry of biological time*, volume 12. Springer Science & Business Media, 2001.

87. **Wojewoda, J.**, **K. Czolczynski**, **Y. Maistrenko**, and **T. Kapitaniak** (2016). The smallest chimera state for coupled pendula. *Scientific Reports*, **6**, 34329.

88. **Wolfrum, M.** and **E. Omel'chenko** (2011). Chimera states are chaotic transients. *Physical Review E*, **84**(1), 015201.

89. **Yang, T.**, **X. Xia**, and **P. Zhang** (2019). Vortex-dynamical interpretation of anti-phase and in-phase flickering of dual buoyant diffusion flames. *Physical Review Fluids*, **4**(5), 053202.

90. **Yeoh, G. H.** and **K. K. Yuen**, *Computational fluid dynamics in fire engineering: theory, modelling and practice*. Butterworth-Heinemann, 2009.

91. **Yoshida, T.**, **L. E. Jones**, **S. P. Ellner**, **G. F. Fussmann**, and **N. G. Hairston Jr** (2003). Rapid evolution drives ecological dynamics in a predator–prey system. *Nature*, **424**(6946), 303.

LIST OF PAPERS BASED ON THESIS

Refereed Journals Based on the Project Report

1. **Krishna Manoj**, Samadhan A. Pawar and R. I. Sujith (2018), "Experimental Evidence of Amplitude Death and Phase-Flip Bifurcation between In-Phase and Anti-Phase Synchronization". Scientific Reports, **8**, 11626

2. **Krishna Manoj**, Samadhan A. Pawar, Suraj Dange, Sirshendu Mondal, R. I. Sujith, Elena Surovyatkina, and Jurgen Kurths (2019), "Synchronization route to weak chimera in four candle-flame oscillators". Physical Review E, **100**, 062204.

3. **Krishna Manoj**, Samadhan A. Pawar and R. I. Sujith (2020), "Experimental investigation on the susceptibility of minimal networks to a change in topology and number of oscillators". (Under Preparation)

Refereed Journals (Others)

1. Suraj Dange, **Krishna Manoj**, Subham Banerjee, Samadhan A. Pawar, Sirshendu Mondal and R. I. Sujith (2019), "Oscillation quenching and phase-flip bifurcation in coupled thermoacoustic systems". Chaos: An Interdisciplinary Journal of Nonlinear Science, **29**, 093135.

2. Suraj Dange, Samadhan A. Pawar, **Krishna Manoj**, and R. I. Sujith (2019), "Role of buoyancy-driven vortices in inducing different modes of coupled behaviour in candle-flame oscillators". AIP Advances, **9**(1), 015119.

3. D. Premraj, **Krishna Manoj**, Samadhan A. Pawar and R. I. Sujith (2020), "General model for a thermoacoustic oscillator: Stuart-Landau versus van der Pol oscillators". (Under Preparation)

Presentation in Conferences

1. **Krishna Manoj**, Samadhan A. Pawar, and R. I. Sujith (2017), Experimental Evidence of Amplitude Death in Coupled Candle Flame Oscillators. 70th Annual Meeting of the APS Division of Fluid Dynamics, November 19 - 21, Denver, Colorado.

2. **Krishna Manoj**, Samadhan A. Pawar, Subham Banerjee, Suraj Dange, Sirshendu Mondal and R. I. Sujith (2019), Amplitude Death: A new approach to quench

thermoacoustic oscillations in coupled systems" Conference on Nonlinear Systems & Dynamics. December 12 - 15, IIT Kanpur, India